GDAŃSK UNIVERSITY OF TECHNOLOGY
FACULTY OF CHEMISTRY

GDAŃSK UNIVERSITY OF TECHNOLOGY
FACULTY OF CHEMISTRY

The author of the PhD dissertation: Paulina Słonimska

Scientific discipline: Chemical Sciences

DOCTORAL DISSERTATION

Title of PhD dissertation: **Pro-regenerative alginate-based formulations of zebularine and retinoic acid for subcutaneous delivery**

Title of PhD dissertation (in Polish): **Proregeneracyjne formulacje zebularyny i kwasu retinowego na bazie alginianu do podania podskórnego**

Supervisor *signature*
Prof. dr hab. inż. Paweł Sachadyn

Gdańsk, 2025

GDAŃSK UNIVERSITY OF TECHNOLOGY
FACULTY OF CHEMISTRY

GDAŃSK UNIVERSITY OF TECHNOLOGY | FACULTY OF CHEMISTRY

STATEMENT

The author of the PhD dissertation: Paulina Słonimska
I, the undersigned, agree/~~do not agree~~* that my PhD dissertation entitled:
Pro-regenerative alginate-based formulations of zebularine and retinoic acid for subcutaneous delivery.

may be used for scientific or didactic purposes.[1]

Gdańsk,.....

signature of the PhD student

Aware of criminal liability for violations of the Act of 4th February 1994 on Copyright and Related Rights (Journal of Laws 2006, No. 90, item 631) and disciplinary actions set out in the Law on Higher Education (Journal of Laws 2012, item 572 with later amendments),[2] as well as civil liability, I declare, that the submitted PhD dissertation is my own work.

I declare, that the submitted PhD dissertation is my own work performed under and in cooperation with the supervision of Prof. Paweł Sachadyn

This submitted PhD dissertation has never before been the basis of an official procedure associated with the awarding of a PhD degree.

All the information contained in the above thesis which is derived from written and electronic sources is documented in a list of relevant literature in accordance with art. 34 of the Copyright and Related Rights Act.

I confirm that this PhD dissertation is identical to the attached electronic version.

Gdańsk,.....

signature of the PhD student

I, the undersigned, agree/~~do not agree~~* to include an electronic version of the above PhD dissertation in the open, institutional, digital repository of Gdańsk University of Technology, Pomeranian Digital Library, and for it to be submitted to the processes of verification and protection against misappropriation of authorship.

Gdańsk,.....

signature of the PhD student

[1] Decree of Rector of Gdansk University of Technology No. 34/2009 of 9th November 2009, TUG archive instruction addendum No. 8.

[2] Act of 27th July 2005, Law on Higher Education: Chapter 7, Criminal responsibility of PhD students, Article 226.

GDAŃSK UNIVERSITY OF TECHNOLOGY
FACULTY OF CHEMISTRY

DESCRIPTION OF DOCTORAL DISSERTATION

The Author of the PhD dissertation: Paulina Słonimska
Title of PhD dissertation: Pro-regenerative alginate-based formulations of zebularine and retinoic acid for subcutaneous delivery

Title of PhD dissertation in Polish: Proregeneracyjne formulacje zebularyny i kwasu retinowego na bazie alginianu do podania podskórnego

Language of PhD dissertation: English

Supervision: Prof. Dr.hab.eng. Paweł Sachadyn

Date of doctoral defense: <day, month, year>

Keywords of PhD dissertation in Polish: regeneracja, gojenie ran, małżowina uszna, epigenetyka, alginian

Keywords of PhD dissertation in English: regeneration, wound healing, ear pinna, epigenetic, alginate

GDAŃSK UNIVERSITY OF TECHNOLOGY
FACULTY OF CHEMISTRY

Summary of PhD dissertation in Polish:

Regenercja tkanek, jak wiele procesów życiowych podlega regulacji epigenetycznej. Inhibitory epigenetyczne umożliwiają odblokowanie ekspresji genów wyciszonych epigenetycznie. Celem tej pracy było opracowanie formulacji leków małocząsteczkowych z nośnikiem alginianowym pobudzających regenerację tkanek poprzez aktywację genów istotnych w jej mechanizmach. Jako substancje czynne wybrałam zebularynę, inhibitor metylotransferazy DNA, i regulator transkrypcji, kwas retinowy. Do badania odpowiedzi regeneracyjnej, wykorzystałam model uszkodzenia małżowiny usznej u myszy. Formulacje zebularyny i kwasu retinowego przygotowałam stosując opracowaną przeze mnie metodę opartą na użyciu młyna kulkowego. Obserwacje mikroskopowe wykazały, że zebularyna tworzyła jednorodną formulację z 2% alginianem sodowym, podczas gdy kwas retinowy, praktycznie nierozpuszczalny w roztworach wodnych, rozpraszał się w postaci drobnych kryształów. Stopniowa absorpcja nośnika wizualizowana za pomocą przeżyciowej ultrasonografii może wyjaśnić podskórnie uwalnianie związków czynnych i obserwowaną regenerację małżowiny usznej. Badania na poziomie molekularnym polegające na oznaczeniu aktywności genów o potencjalnym znaczeniu w gojeniu się ran i regeneracji ujawniły dynamiczne czasoprzestrzenne odpowiedzi transkrypcyjne w regenerujących się tkankach i znaczący wpływ terapii epigenetycznej.

GDAŃSK UNIVERSITY OF TECHNOLOGY
FACULTY OF CHEMISTRY

Summary of PhD dissertation in English:

Tissue regeneration, like many life processes, is subject to epigenetic regulation. The activity of epigenetically silenced genes can be activated using epigenetic inhibitors. This work aimed to develop formulations of small-molecule drugs with an alginate carrier to stimulate tissue regeneration by inducing silenced genes critical in regenerative mechanisms. As active compounds, I selected zebularine, a DNA methyltransferase inhibitor, and retinoic acid, a potent transcriptional regulator, and used an ear pinna punch wound model in mice to study regenerative responses. The formulations of zebularine and retinoic acid were prepared according to a procedure based on using a bead mill homogenizer I developed. Microscopic observations revealed that zebularine formed a homogenous formulation with 2% sodium alginate, while retinoic acid, practically insoluble in aqueous solutions, dispersed as fine crystals. Gradual carrier absorption visualised by live ultrasonography may explain the subcutaneous release of active compounds and the observed ear pinna regeneration. At the molecular level, analyses focusing on the activity of selected gene panels with potential importance in wound healing and tissue regeneration revealed dynamic spatiotemporal transcriptional responses in the regenerating tissues and a significant impact of the epigenetic treatment.

The research presented in this doctoral dissertation was supported by the National Centre for Research and Development of Poland under the project "New generation bioactive molecules delivery systems, based on chemically synthesised and obtained through genetic engineering nanobiomaterials" No. TECHMATSTRATEG2/410747/11/NCBR/2019 (acronym BIONANOVA) realized under the strategic programme "Modern Material Technologies TECHMATSTRATEG"

A part of the results presented in this doctoral dissertation is included in the patent "Pharmaceutical composition based on hydrogel formulations for use as a two-component preparation stimulating tissue regeneration" (No. Pat. 246411) granted by the Patent Office of the Republic of Poland on September 18 2024. A related patent application, "Hydrogel formulation comprising zebularine and retinoic acid" (No. EP22214353.9A) has been filed with the European Patent Office on December 16 2022.

GDAŃSK UNIVERSITY OF TECHNOLOGY
FACULTY OF CHEMISTRY

GDAŃSK UNIVERSITY OF TECHNOLOGY
FACULTY OF CHEMISTRY

Acknowledgements

I want to express my sincere thanks to:

Professor Paweł Sachadyn, for his valuable guidance throughout my Eng, MSc and PhD studies, and above all, for the enormous support in my scientific development and fascination with science, thanks to which I am where I am now;

Co-workers from the Laboratory for Regenerative Biotechnology for the warm welcome in the team, kindness and interesting cooperation;

My parents for their continued support.

Table of contents

THE AIM OF THE STUDY

My research involves developing alginate formulations of pro-regenerative epigenetic inhibitors. The aim was to develop a method for the effective delivery of pro-regenerative drugs activating endogenous regenerative potential and analyze responses to the treatment in regenerating tissue at the molecular level.

In the study, I used a model of the ear pinna injury in laboratory mice. The model enables tracking regeneration progress under the action of tested pharmacologicals. The ear pinna is an organ with a complex structure composed of various tissue types. Therefore, in the ear pinna model, one can observe skin regeneration and other tissues, such as muscles, cartilage, nerves and vessels. The regenerative effect of the drug in this model may constitute a basis for conducting tests in other injury models and in other organs.

In my work, as active substances with pro-regenerative properties, I used an epigenetic drug - zebularine, combined with a transcription activator - retinoic acid. Zebularine is a cytidine analogue, a nucleoside inhibitor of DNA methyltransferases. Previous research in the Laboratory for Regenerative Biotechnology at the Gdańsk University of Technology showed that it stimulates ear pinna regeneration in mice (Sass, Sosnowski *et al*. 2019). A decrease in DNA methylation and transcriptional activation of neurodevelopmental and pluripotency genes in regenerating tissues was observed. Combining zebularine with retinoic acid further enhanced and accelerated this effect, resulting in a complete closure of excisional, through-and-through ear pinna wounds within three weeks post-injury (Sass, Sosnowski *et al*. 2019).

In my experiments, I combined zebularine and retinoic acid in a formulation with sodium alginate. I expected that using an alginate carrier would enable gradual drug release, simplify the administration regimen, and increase the delivery of active substances to internal lesions, even in hard-to-reach sites.

To study the effect of alginate-based regenerative formulations of zebularine and retinoic acid at the molecular level, I focussed on transcriptional responses of genes involved in pluripotency, neurodevelopment, fibrosis, and Wnt signalling in regenerating ear pinnae.

1. Wound healing and regeneration

Both wound healing and regeneration respond to injury. While the first is needed to rapidly seal the wound to stop bleeding and prevent contamination, leading to replacing the lost tissue with a scar consisting primarily of connective tissue, the latter involves restoration of tissue architecture and functions.

1.1 Skin wound healing

Wound healing relates to responses to injuries in various tissues (Stroncek and Reichert 2008); however, skin wound healing is one of the most extensively studied. The skin is a complex organ consisting of the *epidermis* and *dermis*, including subcutaneous fat, a layer of dermal adipocytes, skin appendages such as hair follicles, sebaceous and sweat glands (Takeo, Lee *et al*. 2015), and supplied with the networks of nerves, blood and lymphatic vessels (Hodge, Sanvictores *et al*. 2018). In mice but also in some parts of human skin, the subcutaneous fat layer under the skin is separated from the rest of the body by a residual layer of striated muscles known as *panniculus carnosus* (McGrath, Eady *et al*. 2004, Rittié 2016). The outermost layer is the *stratum corneum*, where the cells have lost their nuclei. Other epidermal cells include melanocytes, Langerhans cells and Merkel cells. Melanocytes are dendritic cells that distribute packets of melanin pigment to the surrounding keratinocytes, giving the skin its colour. Langerhans cells, located in the *epidermis*, are one of the components of the skin's defence system. They can present antigens and are located in the basal and suprabasal layers of the *epidermis*. They travel from the skin to the draining lymph nodes, increasing their migration rate during inflammation. Langerhans cells also play a role in maintaining tolerance in normal skin by inducing activation and proliferation of skin-resident regulatory T cells (Rajesh, Wise *et al*. 2019). Merkel cells function as sensory touch in the skin (Moll, Roessler *et al*. 2005). They are situated in the basal layer of the epidermis and certain distinct areas of the hairy skin of mammals (Merkel 1875). In humans, Merkel cells occur in the basal layer of the *epidermis*, concentrated in secretory glandular processes, hair follicles, and some mucosal tissues. They contain heterogeneously distributed neuropeptides, some acting as neurotransmitters through which Merkel cells and their associated nerves perform their classical function as slowly adapting mechanoreceptors (Moll, Roessler *et al*. 2005). The skin appendages include eccrine (although in mice, they are only found on the soles of the feet) and apocrine glands, ducts and pilosebaceous cells (Vestita, Tedeschi *et al*. 2022).

Wound healing is a biological cross-species evolutionary process and involves spatially and temporally overlapping processes. Wound healing is achieved through four precisely coordinated and partially overlapping phases. These phases are haemostasis, inflammation, proliferation, and remodelling (Guo and DiPietro 2010, Richardson, Slanchev *et al*. 2013). Haemostasis initiates wound healing (Guo and DiPietro 2010). This phase begins immediately after the injury and usually lasts some hours (Reinke and Sorg 2012). Blood vessels are narrowed at this time, and the fibrin clot is formed. The clot and tissues surrounding the wound release pro-inflammatory cytokines. The levels of platelets, transforming growth factor, fibroblast growth factor, and epidermal growth factor increase (Guo and DiPietro 2010). In the inflammation phase, the wound is cleaned of foreign matter. Neutrophils remove dead tissues, bacteria and other foreign bodies in the wound area. The activity of macrophages is also crucial at this stage. Macrophages play diverse roles in maintaining body integrity, participating in eliminating pathogens or tissue repair under inflammatory conditions. There are different subpopulations of macrophages, each with its characteristics and functions. Subpopulations of macrophages have been distinguished: classically activated macrophages (M1) and alternatively activated macrophages (M2), although there are still macrophages whose origin and characteristics are still not fully explored. M1 macrophages produce pro-inflammatory cytokines that mediate resistance to pathogens and have strong bactericidal properties. In contrast, M2 macrophages play a key role in parasite responses, tissue remodelling, and angiogenesis (Chávez-Galán, Olleros *et al*. 2015). Moreover, macrophages stimulate keratinocytes and fibroblasts, thus supporting tissue regeneration (Guo and DiPietro 2010). The next phase is proliferation (Enoch and Leaper, 2008). It occurs after the inflammatory phase and lasts 3 to 10 days (Reinke and Sorg 2012). In this phase, the multiplication of fibroblasts, keratinocytes and other epithelial cells occurs (Enoch and Leaper 2008). In the proliferative phase, granulation tissue is formed. It will fill the wound before reepithelialisation. Epithelial cells migrate through the new tissue to create a barrier between the wound and the environment. Granulation tissue appears approximately 4 days after wounding and simultaneously initiates regenerative polarization of M2 macrophages, fibroblast proliferation, and myofibroblast differentiation (Jiang and Scharffetter-Kochanek 2020). Granulation tissue is supplied by a very dense network of vessels. Granulation tissue contains fibroblasts and endothelial cells in the ECM (extracellular matrix) composed of fibronectin, elastin, laminins, collagens, glycosaminoglycans and proteoglycans

promoting capillary growth (Guo and DiPietro 2010, Ghatak, Maytin *et al*. 2015). New blood vessels provide nutrition and oxygen to growing tissue, allowing leukocytes to enter the wound site (Xue and Jakson, 2015). One of the activities of the proliferative phase is also the repair of peripheral nerves. Restoration of neurological function after traumatic injury to peripheral nerves involves collateral reinnervation and nerve regeneration (Navarro, Vivó *et al*. 2007). Homeostasis begins immediately after the injury and lasts from a few to a dozen or so hours; the inflammatory phase also starts immediately after the injury and usually lasts about 3-5 days or longer in the case of chronic wounds. Proliferation appears about 3 days after the injury and lasts up to 10 days (Reinke and Sorg, 2012).

The wound undergoes physical contraction via contractile myofibroblasts that emerge from the wound (Ghatak, Maytin *et al*. 2015). In a healing wound, fibroblasts synthesise collagen. The type, amount, and organisation of collagen change in a healing wound and determine the tensile strength of the healed skin. Collagen III is the first to be synthesised in the early stages of wound healing and is replaced by collagen I, the dominant type of skin collagen. The initial random deposition of collagen during granulation tissue formation is further enhanced by covalent cross-linking induced by the enzyme lysyl oxidase. This process matures the collagen into complex structures that change to restore tensile strength. Collagen remodelling continues for many months after wound closure (Mathew-Steiner, Roy *et al*. 2021). Wound healing requires cellular interactions between fibroblasts, myofibroblasts, keratinocytes, smooth muscle cells, endothelial cells, and immune cells. Growth factors mediate these interactions. Growth factors necessary in the process of wound healing and regeneration include epidermal growth factor EGF, fibroblast growth factor FGF, insulin-like growth factor IGF, keratinocyte growth factor KGF, platelet-derived growth factors PDGF, transforming growth factors TGF, and vascular endothelial growth factor VEGF. The growth factors have diverse roles in wound healing and regeneration processes. EGF is produced mainly by platelets and is found in high concentrations in the earliest stages of wound healing. EGF increases the rate of wound epithelialisation and reduces scarring by preventing excessive wound contraction. EGF can stimulate keratinocyte proliferation and migration, and KGF can then stabilise the *epidermis*. PDGF is stored in platelets and released in large amounts by platelet degranulation during coagulation after injury. PDGF is a potent chemoattractant for neutrophils, monocytes, and fibroblasts. It

stimulates mesenchymal cells to synthesise extracellular matrix components, collagenase and other growth factors. VEGF is specific for endothelial cells and is a chemoattractant with permanent angiogenic activity. The role of TGF in wound healing is to promote the chemotaxis of inflammatory cells and the synthesis of extracellular matrix (Słonimska, Sachadyn *et al*. 2024)

Few studies indicate a direct role of pluripotency factors, such as Nanog, Pou5f1 (Aguirre, Escobar *et al*. 2023), cMyc or Sox2, in skin wound healing. For example, Sox2 has been reported to promote skin wound healing in mice (Uchiyama, Nayak *et al*. 2019), cMyc to increase epidermal and stem cell differentiation (Arnold and Watt 2001) (Waikel, Kawachi *et al*. 2001), and Klf4 deficiency to delay skin wound healing in mice (Li, Zheng *et al*. 2012). Pluripotency factors affect the ability of cells to self-renew. Replacing old, worn-out cells with new ones is an essential step in wound healing (Ho, Wagner *et al*. 2005) and with a deficit of these factors, cells lose the ability to self-renew and spontaneously differentiate (Hattori, Imao *et al*. 2007). Notably, activation of pluripotency factors has been observed in ear pinna regeneration in mice (Sass, Sosnowski *et al*. 2019).

In conjunction with re-epithelialisation, reconstruction of the *dermis* occurs through the migration and proliferation of fibroblasts. The response of fibroblasts during wound healing determines the outcome of tissue repair. In response to wounding, macrophages and fibroblasts release growth factors leading to further migration and proliferation. They also release inflammatory cytokines that induce an immune response (Schmidt and Horsley 2013). Fibroblasts also produce collagen and other extracellular matrix proteins that promote wound healing. Although collagen and extracellular matrix deposition are indeed necessary to complete wound closure, excessive collagen deposition is responsible for skin fibrosis and scarring (Takeo, Lee *et al*. 2015).

Although, as previously mentioned, wound healing is an interspecies process, the outcome of the skin wound healing process varies depending on the species. Some lower vertebrates, including fish (zebrafish) and amphibians (axolotl and African clawed frog), show excellent skin regeneration. Round wounds with a diameter of about 2 mm after skin excision regenerate entirely, including the secretory appendages. Zebrafish skin can regain its striped pigmentation pattern after healing, and subcutaneous adipocytes and scales are regenerated. This makes the regenerated skin almost indistinguishable from the original structure (Richardson, Slanchev *et al*. 2013).

Scarless skin wound healing has also been reported in a mammalian species, the African spiny mouse (*Acomys*) (Gaire, Varholick *et al*. 2021). However, wound healing in adult mammals typically results in the formation of subfunctional scars within the injury site. Scars consist primarily of connective tissue and are characterised by abundant collagen deposition (Sephel and Woodward 2001, Estiragues, Morillo *et al*. 2023). Scars are often considered an inevitable consequence of surgical intervention (Estiragues, Morillo *et al*. 2023). Scars are not only an aesthetic problem. The resulting tissue is devoid of appendages that constitute an integral part of the biological and physiological functionality of the skin (Takeo, Lee *et al*. 2015). Although the scar fulfils the essential functions of the skin, namely preventing infections and contaminations, the scarring process has many harmful effects, such as decreased extensibility and reduced tensile strength (Takeo, Lee *et al*. 2015). In addition, hair follicles and sebaceous glands serve as sensory and thermoregulatory organs for the skin (Li, Frank *et al*. 2011). Furthermore, the markedly different appearance of scarred skin tissue compared to the original intact skin can result in devastating cosmetic and psychological consequences, reducing the quality of life. Scarring prevents the complete recovery of functional skin. Therefore, restoring the skin to its original state, namely skin regeneration, is a significant research challenge (Takeo, Lee *et al*. 2015). Foetal skin wounds attracted interest as a model that can help reveal mechanisms of scarless healing.

1.1.1 Scarless wound healing process in mammalian foetuses

Mid-pregnancy mammalian foetuses can heal wounds quickly without scarring. However, after a process known as the foetal transition occurs, mammals lose the capability for scarless skin wound healing. In mice, the foetal transition occurs between 16 and 17 days of gestation (Podolak-Popinigis, Górnikiewicz *et al*. 2015). The ability of organisms to heal wounds without scarring has been demonstrated in embryos of several mammals, including marsupials, mice, rats, sheep, pigs, and rabbits. Although the understanding of scarless wound healing mechanisms remains insufficient, multiple differences between foetal and adult mammalian wound healing have been identified. It is known that re-epithelialisation at the level of keratinocytes in adults is much slower than in the foetus. Myofibroblasts have been detected at later stages of wound healing in adults than in foetuses. Minimal inflammatory infiltration is observed in foetuses, while in adults, there is an increased number of leukocytes, mast cell infiltration and macrophages. Differences in the structure of collagen are also visible. In adult

organisms, collagen bundles are highly cross-linked, while in foetuses, the weave is fine, reticular, and enriched with type III collagen. Hyaluronic acid in adult organisms is at a shallow level; the low molecular weight form predominates, while in foetuses, its high levels with more persistent expression are visible, and the macromolecular forms dominate (Ud-Din, Volk *et al*. 2014).

In 1979, scarless skin wound healing in human foetuses was reported (Rowlatt 1979). These reports inspired investigations of the mechanisms underlying the phenomenon by comparing the scarless wound healing and scarring in multiple animal models (Rowlatt 1979, Satish and Kathju 2010, Wulff, Parent *et al*. 2012). A key difference in foetal wound healing is the low inflammatory response resulting from the lack of a fully developed immune system. In scarless wounds, neutrophils, macrophages, and mast cells differ in size and maturity compared to scar wounds (Satish and Kathju 2010, Wulff, Parent *et al*. 2012). The unique healing properties of foetal wounds may be due to the foetal environment, foetal tissues, or a combination. There are many differences between the prenatal and postnatal environments that may play a role in the foetus' response to trauma. A series of reciprocal translocation experiments in which tissues were transplanted between postnatal and foetal animals demonstrated an intrinsic cellular mechanism responsible for the phenomenon of scarless wound healing. In one experiment, full-thickness skin from an adult sheep was grafted onto the backs of fetal lambs on day 60 of gestation. This way, adult skin grafts were perfused with foetal blood and rinsed in amniotic fluid. Forty days later, incisions were made on both the adult skin graft and the adjacent foetal skin. The wound was collected 14 days after the injury. They were analyzed using light microscopy and immunohistochemical examinations. Studies have shown that adult skin grafts healed with scarring, unlike the foetal ones, which healed without scarring. This indicates that the scarless healing of foetal skin is related to the intrinsic properties of the foetal skin and not primarily due to the properties of the foetal environment (Longaker, Whitby *et al*. 1994). Further studies demonstrated extensive repaterning of methylome following the loss of the ability for scarless skin wound healing in foetal mice between days 15 and 18 (Podolak-Popinigis, Ronowicz *et al*. 2016), thus pointing to the importance of epigenetic mechanisms in the foetal transition.

1.2 Regeneration

In contrast to wound healing, which leads to the formation of replacement functionally deficient scar tissue, the regeneration process can be defined as repairing tissues and organs while restoring the lost structure and functionality (Carlson 2007).

1.2.1 Types of regeneration

The ability to regenerate is widespread throughout the animal kingdom. Much knowledge has been gained from analysing regenerative processes in amphibians and fish (Seifert and Muneoka 2018). However, proper regeneration is rarely observed in mammals, except for the foetal and neonatal phases of development (Rowlatt 1979, Longaker, Whitby *et al*. 1994, Satish and Kathju 2010, Wulff, Parent *et al*. 2012, Iismaa, Kaidonis *et al*. 2018). Response to injury in mammals usually results in the formation of nonfunctional fibrotic tissues.

Lower species, such as planarians, salamanders, and reptiles, can overcome scarring and tissue loss through complex adaptations that allow them to regenerate various anatomical structures through epimorphic regeneration (Londono, Sun *et al*. 2018). Epimorphosis is the reconstruction of a missing part of a tissue or organ. This type, seen in higher-order species, involves the development of the blastema, a mass of undifferentiated cells formed in the injury site, e.g. in the stump of the amputated limb in amphibians.

Another type of regeneration is morphallaxis. Morphalaxis is a unique form of regeneration, which is, in some way, a more impressive type of regeneration than epimorphosis, as it involves the reconstruction of the entire organism from a vestigial fragment. This process, observed among lower-order species, involves the direct transformation of a part into a new organism or parts of an organism without multiplying on cutting surfaces (Pellettieri 2019). It occurs in the absence of cell proliferation and involves the transformation of existing body parts or tissues into newly organised structures (Bosch 2007). This leads to a complete reorganisation of the remaining tissues, resulting in an overall smaller but complete organism (Londono, Sun *et al*. 2018). Morphallaxis has been demonstrated in hydras, planaria, and *Sabella* (marine fanworm).

Spectacular regenerative phenomena, such as morphalaxis, are unknown in mammals (Carlson 2007), and epimorphosis is questionable. However, regeneration is

vital to life in multicellular organisms, including mammals. This type of regeneration is known as physiological regeneration. It involves constantly replacing dead cells. Physiological regeneration is a regular and repetitive body regeneration that occurs spontaneously and is not caused by injury (Seifert, Kiama *et al*. 2012). Examples include blood replacement, menstruation, *epidermis* replacement, intestinal mucosa regeneration, the physiological regeneration of the liver, and some species-specific phenomena, e.g. antler replacement in the deer (Carlson 2007, Chuong, Randall *et al*. 2012).

1.2.2 Organ and system regeneration

Mammalian organs in adults show varied regenerative abilities. For example, the heart and central nervous system have minimal regenerative capacity, while the liver presents an immense but not limitless regenerative potential (Baddour, Sousounis *et al*. 2012). As indicated below, the regenerative responses have different mechanisms and outcomes depending on organ and tissue type.

The liver is t known for its excellent regenerative abilities. It can regenerate even after 70% of the organ is removed (Higgins 1931).

The mature peripheral nerves in adult mammals have an innate ability to regenerate after axotomy (Wood, Kemp *et al*. 2011). When regeneration occurs immediately after injury, the peripheral nerve environment best supports nerve regeneration and reinnervation (Burnett and Zager 2004). However, nerve damage is often associated with destroying the basal lamina and Schwann cells, creating fibroblastic scar tissue that traps the growing axon and hinders regeneration (Morgenstern, Asher *et al*. 2003). Furthermore, chronic axotomy and denervation often impair basic neural cell regenerative mechanisms (Wood, Kemp *et al*. 2011).

The thymus gland is another organ capable of regeneration. The adrenal gland consists of two areas: the cortex and the medulla. The medulla does not have the intrinsic ability to regenerate, but the cortex does. It can regenerate after injury. Cortical regeneration is achieved by dedifferentiation, proliferation, and redifferentiation of remaining cells in the cortex and stem cells in the glomerular zone (Mitani, Mukai *et al*. 2003). The thyroid gland regeneration can be mediated by epidermal stem cells (ESC) and bone marrow-derived mesenchymal stem cells (BMMSC). In 2007, Lan *et al.*, induced stem cells in the thyroid gland to acquire regenerative properties (Lan, Cui *et*

al. 2007). However, using thyroid stem cells to improve regeneration is not entirely safe because these cells have, in some cases, been associated with the development of thyroid cancer (Gibelli, El-Fattah *et al*. 2009).

Although the lung is not a regenerative organ, it has been shown that neuroepithelial bodies in the lung function as progenitor cells capable of regenerating the proximal bronchiolar epithelium (Reynolds, Giangreco *et al*. 2000).

The heart can serve as an emblematic example of non-regenerating organs in mammals. Mammalian hearts typically respond to injury by scarring, with the damaged heart muscle being replaced by fibrotic scar tissue. Cardiac muscle tissue consists of specialised cells - cardiomyocytes - their deficiency results in heart failure, which is one of the most common causes of death worldwide. Cardiomyocytes are destroyed due to hypertension and cardiac overload disorders, as a result of myocardial infarction, and as a result of ageing (Laflamme and Murry 2011). However, the hearts of one-day-old newborn mice can regenerate, with only minimal fibrosis, after partial surgical resection. This ability is lost at the age of 7 days. The regenerative capacity of the heart of one-day-old mice is characterized by cardiomyocyte proliferation with minimal hypertrophy or fibrosis. Genetic mapping showed that most cardiomyocytes in the regenerated tissue were derived from pre-existing cardiomyocytes. It has also been demonstrated that two months after the injury, the regenerated apex of the heart ventricle shows normal contractile function (Porrello, Mahmoud *et al*. 2011). The integrity of the endothelial barrier is required to maintain vascular homeostasis and fluid balance between the circulation and surrounding tissues and prevent vascular disease development. Endogenous and exogenous repair mechanisms serve to reverse vascular damage and restore endothelial barrier function by regenerating functional endothelium and re-engaging endothelial junctions (Evans, Iruela-Arispe *et al*. 2021). Following endothelial damage, the vascular repair process involves rebuilding a functional endothelial monolayer and reestablishing endothelial junctions to reform the semipermeable barrier. This regeneration may include resident (Blum and Begemann 2013) endothelial cells and other exogenous cells, such as circulating stem and progenitor cells (Evans, Iruela-Arispe *et al*. 2021). The process of endothelial regeneration is thought to involve the migration and proliferation of endothelial cells and the recruitment of circulating endothelial stem and progenitor cells that differentiate into endothelial cells. Some circulating cells express the same surface markers and

exhibit some in vivo properties similar to mature endothelial cells. These circulating cells can implant in damaged endothelium and thus regenerate it (Evans, Iruela-Arispe *et al*. 2021). However, increasing evidence indicates that circulating monocytic cells do not directly contribute to endothelial regeneration (Ohle, Anandaiah *et al*. 2012). The vascular endothelium can be repaired by mature endothelial cells lining the vessel wall that migrate into the damaged area. In a porcine model, it has been shown that endothelial regeneration can occur, but the regenerated tissue is not fully functional (Vanhoutte 2010). One month after the endothelium of part of the artery was removed *in vivo*, the endothelial surface was lined entirely, but the regenerated endothelium showed significant impairment in endothelium-dependent relaxation to aggregating platelets, serotonin, ergonovine, or thrombin and a greater tendency to exhibit endothelium-dependent contractions.

1.2.3 Blastema in regeneration

Blastema is a mass of undifferentiated cells capable of growing and regenerating into organs or body parts. It is widely accepted that blastema formation mediates epimorphosis and is a hallmark of this regeneration type. Blastema usually occurs in the early stages of organism development, e.g., in embryos and regenerating tissues (Hashemzadeh, Mahdavi-Shahri *et al*. 2015). In adult amphibians, blastema, from which an entire limb develops, is formed in the stump shortly after amputation. Blastema formation requires adequate nerve supply, permeable wound epithelium, and connective tissue cells. These cells signal between the neuroepithelium and vascular cells and function primarily to recruit regeneration-competent cells (McCusker, Bryant *et al*. 2015). At the end of blastema formation, cells begin to multiply rapidly. At the beginning of the proliferation phase, cells have relatively abundant, granular cytoplasm, but as cell division progresses, its amount decreases. Dividing cells are usually densely clustered at the limb tip in the older blastema, whereas in the younger blastema, they are more evenly distributed (Hashemzadeh, Mahdavi-Shahri *et al*. 2015). Recent studies on fish, frogs, salamanders, and also in a mammalian model, the spiny mouse, confirmed that immune cells and their products are necessary for blastema formation and effective regeneration. For example, when macrophages are depleted during adnexal amputation in adult fish or salamanders, subsequent re-epithelialisation prevents blastema formation and regeneration (Seifert and Muneoka 2018).

In mammals, the blastema or blastema-like forms were reported during the heart regeneration of neonatal mice (Tan and Bronner 2024), the fingertip of adult mice (Simkin, Sammarco *et al*. 2015), ear pinna hole closure in the MRL mouse (Gourevitch, Clark *et al*. 2003, Bedelbaeva, Cameron *et al*. 2023) and the regeneration of the ear pinna of adult spiny mice (Tomasso, Disela *et al*. 2024). However, the extent of regeneration is markedly inferior in these models compared to that of the amphibian limb.

2.1. Ear pinna wound closure as a model of mammalian regeneration

The ear pinna is an organ found only in mammals (Webster 1966). The ear pinna of adult mice is approximately 10 mm at the base and approximately 11 mm from the base to the edge of the ear pinna and approximately 300 μm thick. The inner elastic layer of cartilage is two chondrocytes-thick, which is approximately 60 μm. It is sandwiched between two thin layers of skin with a few hair follicles. The thickness of the epithelium varies between 25 and 40 μm and consists of 2-3 layers of keratinocytes covered with the *stratum corneum* with a thickness of 10 μm. The 25-60 μm-thick *dermis* contains a dense extracellular matrix and few elongated fibroblasts (Sosnowski, Sass *et al*. 2022). Ear pinna is supplied by dense networks of peripheral nerves and blood vessels (Yamazaki, Li *et al*. 2018) as well as lymphatic vessels (Yousefi, Zhi *et al*. 2014)

The ear pinna injury model was examined as early as 1953. It was then shown that punctures with a diameter of 1 cm in the ear pinna of rabbits completely closed within 8 weeks (Williams-Boyce and Daniel Jr 1980). Later, similar observations were made in 1972 (Goss and Grimes 1972). In 1980, it was demonstrated that holes punched in rabbits' ears are repaired by regenerating blastema, i.e. undifferentiated cells formed in the injury site at the periphery of wounds (Williams-Boyce and Daniel Jr 1980). It was observed that the cartilage layer was thicker after regeneration (Williams-Boyce 1982). Later, the innate ability to regenerate the ear pinna was discovered in other species: the MRL/MpJ mouse and *Acomys*, also known as the African spiny mouse (Sosnowski, Sass *et al*. 2022). In most laboratory strains, including the common-use ones such as C57BL/6 and BALB/c, punching out holes in the ear pinna used to be a method to mark animals permanently. In MRL/MpJ mice, 2-mm holes close entirely within 30 days without scarring. The regeneration of this complex tissue was reported to occur through the formation of blastema-like structures (Blankenhorn, Troutman *et al*.

2003, Gourevitch, Clark *et al*. 2003). The structure of the skin, muscles, blood vessels, and cartilage was restored (Clark, Clark *et al*. 1998) and peripheral nerves were identified in the regrowing tissues (Buckley, Metcalfe *et al*. 2011). The model was even termed as "classical epimorphic regeneration (Blankenhorn, Troutman *et al*. 2003), although it does not involve the re-growth of a complete complex organ like the limb, and some authors challenge the regenerative nature of ear hole closure in the MRL mouse (Gawriluk, Simkin *et al*. 2016). Nevertheless, subsequent studies from several laboratories reported enhanced regenerative responses in organs other than ear pinna, including the heart (Leferovich, Bedelbaeva *et al*. 2001), cornea (Xia, Krebs *et al*. 2011), digit tips (Chadwick, Bu *et al*. 2007), articular joints (Fitzgerald, Rich *et al*. 2008), spinal cord (Thuret, Thallmair *et al*. 2012), and tendons (Lalley, Dyment *et al*. 2015), which suggests that the ability to close ear pinna may correlate with the organism capacity for regeneration. The studies of MRL crosses with C57BL/6 mice demonstrated that the phenomenon of ear pinna hole closure was genetically determined, and multiple *loci* contribute to this quantitative trait (Blankenhorn, Troutman *et al*. 2003). It is worth noting that the *nude* mice show enhanced ear pinna hole closure resulting from a monogenic mutation in the *Foxn1* gene, which was observed in different strain backgrounds (Gawronska-Kozak 2004).

The previously mentioned *Acomys*, specifically their two species, *Acomys kempi* and *Acomys percivali*, were shown to regenerate full-thickness excisional injuries of ear pinna and dorsal skin. These species completely close 4-mm circular through-and-through wounds in the ear pinnae and regenerate the lost tissue (Seifert, Kiama *et al*. 2012). Thomas *et al.* showed that the ear pinna regeneration in *Acomys* involved the formation of a blastema-like structure (Gawriluk, Simkin *et al*. 2016). The blastema-like structure consists of a specialised wound *epidermis* that attracts migrating cells and secretes factors that stimulate cell cycle progression and proliferation. These studies demonstrate that blastema-mediated regeneration in *Acomys* parallels epimorphic regeneration in other vertebrates, such as salamanders, newts, and zebrafish (Gawriluk, Simkin *et al*. 2016).

The ear pinna is an organ with a complex structure consisting of various types of tissues (Fig. 1). However, the model of ear pinna punch wound is characterised by its experimental simplicity (Fig. 2) and convenient quantification (Sass, Sosnowski *et al*. 2019). Therefore, the ear pinna hole closure can be effective for the assessment of the

pro-regenerative activity of chemical compounds (Bastakoty, Saraswati *et al*. 2015, Zen, Nawrot *et al*. 2016, Zhang, Kurpad *et al*. 2017, Sass, Sosnowski *et al*. 2019, Sosnowski, Sass *et al*. 2022). The model benefits from the nature of ear pinna wound closure: in contrast to 6-mm excisional dorsal skin wounds, which close without treatment intervention in approximately 2 weeks (Sass, Sosnowski *et al*. 2019), 2-mm holes in the ear pinna in normal laboratory mice such as BALB/c or C57BL/6 do not show complete closure without treatment, which facilitates the demonstration of regenerative effects. Studies utilising ear pinna wounds published in top-ranked scientific journals indicate the growing recognition of the model (Seifert, Monaghan *et al*. 2012, Shyh-Chang, Zhu *et al*. 2013, Wei, Kim *et al*. 2020).

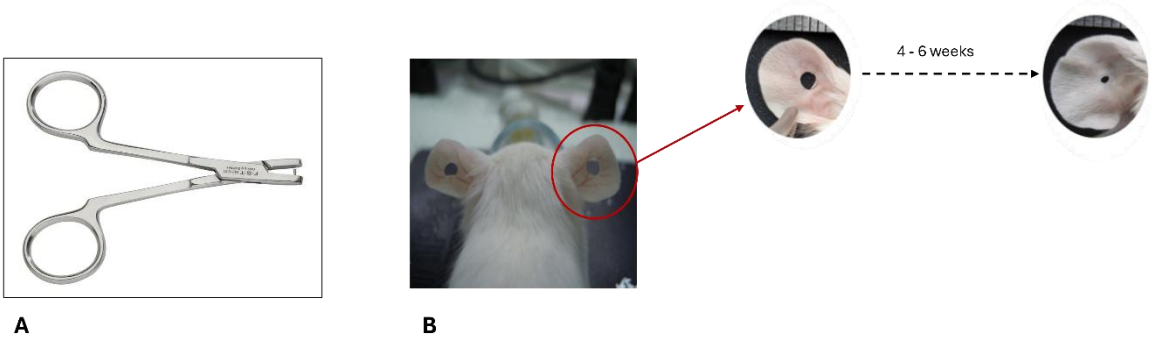

Figure 1 Principles of ear pinna punch experiment: 1A - A laboratory scissors punch that was used to make holes in the ear pinna of a mouse, 1B - Photo of mice with holes made in the ear pinna and the size of the hole in the ear pinna of a selected representative mouse immediately after injury and after the regeneration time, i.e., about 4-6 weeks

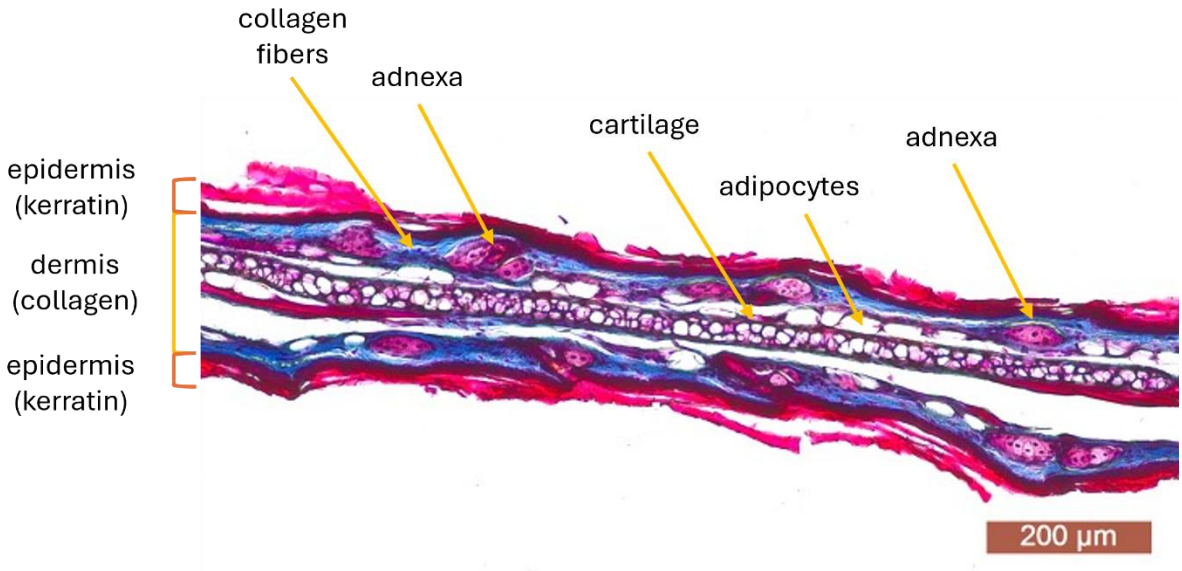

Figure 2 Histological imaging of ear pinna. A cross-section of the central part of the ear pinna stained with Masson's methods (Słonimska, Baczyński-Keller et al. 2024). Dermis (collagen) stains blue; epidermis (keratin), muscles, cartilage, sebaceous glands, and nuclei stain purple.

2.2 Can the ear pinna serve as a skin regeneration model?

Thanks to this organ's complexity revealed by histology imaging (Fig. 2), the ear pinna punch wound closure can be used to investigate regeneration responses in various types of tissues, including skin, cartilage, muscles, nerves and vessels, which is an advantage of this model (Sosnowski, Sass *et al*. 2022). However, there is a question as to whether the ear pinna can be used as a skin wound model.

2.2.1 The role of various tissues in the regeneration process of the ear pinna and dorsal skin

Research on skin wound healing often concentrates on the growth of the *dermis* and *epidermis* and their main cellular components, i.e., fibroblasts and keratinocytes. However, the roles of adipose tissue, subdermal muscle layers, hair follicles, peripheral nerves and blood vessels, and cartilage in the case of the ear pinna, can be significant if not decisive, and therefore they are shortly delineated below.

The presence of perichondrium surrounding the cartilage layer in the ear pinna promotes the recruitment of injury-activated cartilage progenitor cells, which contribute to the formation of fully differentiated tissue (Togo, Utani *et al*. 2006, Abarca-Buis and Krötzsch 2023). Damage to larger blood vessels promotes the release of blood components, including monocyte-derived macrophages, which are very important in the progression of wound healing and regeneration (Lucas, Waisman *et al*. 2010, Godwin, Pinto *et al*. 2013, Simkin, Gawriluk *et al*. 2017). Muscle and fat tissue abundance can activate limited progenitor stem cells in response to injury (Kragl, Knapp *et al*. 2009, Lehoczky, Robert *et al*. 2011).

Until recently, it was believed that adipose tissue played a negative role in wound healing. It was considered harmful in treating extensive and deep burns due to poor circulation and easy liquefaction of wound beds, which provide an excellent breeding ground for bacteria (Fu, Fang *et al*. 2007). Currently, adipose tissue is perceived as one of the largest endocrine organs in the body, containing various types of cells and having many potential applications in regenerative medicine. It has been shown that only one-third of adipose tissue consists of mature adipocytes. In contrast, the remainder consists of a heterogeneous group of preadipocytes, fibroblasts, mesenchymal stem cells (MSCs), endothelial progenitor cells (EPCs), pericytes,

macrophages, T cells, and erythrocytes in vascular stromal cell networks (Trevor, Riches-Suman *et al*. 2020). Fu *et al.* examined the effect of endocrine adipose tissue extract on wound healing. Four full-thickness wounds measuring 3.0 cm x 2.5 cm were made on the back of male Wu Zhi Shan minipigs. In the case of treatment with adipose tissue, an acceleration in the reduction of the wound surface and volume was observed in relation to the groups treated with the growth factor and to the control groups (in the control groups, animals received physiological saline). In wounds treated with adipose tissue, a significant increase in the thickness of the regenerated epidermis and the number of new vascular networks was observed. Regenerated wounds treated with adipose tissue showed increased proliferative cell nuclear antigen (PCNA) and factor VIII-related antigen expression, indicating active cell differentiation and proliferation. Cultured adipose tissue-derived stromal cells, or ASCs, secrete many regenerative growth factors and immune mediators that influence processes during wound healing, such as angiogenesis, modulation of inflammation, and extracellular matrix remodelling (Van Dongen, Harmsen *et al*. 2018).

Hair follicles also participate in wound healing. Hair follicles are sensory organs associated with the immune response against pathogens, thermoregulation, sebum production, angiogenesis, neurogenesis, and wound healing. Skin hair follicles are the main appendages of the skin. They originate from the ectoderm. As a repository of stem cells, they contribute to the reconstruction of the skin microenvironment, including the innervation and vascular system of the skin. HFSCs (hair follicle stem cells) in the bulge area of the hair follicle may serve as a reservoir for transient amplifying cells capable of generating different cell types during hair follicle regeneration. HFSCs can also differentiate into epidermal and sebaceous glands involved in skin wound healing (Chen, Sun *et al*. 2021).

The peripheral nervous system plays a vital role in nerve-dependent regeneration. The peripheral nervous system presents a niche containing peripheral neural crest-derived glial cells or multipotent neural crest-like cells throughout the body. These multipotent nerve-adjacent cells can be reprogrammed *in vivo* to play several roles, such as pigmentation and regeneration of limbs in amphibians and skin in rodents (Suzuki, Satoh *et al*. 2005, Yokoyama, Maruoka *et al*. 2011, Kaucká and Adameyko 2014). Buckley *et al*., in their studies, showed that the MRL/MpJ mouse also

has an increased ability to regenerate peripheral nerves in the ear wound (Buckley, Metcalfe *et al*. 2011). Moreover, surgical denervation of the ear pinna resulted in the loss of neurofilament expression in the wound, prevented blastema formation and severely impaired routine healing, disrupting re-epithelialisation, increasing wound size, and progressive necrosis toward the ear tip. These observations suggest that innervation may be necessary for regeneration and normal wound-healing processes (Buckley, Wong *et al*. 2012). Notably, diabetic peripheral neuropathy is considered one of the main causes of the failure of diabetic foot ulcers to heal (Falanga 2005, Ackermann and Hart 2013, Tecilazich and Veves 2018).

As previously signalled, skin regeneration in mammals is vessel and nerve-dependent (Suzuki, Satoh *et al*. 2005, Yokoyama, Maruoka *et al*. 2011, Kaucká and Adameyko 2014). The ear pinna allows straightforward visualisation of blood vessels and peripheral nerve networks (Yamazaki, Li *et al*. 2018, Sosnowski, Sass *et al*. 2022), so the ear pinna model can add to the studies on this aspect of wound healing.

2.2.2 Differences between ear pinna and dorsal skin wounds

A fundamental difference exists between through-and-through wounds in the ear pinna and full-thickness excision wounds in the dorsal skin (Sami, Heiba *et al*. 2019). The ear pinna consists of two layers of skin and cartilage between them (Suzuki, Ebara *et al*. 2012). A sheet of cartilage between the layers of the *dermis* prevents the rapid wound contraction seen in the loose skin of the back in mice. Therefore, some researchers have noted auricular skin excision as an alternative to the dorsal wound model to study the epithelium (Sami, Heiba *et al*. 2019). However, on the back, the entire excision surface is an open wound, while wounds in the ear pinna can be considered as the edges around the punch holes. The formation of undifferentiated blastema-like tissues in healing ear pinnae suggests resemblances with epimorphic regeneration, a type of regeneration observed during limb regrowth in amphibians, where a mass of undifferentiated cells gives rise to a new limb. In addition, the ear pinna skin contains a thinner layer of *dermis*, fewer hair follicles, and less fatty tissue than most of the remaining body parts. For comparison, the thickness of the *dermis* on the mouse dorsum is, depending on the sex and strain, 500 – 750 μm (Sabino, Deana *et al*. 2016). A conspicuous difference is cartilage, which supports skin layers and prevents rapid wound contraction.

Considering the above-discussed differences between the ear pinna and dorsal skin models, experiments in the ear pinna should not be considered an exact replacement for dorsal skin tissue. The absence of contraction critical in the dorsal wound closure in rodents and convenience in vessel and nerve networks imaging can be seen as the advantages of the ear pinna model. Although the differences between dorsal skin wounds and ear pinna regeneration are essential, the latter undoubtedly involves skin restoration, thus opening an opportunity to investigate skin wound healing.

3. Pharmacological stimulation of regeneration

For now, studies in regenerative medicine are associated most with cell therapies and tissue engineering. The term "regenerative medicine" was preceded by "tissue engineering, " which involves creating organs or tissues *in vitro*. Regenerative medicine uses tissue engineering, stem cell therapy, genetic engineering, materials science, drug delivery, and biomedical engineering to develop therapies that maintain and restore normal function to damaged tissues or organs (Mozzetta, Minetti *et al*. 2009, Lorden, Levinson *et al*. 2015). Although these approaches have great potential, they also have numerous limitations. They are associated with high cost, lack of widespread availability, risks of immunological rejection, production time, and complicated cell isolation (Mozzetta, Minetti *et al*. 2009). Small-molecule drugs, key solutions established in most areas of medicine, deserve attention as an approach to the development of regenerative therapies. Current small molecule drug research on regenerative medicine primarily focuses on compounds that stimulate stem cell differentiation and somatic cell behaviour, such as proliferation, differentiation, and intracellular signalling, to drive and direct tissue regeneration. The advantage of small molecule drugs is that they are cost-effective, have a longer shelf life, and are less complicated both in production and use than biologics, biosimilars or cell-based therapies (Lorden, Levinson *et al*. 2015).

Below, to provide insight into the research interest in regenerative medicines, I summarize several studies on small molecules showing promising regenerative effects in as diverse tissues as the spinal cord, sciatic nerve, bones, and skeletal and cardiac muscles.

Due to the high cost of developing new drugs, previously discovered drugs are often tested for regenerative activity (Lorden, Levinson *et al*. 2015), the strategy known

as drug repositioning. One example of such small-molecule drugs is rolipram. It is an anti-inflammatory drug that inhibits phosphodiesterase. It has been shown to promote axon regeneration (Nikulina, Tidwell *et al*. 2004). Another previously developed small-molecule drug is valproic acid, commonly used to treat epilepsy. It promotes cortical neuron growth *in vitro* and has been shown to improve sciatic nerve regeneration in rats (Hao, Creson *et al*. 2004). The next example is zoledronic acid, the drug used to treat osteoporosis was shown to promote the formation of new bone (Wang, Zhan *et al*. 2022). A small molecule, kartogenin, has the ability to induce chondrogenesis of human MSCs *in vitro* and does not increase cartilage hypertrophy or calcification (Hayek, Kerstetter-Fogle *et al*. 2012, Johnson, Zhu *et al*. 2012, Wang, Wang *et al*. 2019, Chen, Sun *et al*. 2021). Parthenolide has been shown to reduce microtubule detyrosination in axon terminals of cultured dorsal ganglion (DRG) neurons in a concentration-dependent manner and to almost double axonal growth in culture. Even low doses of parthenolide have been shown to accelerate axon regeneration significantly after nerve damage in animals. A single injection into mice into the injured sciatic nerve or its systemic intraperitoneal administration is sufficient to increase the number and length of regenerating axons in the distal nerve 3 days after injury (Gobrecht, Andreadaki *et al*. 2016). Small-molecule drugs that stimulate the regeneration of the nervous system include 7,8-dihydroxyflavone, which supports neurogenesis and neuronal regeneration. It is an agonist of the tropomyosin B receptor (TrkB), mimicking the action of brain-derived neurotrophic factor (BDNF). Upon binding to the TrkB receptor, signalling cascades are initiated that can promote neuronal survival and regeneration. Thanks to these properties, as well as its long half-life and ability to penetrate the blood-brain barrier, 7,8-dihydroxyflavone can be used to treat traumatic brain injury. In particular, the beneficial effects of 7,8-dihydroxyflavone have been observed in animal models of Parkinson's disease, Alzheimer's disease, amyotrophic lateral sclerosis, Huntington's disease, stroke, and depression. Studies have shown that 7,8-dihydroxyflavone can increase neuronal survival through antiapoptotic effects in the Parkinson's model. Treatment with 7,8-dihydroxyflavone can improve learning and memory in healthy young and aged rats. In a mouse model of Alzheimer's disease, treatment significantly improved hippocampus-dependent learning and memory functions (Romeika, Wurzelmann *et al*. 2017). Another low molecular weight compound is rapamycin. It has been shown that mice with hypercapnia (i.e., CO_2 retention causing muscle atrophy) receiving rapamycin showed improved satellite cell autophagy flux, activation,

replication rate, and myogenic capacity, i.e., improved myogenesis previously disrupted by hypercapnia (Balnis, Jackson *et al*. 2025). Recently, a novel histone deacetylase inhibitor SR-4370 was identified that ameliorated skeletal muscle degeneration in zebrafish with a Duchenne muscular dystrophy mutation (Louie, Hasegawa *et al*. 2025). It was also demonstrated that the combination of CHIR99021 and A-485 significantly improved survival and function after myocardial infarction in adult mice hearts. CHIR99021 is crucial for transcriptional and epigenetic activation of genes essential for cardiac cell development. At the same time, A-485 promotes cardiomyocyte dedifferentiation into regenerative cells by epigenetic suppression of cardiomyocyte-specific gene expression. A-485 primarily suppresses H3K27Ac (Zhou, He *et al*. 2024). A rat model showed that the euchromatic histone lysine methyltransferase 2 inhibitor BIX01294 could increase the number of cardiac progenitor cells without impairing their differentiation capacity. This suggests that this drug may have an effect on the production of a large number of cardiac progenitor cells for cardiac repair. In addition, after pretreatment with BIX01294, the levels of cardiomyocyte markers GATA4, Nkx2.5, and myocardin produced by Wnt11-induced mesenchymal stem cells were 2.6-5.6 times higher than those in the untreated group (Xu, Jin *et al*. 2022).

Currently, a wide array of phase II clinical trials are in progress, each investigating the potential of different drugs for regenerative indications. At the time of writing, the ClinicalTrials database found 1 059 studies by search category: Condition/disease: Wounds and Injuries, Intervention/treatment: Drug, Study Phase: Phase 2, and 69 studies by search category: Condition/disease: Regeneration, Intervention/treatment: Drug, Study Phase: Phase 2 (access date April 14 2025). For example, nicotinamide riboside in small fibre neuropathy (clinical trial identifier NCT02851797), Rifaximin as a pro-regenerative substance after liver resection (clinical trial identifier NCT02555293), DP001, a vitamin D analogue that has shown bone formation-stimulating effects in preclinical studies (clinical trial identifier NCT00715676).

4. Epigenetic aspects of regeneration

4.1. Epigenetic regulation of gene expression

The concept of epigenetics has emerged as a potential mechanism by which environmental stimuli can cause lasting changes in gene expression. Epigenetic

mechanisms function alongside DNA sequences to modulate gene expression and ultimately influence protein production (Dalton, Kolshus *et al*. 2014). Epigenetics is one of the fastest-growing scientific fields of biology. Characterising the human DNA methylome at single-nucleotide resolution, the discovery of CpG island shores, new histone variants and modifications, and genome-wide nucleosome positioning maps highlight the increasing pace of discovery. The growing interest in epigenetics is accompanied by technological breakthroughs enabling large-scale epigenomic research. They allow the mapping of epigenetic markers such as DNA methylation, histone modifications and nucleosome positioning, which are crucial for regulating gene and non-coding RNA expression. It is possible to check how these markers correlate with the disease development or therapeutic effects. Therefore, a comprehensive understanding of epigenetic mechanisms, their interactions and differences between the normal state of the body and disease is essential in biomedical research (Portela and Esteller 2010).

Epigenetic alterations regulate biological processes from conception to death, including genome reprogramming during initial embryogenesis and gametogenesis, cell differentiation, and maintenance of established lineage. Key epigenetic mechanisms are DNA methylation and histone post-translational modifications, which interact with each other, regulatory proteins and non-coding RNAs to remodel chromatin into domains such as euchromatin, constitutive or facultative heterochromatin. In addition to epigenetic mechanisms such as imprinting, X-chromosome inactivation, or mitotic bookmarking that establish heritable states, other rapid and transient mechanisms such as histone H3 phosphorylation enable cells to respond and adapt to environmental stimuli. Epigenetic changes can also be responsible for carcinogenesis (Delcuve, Rastegar *et al*. 2009).

Epigenetic factors regulate gene expression through chromatin remodelling and DNA methylation. Chromatin can be remodelled in open or closed functional states that regulate the accessibility of transcriptional factors. When chromatin is open, DNA is available to factors that initiate mRNA transcription and activate gene expression. Chromatin in a closed state limits the availability of DNA to factors that initiate mRNA transcription, thereby suppressing gene expression (Dalton, Kolshus *et al*. 2014). DNA methylation is another epigenetic mechanism that may influence gene expression at the transcriptional level. DNA methylation in the promoter regions can suppress gene

expression. The promoter regions of a gene typically contain many pairs of cytosine-guanine nucleotides distributed multiple times throughout the area, known as cytosine-phosphate-guanine dinucleotide (CpG) sites. DNA methylation involves adding a methyl group at CpG sites in the promoter region of a target gene by DNA methyltransferases. Methylation of CpG sites can directly repress gene expression by preventing enzymes important in RNA synthesis from binding to the promoter region. CpG methylation can also act indirectly by recruiting enzymes and other proteins that promote gene-inhibitory chromatin remodelling, ultimately reducing gene expression, as described above (Dalton, Kolshus *et al*. 2014). CpG-poor regions found in repetitive elements within the intergenic and intronic regions of the genome are methylated and thus maintain a closed chromatin structure (Miranda and Jones 2007). It was initially thought that the DNA methylation pattern was established before birth and was irreversible in adulthood. However, accumulating evidence reveals that DNA methylation responds to and can be altered by environmental signals (Martin and Fry 2018).

Methylation may occur *de novo*, which involves establishing new methylation patterns during embryonic development or copying the methylation pattern onto a newly synthesized DNA strand during replication (Cedar and Bergman 2012). In vertebrates, *de novo* DNA methylation of m5CpG dinucleotides is catalyzed by DNA methyltransferase DNMT3a and DNMT3b, mainly using unmethylated DNA as a substrate. DNMT1, which recognizes preferentially hemimethylated DNA, catalyzes methylation of the nascent, unmethylated strand to maintain methylation during semiconservative DNA replication. When the maintenance methylation is impaired, e.g., due to inhibition, depletion, or nuclear exclusion of DNA methyltransferases, passive demethylation of m5CpG may occur in proliferating cells due to progressive loss of m5C with each round of DNA replication. Passive demethylation is a relatively slow process. It cannot function in terminally differentiated cells because it requires DNA replication. In addition to the passive replication-based process, there is another mechanism of active demethylation. This may include demethylation of DNA in resting cells, which does not undergo replication, or demethylation of transfected plasmid DNA, which is usually non-replicating. Demethylation in dividing cells can also be classified as active when replication is inhibited or when the kinetics of demethylation

are too rapid to be explained by replication. Active demethylation occurs both during development and in differentiated cells (Niehrs 2009).

The DNA methylation described above, like other epigenetic modifications, is regulated by – already mentioned - enzymes divided into: "writers," "erasers," "readers," and "remodelers." "Writers" modify specific bases or amino acids, and "erasers" remove these modifications, thus affecting gene expression. For example, DNA methyltransferase catalyzes the addition of methyl groups to form 5-methylcytosine in DNA bases, while translocation enzymes (Wakizono, Nakashima *et al*.) initiate DNA demethylation, converting 5-methylcytosine into derivatives such as 5-hydroxymethylcytosine, 5-formylcytosine, 5-carboxylcytosine. 5-formylcytosine and 5-carboxylcytosine are excised by thymine-DNA glycosylase. An unmethylated cytosine fills the resulting apyrimidinic site through a base excision repair mechanism. "Readers" are proteins containing specific motifs that recognize and bind these modifications, such as the methyl-CpG binding domain responsible for recognizing 5-methylcytosine. These proteins influence the chromatin state and recruit or cooperate with other enzymes to regulate gene expression. "Remodelers" play a role in chromatin remodelling, relocating, or removing nucleosomes at essential regulatory elements such as enhancers and promoters to modify chromatin accessibility (Dai, Liu *et al*. 2024).

Genomic DNA is organised as chromatin to enable highly condensed genomic information to be stored in the cell nucleus. The basic unit of chromatin is called a nucleosome and consists of negatively charged 146 bp DNA wrapped around a histone octamer core. The histone core of the nucleosome contains four histone proteins, H2A, H2B, H3, and H4, in two copies each. Each core histone protein has an outward-facing tail consisting of lysine. The fifth histone protein, H1, acts as a link between nucleosome units. Modifications such as the addition of acetyl or methyl groups to lysine residues on histone tails can alter the interaction between genomic DNA and the histone core and are involved in the control of gene expression. Chromatin enters an active state when acetyl groups are added (hyperacetylated) to the histone tail by enzymes called histone acetyltransferases (HATs). This promotes the unfolding of the histone 1 unit of chromatin decondensation, allowing mRNA transcription initiation factors to access the genomic DNA and promote gene expression (Dalton, Kolshus *et al*. 2014).

Histone methylation is also crucial at almost all stages of development, and its proper regulation is essential to ensure the coordinated expression of the gene network that regulates pluripotency, differentiation, and organogenesis (Jambhekar, Dhall *et al*. 2019). Chromatin remodelling enzymes and histone methylation are essential for maintaining DNA methylation patterns. Methylation of a lysine residue on the tails of histones H3 and H4 provides an additional layer of control over chromatin structure and, ultimately, gene expression. The conversion from an active to an inactive chromatin state is regulated by various modifications of different locations of the histone H3 and H4 tails, some of which act antagonistically. The methylation of a lysine residue on the histone H3 tail is closely related to the DNA methylation status of a specific chromatin region (Geiman and Robertson 2002). In contrast to histone acetylation, which is connected primarily with chromatin relaxation, the associations of histone methylation with chromatin status and gene expression are more complex and depend on the modification site. E.g. H3K4me2, H3K4me3, and H3K79me3 mark transcriptional activity, while H3K9me2, H3K9me3, H3K27me2, H3K27me3, and H4K20me3, transcriptional repression (Kooistra and Helin 2012). Epigenetic histone-modifying enzymes characterized as “writers” are lysine acetyltransferases (KAT) and lysine methyltransferases (KMT). “Erasers” include histone-lysine deacetylases (HDACs) and lysine demethylases (KDMs) (Lillico, Stesco *et al*. 2016).

One of the main epigenetic mechanisms is chromatin remodelling protein complexes. These are large protein assemblies whose task is to change the structure of chromatin. They use energy from ATP hydrolysis to change the structure of chromatin by moving, throwing out, or restructuring the nucleosome, which is the basic repeating unit of chromatin structure. Chromatin remodelling protein complexes include the SWI/SNF (Switch/Sucrose Non-Fermentable) family. This is one of the better-known families of remodelers. These complexes move nucleosomes or remove them from DNA, enabling transcription. Another family is the group of ISWI (Imitation SWI) protein complexes. These complexes organize and move nucleosomes, thus maintaining chromatin structure. NuRD/Mi-2/CHD complexes are important in cell differentiation and gene repression. They combine chromatin remodelling with histone deacetylation. The INO80 complex is significant in DNA damage response processes. It participates in DNA repair, DNA replication, and transcription control (Clapier and Cairns 2009, Ho and Crabtree 2010).

Many cellular processes are controlled by the Polycomb (PcG) and Trithorax (TrxG) group proteins. These are evolutionarily conserved chromatin-modifying factors. They were initially identified only as part of the epigenetic cellular memory system that maintains repressed or active states of gene expression. Their functional diversity is attributed to their ability to regulate chromatin at many levels - from modifying local structure to three-dimensional genome organization. The Polycomb group of proteins maintains gene repression, acting through histone modifications such as H2A ubiquitination and H3K27 trimethylation. In contrast, the Trithorax group is the opposite of Polycomb because it maintains gene activation. These proteins stabilize the state of active chromatin, for example, by H3K4 trimethylation (Schuettengruber, Bourbon *et al*. 2017).

One more layer of epigenetics, apart from DNA and histone modifications, is considered to be RNA modification, which regulates RNA processing and metabolism. RNA modification occurs in all living forms, and over 150 modifications have been discovered, including 5-methylcytosine (5mC), N6-methyladenosine (m6A), and N1-methyladenosine (m1A). m6A methylation is the most common. It is a dynamic and reversible process in eukaryotic cells regulated by methyltransferases, demethylases, and binding proteins. The m6A methylation process is regulated by methyltransferases, including METTL14, METTL3, and WTAP (Zhang, Zhang *et al*. 2021). This mechanism affects gene expression by changing mRNA stability. It can accelerate mRNA decomposition and thus reduce gene expression, regulate splicing leading to the formation of different transcript variants (Wang, Lu *et al*. 2014), and affect mRNA distribution to specific cellular locations (Shi, Wang *et al*. 2017).

Another mechanism of epigenetic changes is the regulation based on non-coding RNA (ncRNAs) (Dai, Liu *et al*. 2024). ncRNAs play key roles in the regulation of gene expression, splicing, translational, RNA stability, and epigenetic mechanisms (Bartel 2009). ncRNAs include microRNAs (miRNAs), regulating gene expression at the posttranscriptional levels. miRNAs bind to complementary transcripts, inducing degradation or inhibiting translation. (Bartel 2009). Another group of ncRNAs are long-non-coding RNAs (lncRNAs). lncRNAs can bind to proteins and chromosomes, modulating their structural properties, thus affecting the organization of heterochromatin and euchromatin and and influencing gene expression (Ponting, Oliver *et al*. 2009).

4.2 Epigenetic inhibitors and activation of regeneration

The functioning of epigenetic regulation in regenerative processes has not been well recognised. Nevertheless, studies in different tissues and organs provide significant evidence in support of the role of epigenetic mechanisms in regeneration. A selection of articles demonstrating epigenetic repatterning during regenerative processes and its impact on regenerative capacity are presented below.

Neonatal murine hearts perfectly regenerate after apex resection, but this ability is lost by the age of 7 days (Porrello, Mahmoud *et al*. 2011). Sim *et al.* investigated the role of DNA methylation in directing transcriptional changes during the first two weeks of postnatal heart development in mice. Cardiomyocyte maturation was associated with the loss of proliferative capacity and regenerative potential. It has been shown that the vast majority of regions with developmental DNA methylation changes were hypermethylated. Hypermethylated regions were associated with the transcriptional shutdown of crucial developmental signalling pathways (Sim, Ziemann *et al*. 2015).

Examples of the vital role of epigenetic regulation were observed in developing and regenerating nervous tissue. Several studies have been conducted to characterise the epigenome of the developing retina and assess the impact of experimental changes in histone modifications on neurogenesis in this system. DNase mapping of the developing mammalian retina (in transgenic mice) has shown that widespread changes in chromatin accessibility correlate with changes in gene expression. This availability was partly due to dynamic histone modifications highly correlated with the expression of differentiation genes. DNA methylation regulators are expressed at low levels in Müller cells at rest (glial cells found in the vertebrate retina). Still, their levels increase dramatically as early as four days after injury. These include genes essential in CpG methylation, like *Dnmts* (Wilken, Brzezinski *et al*. 2015, VandenBosch and Reh 2020). Loss of regenerative potential in neonatal murine hearts was also correlated with changes in DNA methylation and gene expression patterns. The methylome transition from day 1 to day 7 was characterized by an excess of regions of the genome that gain over those that lose DNA methylation. Promoter genomic regions showing increased DNA methylation on day 7 compared to day 1 were significantly enriched in genes key to cardiac maturation and myocardial development. Extensive changes in DNA methylation patterns during the development of neonatal mouse hearts likely contribute

to the decline in regenerative capacity observed only shortly after birth (Górnikiewicz, Ronowicz *et al*. 2016).

Epigenetic changes demonstrated correlations with the loss of regenerative capacity during the embryonic period. In mice, scarless healing of foetal skin wounds is observed until 16-17 days of gestation until the so-called “foetal transition”. The transcriptome profile analysis of mouse dorsal skin revealed extensive changes in DNA methylation after losing the skin's ability to heal scarless wound wounds in the foetus. These changes correlate with increased gene expression involved in embryonic morphogenesis, synapse functions, neuronal and epithelial development, and repression of genes responsible for epithelial differentiation and inflammatory response. A significant proportion of genes encoding factors involved in wound healing were more than doubled in expression after foetal delivery. The findings indicate the role of epigenetic regulation in scar-free healing (Podolak-Popinigis, Ronowicz *et al*. 2016).

The above-summarised evidence suggests that the transient reversal of these changes may result in enhanced regenerative responses (Sass, Sosnowski *et al*. 2019). The activity of epigenetically silenced genes can be induced using epigenetic inhibitors, like the inhibitors of DNA methylation and histone deacetylation. The concept of epigenetic derepression mechanism based on DNA demethylation is shown in Fig. 3. DNA demethylation induced by an epigenetic inhibitor releases the epigenetic repression, thus enabling gene expression, which an additional transcriptional activator can enhance.

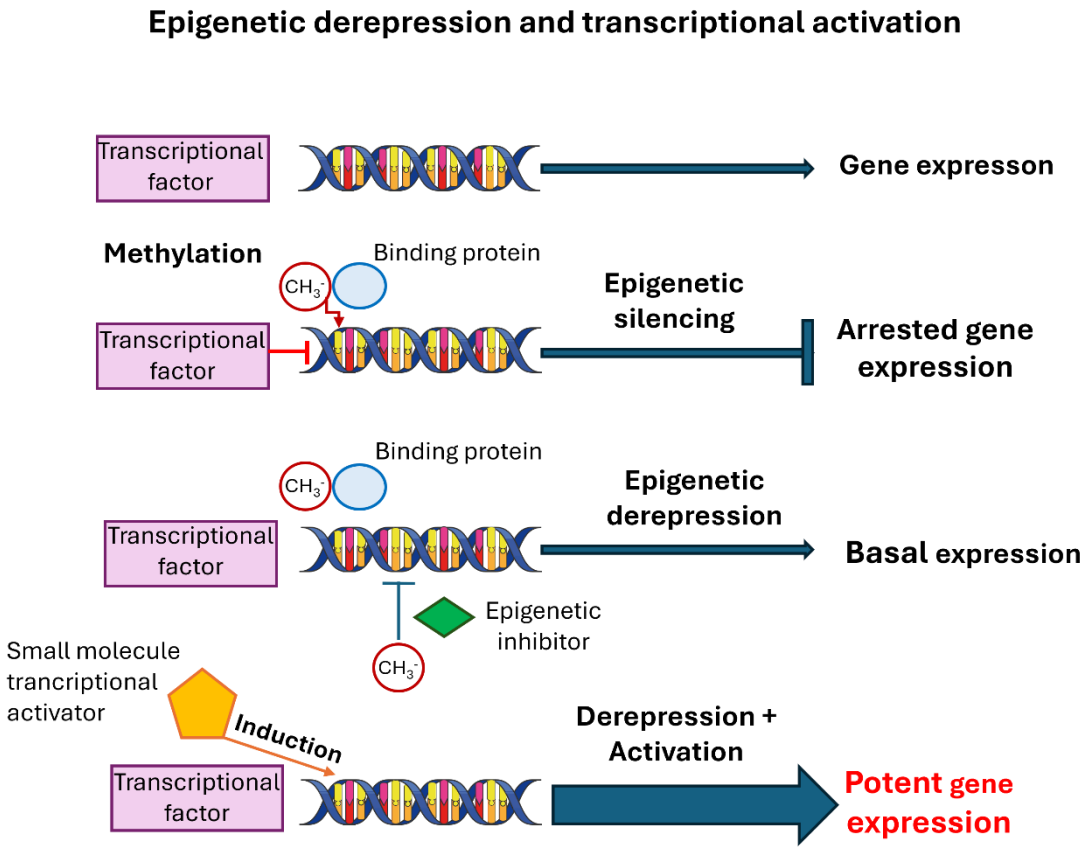

Figure 3 The concept of epigenetic derepression and transcriptional activation (drawn using ServierMedicalArt).

Epigenetic inhibitors are primarily investigated as anti-cancer drugs. Many small-molecule epigenetic inhibitors are under clinical trials (Kaminskas, Farrell *et al*. 2005, Wijermans, Rüter *et al*. 2008, Jin, Liu *et al*. 2022, Wang, Zhan *et al*. 2022), while a few are already in clinical use. So far, two DNA methyltransferase inhibitors, 5'-azacitidine (brand name Vidaza) (Kaminskas, Farrell *et al*. 2005), 5-aza-2′-deoxycytidine (generic name Decitabine), have been approved to treat myelodysplastic syndromes and acute myeloid leukaemia (Wijermans, Rüter *et al*. 2008). Also, several HDAC inhibitors have been approved as anti-cancer drugs, including Vorinostat (brand name Zolinza) indicated for the treatment of cutaneous T-cell lymphoma (Giannini, Cabri *et al*.), Romidepsin (brand name Istodax) indicated for the treatment of peripheral T-cell lymphoma and cutaneous T-cell lymphoma (VanderMolen, McCulloch *et al*. 2011), Belinostat (brand name Beleodaq) indicated for the treatment of peripheral T-cell lymphoma, and Panobinostat (brand name Farydak) indicated for the treatment of myeloma (Moskowitz and Horwitz 2017). Both DNMT and HDAC inhibitors are

reported to act through the activation of epigenetically silenced genes (Mund, Brueckner *et al*. 2006, Delcuve, Khan *et al*. 2012).

There are also investigations into using epigenetic drugs to treat conditions other than cancer, such as neurodegenerative disorders (Xu, Li *et al*. 2012, Singh, Halder-Sinha *et al*. 2018, Kaur, Rathod *et al*. 2022). One of HDAC inhibitors, Valproate, has been in use to treat seizures since 1978 (Henry 2003). It is also indicated in bipolar disorder and migraines. Valproic acid has been shown to promote neuronal differentiation and survival (Wakizono, Nakashima *et al*. 2021). However, it is worth noting that the molecule has several other targets besides HDACs, and its therapeutic effects may involve other mechanisms than histone hyperacetylation-mediated transcriptional derepression. Valproate has been reported to be teratogenic and hepatogenic but not cancerogenic (Blaheta and Cinatl Jr 2002, Brotzmann, Escher *et al*. 2022), which is important, considering the potential risks of cancers associated with epigenetic modifications.

Several other HDAC inhibitors are under investigation in non-cancerous diseases (Ramaiah, Tangutur *et al*. 2021, Noce 2024). Experimental and preclinical evidence indicates that these epigenetic drugs may be effective in treating inflammatory diseases, neurodegenerative disorders, and muscular dystrophy.

Few attempts to apply epigenetic inhibitors, including both those already approved to treat other conditions and investigational ones, to promote tissue regeneration in animal models have been reported. An example of therapy based on epigenetic derepression of neuronal genes is using the epigenetic inhibitor suberoylanilide hydroxamic acid (SAHA), known under the generic name Vorinostat, already approved as an anticancer drug, as mentioned above. As demonstrated in a mouse mechanical-sensory ear hair cell model, it induces neuronal genes in mutant cells, preventing hearing loss. Vorinostat was found to activate the formation of a splicing variant of the REST gene. In neuronal cells, controlled alternative frameshift exon splicing into the REST transcript is needed to activate neuronal genes. The resulting truncated REST variant allows neuronal gene expression, unlike the complete REST repressor silencing neuronal gene expression in non-neuronal cells (Nakano, Kelly *et al*. 2018).

The ability of HDAC inhibitors to counteract the progression of muscular dystrophies points to histone modifications as a critical link between specific genetic mutations and further determinants of disease progression. This also suggests the involvement of epigenetic events in the pathogenesis of muscular dystrophy (Consalvi, Saccone *et al*. 2011). Duchenne muscular dystrophy (DMD) is caused by mutations in the dystrophin gene, leading to dystrophin deficiencies, muscle fibre degeneration, and progressive fibrotic muscle replacement. Givinostat, an HDAC inhibitor, was observed to significantly reduce fibrosis and promote compensatory muscle regeneration in mice. A study was conducted to evaluate whether the beneficial histological effects of givinostat could be extended to boys with DMD. Givinostat treatment significantly increased the muscle tissue fraction in biopsies and reduced the amount of fibrotic tissue. It also substantially reduces tissue necrosis and fat replacement. Treatment with Givinostat for more than one year has been shown to significantly prevent the progression of histological disease progression in boys with DMD (Bettica, Petrini *et al*. 2016). Givinostat (brand name Duvyzat) was approved to treat boys with DMD ages six years and over in March 2024 (Lamb 2024).

Sodium phenylbutyrate is another HDAC inhibitor connected with promising pro-regenerative actions. It exerts anti-inflammatory effects in lipopolysaccharide-activated microglial cells, reducing nitric oxide release and cytokine secretion. Sodium phenylbutyrate was first indicated to treat urea cycle disorders, later introduced in combination with tauroursodeoxycholic acid to treat amyotrophic lateral sclerosis (Bouhadir, Lee *et al*.) (Peña-Quintana, Llarena *et al*. 2017, Ketabforoush, Faghihi *et al*. 2024). Sodium phenylbutyrate has been shown to have the potential to regulate the balance of pro-inflammatory cytokine expression, resulting in improved axonal regeneration, remyelination, and reinnervation in an *in vivo* sciatic nerve transection injury model (Yadav, Huang *et al*. 2021).

Interesting trials with small molecules targeting mechanisms of epigenetic regulation other than histone deacetylation to promote regeneration were conducted in *ex vivo* models.

The FDA-approved drug excipients N-methylpyrrolidone (NMP) and N, N-dimethylacetamide (Birsoy, Chen *et al*. 2008) act as BET bromodomain inhibitors, which prevent bromodomain binding to acetyl histone groups, resulting in gene

downregulation. Both NMP and DMA reduce inflammation and positively affect bone remodelling by inhibiting osteoclastogenesis and promoting the anabolic effects of BMP2. Pretreatment with NMP and DMA recovered TNFα-inhibited osteoblastic gene expression and mineralization in multipotent stem cells but not in preosteoblasts and cranial osteoblasts (Chen, Weber *et al*. 2019).

Shah *et al.* examined the effect of zebularine on corneal epithelial wound healing in *ex vivo* diabetic models. Diabetic corneal complications may cause permanent epithelial defects and impaired wound healing due to limbal epithelial stem cell dysfunction. DNA methylation profiling of nondiabetic and diabetic limbal epithelial cells showed that the *WNT5A* promoter was significantly hypermethylated in the latter. The hypermethylation was accompanied by a significant reduction in the WNT5A protein. WNT5A belongs to the Wnt family of secreted signalling lipoproteins essential for developing homeostasis and maintaining and regenerating stem cells. WNT5A is also associated with the immune response. Zebularine, a DNA methylation inhibitor, was selected to reverse the hypermethylation of *WNT5A* promoter, and thus promote corneal epithelial wound healing in diabetic patients. Zebularine-treated diabetic cells showed significantly reduced 5-methylcytosine levels and significantly reduced DNMT1 levels, indicating effective DNA demethylation. Zebularine treatment increased WNT5A levels 1.37-fold and stimulated healing in a dose-dependent manner in a scratch wound assay with a 1.6-fold increase over 24 hours compared to the untreated control group in human limbal epithelial cells. The result was consistent with accelerated wound healing in zebularine-treated diabetic organ-cultured corneas. Shah *et al.* connected the regenerative zebularine effect with the reversal of *WNT5A* hypermethylation (Shah, Spektor *et al*. 2023).

Specific molecular mechanisms by which epigenetic modulators can promote reprogramming by activating pluripotency genes still need to be explained. Most current research is in the early preclinical phase. One of the main points limiting the use of epigenetic drugs is that their action affects the entire epigenome. They are not targeted to specific *loci* but to induce cellular reprogramming or differentiation. This way, epigenetic modulators can activate genes with undesirable functions and generate global effects. Targeted chromatin remodelling could be a solution. On the other hand, the examples of epigenetic inhibitors already approved as drugs indicate that the risk of epigenetic changes is considered acceptable in the case of severe diseases.

4.2.1 Synergistic pro-regenerative effect of zebularine and retinoic acid

An example of an epigenetic inhibitor successfully applied to induce regeneration is zebularine, known under the IUPAC name 1-[(2R,3R,4S,5R)-3,4-dihydroxy-5-(hydroxymethyl)oxolan-2-yl]pyrimidin-2-one. It is a cytidine analogue, a nucleoside inhibitor of DNA methyltransferases. The synthesis of zebularine was first described in 1961 (Funakoshi, Irie *et al*. 1961). Initially, zebularine was tested as a potential bacteriostatic agent, the inhibitor of thymidylate synthase (Votruba, Holý *et al*. 1973), and cytidine deaminase (Kim, Marquez *et al*. 1986). Later, zebularine was tested for its anticancer activity in cell lines and considered a promising anticancer drug candidate, but ultimately, the molecule has never entered clinical trials, which was explained by its rapid metabolic degradation in the body (Ganesan, Arimondo *et al*. 2019), although zebularine displays excellent stability in aqueous solutions (estimated as 508 h at pH 7.4 in PBS) (Cheng, Matsen *et al*. 2003).

Zebularine was found to stimulate the regenerative response in mouse ear pinnae. The effect was manifested by over 80% ear hole closure compared to approximately 40% in the controls within 6 weeks post-injury (83.2 ± 9.4% vs 43.6 ± 15.4%). Zebularine was selected for this experiment owing to its low toxicity and established DNA demethylating activity (Sass, Sosnowski *et al*. 2019). To my knowledge, this was the first successful treatment with an epigenetic inhibitor to induce complex tissue regeneration in an animal model. Combined delivery of zebularine with retinoic acid potentiated and accelerated zebularine's regenerative effect, resulting in complete ear hole closure within three weeks after injury. The regenerated tissue architecture resembled that in the normal ear pinna. In response to zebularine treatment, the regenerating ear pinna tissues showed DNA demethylation and activation of pluripotent and neurodevelopmental genes (Sass, Sosnowski *et al*. 2019). The observations are consistent with the concept that DNA demethylating agents promote pluripotency in cell lines, and passive demethylation may preferentially activate pluripotency genes (De Carvalho, You *et al*. 2010, He, Sun *et al*. 2017). It is important that a subsequent independent study described above showed that zebularine promoted healing in an organotypic wound model developed from epithelial cells collected from diabetic patients (Shah, Spektor *et al*. 2023), and the effect was associated with its DNA demethylating activities.

For demethylating activity, zebularine requires several stages of metabolic activation. The first is phosphorylation to zebularine monophosphate by uridine-cytidine kinase, followed by phosphorylation to zebularine diphosphate by nucleoside phosphate kinase, reduction to deoxyzebularine diphosphate by ribonucleotide reductase, and finally phosphorylation to zebularine triphosphate by nucleoside diphosphate kinase. Deoxyzebularine triphosphate is a substrate of DNA polymerase incorporated into DNA during replication, and the incorporated nucleoside acts as an irreversible inhibitor, covalently binding DNA methyltransferases (Sass, Sosnowski *et al*. 2019). Zebularine has a mechanism of action similar to 5-azacytidine. It is also incorporated into DNA during replication, forming covalent complexes with DNA methyltransferases. This depletes active DNMTs and induces replication-dependent global demethylation and gene reactivation (Orta, Pastor *et al*. 2017). However, zebularine reveals much lower cytotoxicity than 5-azacitidine in both cellular and animal models. For example, the IC_{50} values determined in human bladder carcinoma T24 cells were 17.4 and 120 μM for 5-azacitidine and zebularine, respectively (Ben-Kasus, Ben-Zvi *et al*. 2005). The reported LD_{50} of 5-azacitidine in mice was 2.48 mg/kg i.p. for five days (European Medicines Agency. European public assessment report Vidaza. EMEA/593162/2008; 2008), while no toxicity signs were observed following long-term daily i.p. administration of zebularine at 400 mg/kg for 78 days (Herranz, Martín-Caballero *et al*. 2006). Also, mice receiving seven i.p. zebularine doses at 1000 mg/kg within 10 days of treatment showed weight loss or other adverse effects (Sass, Sosnowski *et al*. 2019). Another significant difference between zebularine and 5-azacitidine is the preferential targeting of cancer cells over normal fibroblasts, as assessed by DNA incorporation, growth inhibition, and DNMT depletion (Cheng, Yoo *et al*. 2004). Interesting effects of zebularine on dermal cells were observed in cultured human keratinocytes (HaCaT) and fibroblasts (46BR.1N). Zebularine slightly stimulated the viability of fibroblasts and keratinocytes after 72 hours at low concentrations of 0.1 and 1.0 μg/ml, respectively, but exerted inhibitory effects at 0.01 μg/ml. A more potent decrease in viability was observed at 10–150 μg/ml concentrations and 50–150 μg/ml for fibroblasts and keratinocytes, respectively (Sass, Sosnowski *et al*. 2019).

While the use of zebularine as a drug promoting tissue regeneration was first discovered in the Laboratory for Regenerative Biotechnology, retinoids' involvement in the regulation of regeneration processes was well recognised, first in amphibian limb

regeneration (Blum and Begemann 2013), then in mammals. Retinoic acid (all-trans retinoic acid), a metabolite of vitamin A (retinol), regulates gene expression at the transcriptional level through its nuclear receptors (RARs). Retinoic acid signalling involves binding to a nuclear RAR, which forms a heterodimer complex with retinoids (Cunningham and Duester 2015). The complex regulates transcription by binding to DNA, which ultimately stimulates a cascade of events that engage transcription coactivators and transcription initiation (Duester 2008, Cunningham and Duester 2015). Retinoic acid modulates development by acting as a distributed signalling element. It performs an essential function in the adult body - it helps maintain epithelial homeostasis, immune functions, brain functions, and spermatogenesis (Cunningham and Duester 2015). Retinoic acid signalling pathways are active during growth, organ development, and regeneration (Maden and Hind 2003). As mentioned previously, retinoic acid regulates limb re-growth after amputation in urodele amphibians (Maden and Hind 2003). In mammals, retinoic acid stimulates alveolar regeneration after injury in adult lungs, which, in principle, lack regenerative capacity (Maden and Hind 2003). It has been shown that retinoic acid can reverse elastosis-induced emphysema in rats following intraperitoneal injections at a dose of 500 μg/kg daily for 10 days. This was observed to correct the function of previously dysregulated Notch, Hedgehog, Wnt, BMP, and TGF-β pathway genes, resulting in the regeneration of the alveolar epithelium (Uniyal, Tyagi *et al*. 2020). Retinoic acid has a distinct effect on the skin. It treats skin cancer, acne, ichthyosis, and psoriasis and reverses skin ageing processes caused by excessive exposure to UV radiation (Lin, Liu *et al*. 2018, Szymański, Skopek *et al*. 2020). *In vitro*, retinoic acid displays toxicity in human dermal fibroblast and keratinocyte cell cultures from neonatal foreskin at concentrations over 6 μM (Varani, Mitra *et al*. 1990). Retinoic acid, approved as a drug under the generic name Tretinoin, is indicated for skin conditions, as listed above, although the molecule is a teratogen (Anisha 2024). It is also an effective drug to treat acute promyelocytic leukaemia, a cancer characterized by abnormal accumulation of immature granulocytes called promyelocytes, where retinoic acid induces differentiation of the immature leukemic promyelocytes into mature granulocytes (Liang, Qiao *et al*. 2021).

A retinoid antagonist, Tazarotene, is an FDA-approved drug indicated for treating skin conditions, including acne vulgaris, plaque psoriasis, and wrinkles. Tazarotene enhances angiogenesis *in vitro* by promoting branching morphogenesis and tubular remodelling.

The proangiogenic phenotype, characterized by the secretion of proangiogenic factors such as hepatocyte growth factors, vascular endothelial growth factors, plasminogen activator, urokinase, and placental growth factor, and reduced secretion of the antiangiogenic factor pentraxin-3 from neighbouring fibroblasts, is mediated by the retinoic acid receptor, but not retinoic acid receptor activation. In an ear-punch wound model in mice, i.p. injected Tazarotene promoted wound closure and growth of mature and functional microvessels and increased blood flow. After wound closure, normal-appearing skin containing new hair follicles and maturing collagen fibres was observed (Zen, Nawrot *et al*. 2016).

5. Hydrogel nanoparticles as drug carriers

Bionanomaterials are molecular structures with nanoscale dimensions - from 1 to 100 nanometers, consisting of biological molecules. Bionanomaterials show physicochemical and biological properties that warrant their use in biomedical applications. They are characterised by small size, large surface area, and the ability to connect to and interact with cells and tissues (Goenka, Sant *et al*. 2014). Bionanomaterials can be used for medical applications as carriers of biologically active substances. Bionanomaterial carriers allow for sustainable drug release and extend the time of action.

Drug delivery by nanocarriers occurs through one of three mechanisms: diffusion, chemical reaction, or solvent activation. In delivery control mediated by chemical reactions, the polymer is degraded by hydrolysis or another chemical reaction to release the drug. The drug can also be attached to the polymer by a covalent bond that can be cleaved by water or an enzyme to release the drug. In the solvent activation mechanism, the drug can be released by swelling of the polymer, where the drug has previously been locked in place in the polymer matrix by an osmotic effect, which can be achieved by water ingress from outside into the drug delivery system due to the osmotic driving force and then pushing out the drug from the system (Langer and Peppas 2003).

Hydrogel nanoparticles were proposed as one of the most promising nanoparticle drug delivery systems (Hamidi, Azadi *et al*. 2008, Thoniyot, Tan *et al*. 2015, Basso, Miranda *et al*. 2018, Hsu, Wu *et al*. 2021). Natural or synthetic polymers are used to produce hydrogels that can be applied for pharmaceutical and biological purposes. Although hydrogels of natural origin have disadvantages - they are more likely to exert

immunogenicity or induce inflammatory reactions due to the presence of immunogens, they still have many advantages. Hydrogels have excellent biocompatibility and biodegradability. Smart hydrogels can respond to environmental stimuli (e.g., heat, pH, light, and ultrasound), allowing *in situ* gelation and controlled drug release, significantly increasing the convenience and efficiency of drug delivery (Sun, Song *et al*. 2019). Moreover, hydrogels have the unique potential to combine the characteristics of extremely high water content systems with the advantages of nanoparticles (Hamidi, Azadi *et al*. 2008).

Several hydrogel nanoparticle systems based on natural and synthetic polymers have been prepared and well-characterized. Among natural polymers, alginate (Hamidi, Azadi *et al*. 2008, Guo and DiPietro 2010) and chitosan (Kato, Onishi *et al*. 2003, Hamidi, Azadi *et al*. 2008) have been widely studied. From the synthetic group, hydrogel nanoparticles based on poly(Coşkun, Karaca *et al*. 2014), poly(ethylene oxide), poly(ethyleneimine), poly(vinylpyrrolidone), poly(ethylene glycol) have been the most researched carriers (Kato, Onishi *et al*. 2003).

New hydrogel drug delivery systems are still being researched, often combining two or more already available hydrogels. For example, Hsu *et al*. designed a complex drug delivery system consisting of drug-loaded poly(lactide-co-glycolide) (PLGA) nanoparticles and chemically cross-linked hyaluronic hydrogel. The active substance was a protein drug, bevacizumab, against vascular endothelial growth factor (anti-VEGF), which is used to treat diseases of the back of the eye. Standard therapy involves monthly anti-VEGF injections, which can lead to complications due to frequent dosing. It has been shown that the designed composite can release the drug for over two months under physiological conditions and further improves the bioavailability of drugs by penetrating deep into the layers of the retina (Hsu, Wu *et al*. 2021).

5.1 Alginates as drug carriers

5.1.1 Characteristics of alginate

Alginate is a naturally hydrophilic polymer derived from brown algae. Alginic acid is an anionic biopolymer consisting of linear chains of alpha-L-glucuronic acid (G) and beta-D-mannuronic acid (M) (Fig. 4). The chemical composition of alginates depends on their origin because of the molecular weight (Mw), configuration (distribution in the polymer chain), and proportion of these two monomers (M to G

ratio), which vary significantly depending on the algae species and the place of collection. The M monomer is responsible for flexibility, and the G monomer ensures the structure's stiffness.

Its characteristic properties are high water solubility, a tendency to form gels with high porosity, biocompatibility and non-toxicity. Sequential cross-linking and the formation of polymer networks, upon addition of counterions to the alginate, like calcium ions, results in the development of hydrogel-structured drug delivery vehicles such as micro- and nanoparticles (Hamidi, Azadi *et al*. 2008).

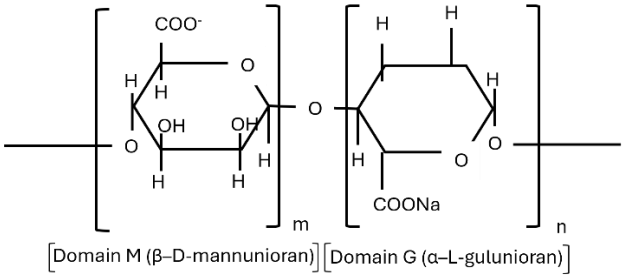

Figure 4 Chemical structure of sodium alginate

5.1.2 Alginate gelling

One of the most important functional properties of alginate is Ca^{2+}-induced gelation. Alginate also forms gels with many other mono-, di-, or trivalent cations, and their gelation may exhibit mechanisms other than Ca^{2+}-induced gelation. The resulting gels also exhibit different properties that lead to various applications. The molecular weight of alginate ranges from 32 to 400 kDa depending on its source, species, or extraction process. The molecular weight of alginate can significantly affect its gelling properties, including swelling, shrinkage, mechanical stiffness, and resistance to monovalent cation interference. Alginate with a higher molecular weight always shows a faster gelation rate, significantly increased gel and fracture strength, and increased elasticity and viscosity compared to alginate with a lower molecular weight. Moreover, the strength of alginate gels increases with increasing molecular weight when the average molecular weight is less than 240 kDa (intrinsic viscosity below 4.8 dl/g). If the molecular weight exceeds 240 kDa, it has a negligible effect on the gel strength (Hu, Lu *et al*. 2021).

As mentioned above, alginate is soluble in water but insoluble in organic solvents. When alginate is dissolved in water, a viscous sol is formed, the volume of

which can increase ten times when water is absorbed. The viscosity of the alginate solution depends on the concentration and degree of polymerization. The solubility of alginate generally increases with increasing ionic strength of the system (except for gelling ions) because high ionic strength can cause reducing the volume of the polymer due to the electrostatic shielding effect and reduced chain winding and viscosity of the system. An aqueous solvent free of cross-linking ions is necessary for dissolution because alginate can form gels in the presence of different gelling cations such as Ca^{2+}, Ba^{2+}, Sr^{2+}, and Cu^{2+}. Moreover, alginate with protonated carboxylic acid groups cannot be thoroughly dispersed in any solvent, including aqueous systems (Hu, Lu *et al*. 2021). Ion-induced alginate gels are formed mainly due to electrostatic interactions between negatively charged carboxyl groups in alginate molecules and positively charged cations, which leads to the formation of polyelectrolyte complexes. Different ion-induced alginate gels may have different properties and gelation properties (Hu, Lu *et al*. 2021). Cross-linking alginate with divalent cations significantly increases its physical stability in aqueous solutions and physiological saline, as shown by the aspect shape factor (Moya, Morley *et al*. 2012).

5.1.3 Kinetics of molecules release from alginate gels

The kinetics of small molecules release from alginate gels can be controlled by regulating drug-alginate interactions. When there is no chemical interaction between drug and polymer, release depends primarily on the charge polarity of the molecule. Hydrophilic molecules can diffuse rapidly, while the hydrophobic ones diffuse slowly (Augst, Kong *et al*. 2006), if any.

5.1.4 Alginate toxicity

Research on the toxicity of sodium alginate dates back to the 1940s. Arora *et al.* showed that the lowest lethal dose, causing haemorrhage, of intraperitoneally administered sodium alginate in mice was 500 mg/kg, but no mortality was observed at a dose of 250 mg/kg (Arora, Chaudhury *et al*. 1968). However, intravenous injections of sodium alginate at a dose of 200-500 mg/kg caused the death of mice within 1 minute to 12 hours (Solandt 1941). In rabbits, the lethal dose of intravenous injections of sodium alginate was determined as 100 mg/kg (data: FAO Nutrition Meetings Report Series., 53A(381), 1974). In cats, intraperitoneal and intravenous injections of sodium alginate at a dose of 250 mg/kg resulted in death within 1 day after intraperitoneal injection and within 2 days after intravenous injection. Brain, liver, and kidney damage was also

observed (Chenoweth 1948). However, the purity of the alginate materials used in the experiments remains unknown, and the observed toxicity might have resulted from contamination. Nowadays, the commercially available alginates marketed as bioreagents are likely to display much lower toxicity. No toxicity was reported in mice following oral administration of alginate. One of the highest-reported doses of alginate administered orally to mice was 5000 mg/kg calcium alginate hydroxyapatite (Hanh, Bich *et al*. 2019).

5.1.5 Alginate biocompatibility

The issue of alginate biocompatibility has already been widely researched, but individual reports are contradictory. It has been proven that when administered intravenously, most commercially available alginates induce a foreign body reaction, leading to fibrosis tissue, such as the liver, rectum, and parietal peritoneum. However, other reports indicate little or no immune response around alginate implants (Martău, Mihai *et al*. 2019). The biocompatibility of alginate has been confirmed *in vivo* studies after ocular administration (Lin, Sung *et al*. 2004), orally (Sosnik 2014), and also in numerous local administrations (Becker, Preul *et al*. 2007, Vériter, Mergen *et al*. 2010, Jayant, McShane *et al*. 2011, Coşkun, Karaca *et al*. 2014). The study by Jayant *et al*. aimed to develop nanoengineered alginate microspheres for local delivery of anti-inflammatory drugs to an implantable glucose biosensor. Biocompatibility was tested *in vitro* using the L929 murine fibroblast cell line and *in vivo* in rats where the test microspheres were dorsally injected. *In vivo* studies have shown that the combined approach of drug-containing carriers with an implanted biosensor is promising for improving the biocompatibility of sensors (Jayant, McShane *et al*. 2011). Becker *et al*. assessed calcium alginate's biocompatibility and *in vivo* stability in porcine aneurysms. Only a minor bioactive response to the alginate gel was observed. No degenerative or inflammatory reaction was observed. The alginate was surrounded by moderate fibrous tissue. Complete filling of the aneurysm with calcium alginate has been shown to provide stability, biocompatibility, and optimal healing in pigs (Becker, Preul *et al*. 2007).

Typically, alginates are available after purification by free-flow electrophoresis and do not cause foreign body reactions at least three weeks after implantation in the peritoneal cavity of rodents. The immunogenic response to intravenous injection may be due to impurities present in the materials (Martău, Mihai *et al*. 2019). The Food and

Drug Administration has classified several alginate salts (calcium, sodium, ammonium, and potassium), as well as propylene glycol alginate derivatives, as Generally Recognized as Safe (GRAS) ingredients for oral administration (Szekalska, Puciłowska *et al*. 2016, Cattelan, Guerrero Gerbolés *et al*. 2020). Noteworthy, alginate has been described as a non-thrombotic material. Therefore, it may be a candidate for cardiac applications such as tissue engineering of heart valves (Liberski 2016).

Experiments in cellular models support the opinion of alginate biocompatibility and high safety profile. The human cell line of HaCaT keratinocytes and 46BR.1N fibroblasts showed no cytotoxic effects and no reduction in viability under exposure to pure sodium alginate extract (Słonimska, Baczyński-Keller *et al*. 2024). Sodium alginate was even observed to moderate drug cytotoxicity in HaCaT cells (Słonimska, Baczyński-Keller *et al*. 2024).

5.1.6 Alginate degradation and elimination from the organism

Following oral administration, the digestive system does not entirely absorb alginate. Alginate preparations react with gastric acid to undergo ionic gelation, creating alginate gel, which may additionally slow down gastric emptying, stimulate gastric stretch receptors, reduce the absorption of nutrients in the intestines, and influence the glycemic response (Dettmar, Strugala *et al*. 2011). In the case of other administration routes, alginate degradation and elimination from the body is poorly recognised, and few studies have addressed this issue. It is known that mammals lack an alginase, a specific enzyme hydrolyzing alginate polymers.

While depolymerization of alginate with a specific enzyme in the body remains unknown, another way of degradation may be considered. As *in vitro* studies suggested, alginate polymer degradation may be mediated by oxidation. Alginate hydrogels dissolve uncontrollably following the loss of divalent cations into the surrounding medium. After the dissolution, they release threads of relatively high molecular weight. Oxidation of alginate with periodate cleaves the carbon-carbon bond of the cis-diol group at the uronate residue and changes the conformation of the chain. This allows the alginate polymers to be hydrolyzed in aqueous solutions (Bouhadir, Lee *et al*. 2001). It has been shown that the degradation rate of alginate polymer can be controlled by changing the degree of oxidation with varying amounts of sodium metaperiodate (Balakrishnan and Jayakrishnan 2005, Gao, Liu *et al*. 2009). The degradation behaviour

of hydrogels was assessed by monitoring changes in molecular weight and mass loss with time. It was found that the course of degradation depended mainly on the degree of oxidation (Gao, Liu *et al*. 2009, Gao, Fan *et al*. 2021).

Eliminating alginate from the body depends on its molecular weight. Twenty-four hours after intravenous administration of low molecular weight alginate (less than 48 kDa) to male Wistar rats, it was excreted in urine. In contrast, a more significant fraction of the polymer remained in the circulation and did not readily accumulate in tissues. In the case of intraperitoneal administration, almost the entire administered dose of alginate was transferred from the peritoneal cavity into the blood within 24 hours, and the low molecular weight polymer fraction was excreted in the urine. After subcutaneous administration, 70% of the injected dose remained at the injection site for 24 hours (Al-Shamkhani and Duncan 1995). The available data on alginate elimination from the organism are limited to a single model and 24-hour observations. Nevertheless, the results indicate that alginate elimination is more likely to occur following the reduction in polymer length.

Experiments with alginate implants provide additional clues on alginate stability in the body. The half-life of alginate hydrogel in the rat hip has been estimated to be about 4 days, while in the rat myocardium, it is estimated to be 6 to 8 days (Shkand, Chizh *et al*. 2016). This study developed a new absorbable biomaterial consisting of a calcium cross-linked alginate, which exhibits low viscosity and undergoes a phase transition to a hydrogel upon injection into the infarct. Calcium cross-linked biotin-labelled alginate was injected into the infarct 7 days after anterior myocardial infarction in the rat to examine the biomaterial effect after the injury. Serial histological examinations showed the formation of an in situ alginate hydrogel implant, which occupied up to 50% of the scar surface. The biomaterial was replaced by connective tissue within 6 weeks. Two months after injection, microscopic examination of sections from the hearts revealed no trace of alginate at the injection site (Landa, Miller *et al*. 2008).

5.1.7 Antihypertensive effect of alginate

Another interesting property characteristic of alginate is a marked antihypertensive effect observed after subcutaneous administration of very low molecular weight sodium alginate in Alzet pumps (Moriya, Shida *et al*. 2013). It affects

salt-induced hypertension in Dahl S rats without affecting sodium transport in faeces and urine. Dahl S rats are susceptible to kidney damage in salt-induced hypertension. The reduction in blood pressure was probably related to decreased urinary protein excretion with the morphological attenuation of glomerulosclerosis. The level of urinary protein excretion in rats treated with sodium alginate was significantly lower than in the untreated animals. At least two mechanisms explaining the antihypertensive alginate effects were proposed: inhibition/delay of sodium absorption in the intestine and direct vasodilator effect (Moriya, Shida *et al*. 2013). While the sodium level excreted in the faeces did not change during the experiment, the alginate treatment completely abolished the increase in blood pressure, thus indicating that the antihypertensive effect was not mediated by inhibition/delay of intestinal sodium absorption. Moreover, no differences were found in the sodium level in urine between rats administered alginate and rats from the control group during the treatment, which suggests that the antihypertensive effects of sodium alginate were not due to reduced salt loading. Consequently, the alginate antihypertensive effect was attributed to the nervous system's adrenergic action or endothelial cell function (Moriya, Shida *et al*. 2013). Independent of the mechanism of action, the data indicate that alginate carriers, though well-tolerated in the body, can have a significant biological impact on its function.

5.1.8 Mucoadhesive properties of alginate

Alginate, though not absorbed after oral administration, may influence gut microflora and intestinal uptake of drugs and nutrients owing to its mucoadhesive properties. The mucoadhesive properties of alginate may aid in its suitability as a potential prebiotic, prebiotic bacteria, or drug carrier for mucosal tissues such as the gastrointestinal tract. Alginate has been shown to have the highest mucoadhesive strength compared to chitosan, carboxymethyl cellulose, and lactic acid. Due to the adhesion of alginate particles to mucosal tissues, the protein transit time is prolonged, and probiotic microorganisms or a specific drug may deposit on the absorbent surfaces. This may improve the bioavailability and effectiveness of probiotics or drugs (Martău, Mihai *et al*. 2019).

Studies were carried out to examine the protective effect of sodium alginate on the intestinal microflora, immunity, and barrier function of the intestinal mucosa in BALB/c mice with reduced immunity induced by cyclophosphamide. In the experiment, sodium alginate was dissolved in 0.2 ml of distilled water and administered to mice by oral

gavage at a dose of 50 mg/kg/day or 250 mg/kg/day for 28 days. At both doses, sodium alginate was shown to alleviate splenic tissue damage and restore impaired immune functions, such as an increase in the immune organ index, a decrease in splenic T lymphocytes, and a significant increase in serum immunoglobulin and cytokine secretion in immunocompromised mice. Moreover, the treatment reversed intestinal mucosa damage and improved intestinal permeability (Huang, Fisher *et al*. 2010).

5.2 Examples of alginate applications in medicine and biomedical research

Several commercial alginate-based products exist, including medical preparations, mainly used to treat heartburn, gastroesophageal reflux, and hyperacidity. Examples of such pharmaceutical products are Gaviscon for protecting the gastric and oesophagal mucosa, Rennie Antacidum used to treat the symptoms of reflux and hyperacidity, Maalox Plus used against heartburn and reflux, and Agicid to treat the symptoms of reflux. Many more advanced alginate applications are under research or clinical trials in diverse medical fields.

- In wound dressings

Dressings with calcium alginate combined with silver were reported to be safe and effective in the treatment of leg ulcers (clinical trial identifier NCT01396304).

- In medicines to treat early gastroenterological tumours, polyps, and fistulas

Sodium alginate mixed with calcium lactate (Gut Guarding Gel) is currently under investigation for mucosal elevation capacity and safety in supporting endoscopic submucosal dissection in the treatment of early gastroenterological tumours and polyps (clinical trial identifier NCT03321396). Calcium alginate is also being investigated for feasibility and safety as a gastrointestinal injection for treating complex cryptoglandular fistulas (clinical trial identifier NCT04740086).

- Drug and cell encapsulation

Alginate is being clinically investigated for β-cell islet encapsulation in the treatment of type I diabetes DIABECELL®, where alginate microcapsules are delivered intraperitoneally (clinical trial identifiers NCT00940173, NCT01736228, NCT01739829), for choroid plexus cell encapsulation in Parkinson's disease NTCELL® (alginate microcapsules are introduced intracranially by stereotactic insertion into the brain under guidance by neuroimaging, clinical trial identifier

NCT01734733), for encapsulation of glucagon peptide-1 (GLP-1)-transfected mesenchymal cells for the treatment of space-occupying intracerebral haemorrhage (GLP-1 CellBeads® alginate microcapsules delivery, by implantation into brain tissue cavity after surgical evacuation of the hematoma, clinical trial identifier NCT01298830) (Ruvinov and Cohen 2016).

Alginate is used in many tissue engineering approaches. As it lacks functionality through interactions with cells and proteins, combining it with other polymers can be effective. Hyaluronan, the main component of glycosaminoglycans, provides CD44-specific interactions with chondrocytes but typically requires chemical cross-linkers to form hydrogels, which may cause unexpected side effects in the body. Park *et al.* proposed a hybrid structure of alginate and valuable hyaluronan for cartilage regeneration. Alginate was used as the framework, and low molecular weight hyaluronan was incorporated into the framework to produce an ethylenediamine-conjugated alginate-hyaluronate hybrid. The prepared hydrogels have proven helpful for effectively regulating chondrogenic differentiation and maintaining the chondrocyte cell phenotype, which may lead to applications in cartilage regeneration (Park, Lee *et al*. 2017).

Alginate can also be used in soft tissue reconstruction. Halberstadt *et al.* created macroporous hydrogel fragments by using unmodified alginate or alginate covalently linked to the fibronectin cell adhesion peptide. They injected these materials subcutaneously into adult female domesticated sheep. Histological tests performed after one and three months showed that the subcutaneous alginate implants supported the growth of tissues and vessels. Minimal inflammatory reaction and peri-implant capsule formation were observed, and the implanted materials maintained their size over the three-month study period (Halberstadt, Austin *et al*. 2002).

Alginate-based Algisyl-LVRTM alginate hydrogel implants were injected into patients with dilated cardiomyopathy in an open chest procedure (clinical trial identifier NCT00847964). The injection mixture was created by combining a separately prepared aqueous solution of sodium alginate (supplemented with 4.6% mannitol) with a calcium-cross-linked alginate hydrogel (supplemented with 4.6% mannitol) immediately before use. A 28% improvement in ventricular ejection fraction was noted over a 24-month follow-up. The continued improvement over this period suggests that

the beneficial reverse ventricular remodelling is maintained long-term after Algisyl-LVR implantation (Lee, Hinson *et al*. 2015).

Alginate has been used as a carrier for a histone deacetylase inhibitor, Vorinostat, to treat kidney diseases, especially acute kidney injury. The currently available HDAC inhibitors cannot be appropriately delivered to the kidneys because of poor solubility in aqueous solutions. Zhang *et al*. proposed calcium alginate (Ca-ALG) microspheres as microcarriers for the delivery of HDAC inhibitors. *In vivo* results showed that Ca-ALG microspheres containing HDAC inhibitors could effectively reduce the regional renal inflammatory response and macrophage infiltration (Zhang, Wang *et al*. 2020).

The above examples demonstrate the potential of alginate as a clinically applicable substance. Alginate is safe and suitable for injection, as evidenced by its numerous applications. However, there are no registered studies yet using alginate as a subcutaneously injectable carrier of small-molecule drugs. Using sodium alginate in this doctoral thesis as a carrier of low-molecular-weight active substances is a new and unique approach.

6. Materials and methods

6.1 Experiments in an animal model

6.1.1 Formulations

Alginate formulations

Sodium alginate solution was prepared by suspending 20 mg of sodium alginate (Merck, Cat. No. 71238-250G, BCCD8789) in 1 ml of water and then processing it in a bead mill homogenizer (Bead Ruptor Elite Omni International) using porcelain beads with a diameter of 2 mm at room temperature in 3 30s-cycles at 4 m/s interrupted with 10-s breaks. The measured pH of the prepared sodium alginate solution was 6.0. According to literature data on the reagent, the weight-average molar mass (Mw) and the number-average molar mass (Mn) were determined as 427 and 186 kDa, respectively, classifying the material as alginate of high viscosity, whereas the mannuronic and guluronic acid contents were determined as 39.6 and 60.4%, respectively, corresponding to an M/G ratio of 0.7, ranking the material among the alginates with the highest guluronic acid content (Gorroñogoitia, Urtaza *et al*. 2022). Drug-alginate formulations were obtained by adding 4 mg of all-trans-retinoic acid (TCI, Cat. No. R0064) or 240 mg zebularine (TCI, Cat. No. Z0022) per 1 ml of sodium alginate solution, followed by bead mill homogenising performed as described above. The Ca^{2+}-crosslinked alginate hydrogels were prepared by adding 10 µl of 7 M $CaCl_2$ to 1 ml of 2% sodium alginate solution, followed by bead mill homogenizing, as detailed above.

Chitosan formulations

Chitosan preparations were provided by Dr. Szymon Mania from the team of Prof. Robert Tylingo at the Department of Food Chemistry, Technology and Biotechnology, Gdańsk University of Technology. Medium molecular weight (MMW) chitosan (Merck, Cat. No. 448869-50G) was dissolved (0.75% w/v) in carbonic acid under mechanical stirring at 300 rpm (RA 2020, Heidolph Instruments GmbH & Co. KG, Kelheim, Germany) at 25ºC (Mania, Partyka *et al*. 2019, Banach-Kopeć, Mania *et al*. 2022). Drug-chitosan formulations were obtained by adding 4 mg of all-trans-retinoic acid (TCI, Cat. No. R0064) or 240 mg zebularine (TCI, Cat. No. Z0022) per 1

ml of chitosan solution, followed by bead mill homogenising performed as described above.

6.1.2 Animals

The experiments were performed on 8 to 10-week-old females of the BALB/c mouse strain. The animals were purchased from the Tri-City Academic Laboratory Animal Centre, where they were maintained. Mice were anaesthetised with isoflurane using SomnoSuite Small Animal Anesthesia System (Kent Scientific Corporation). The animals were first in a chamber where the isoflurane flow was MinVol = 498 mL/min; they were then transferred to the mask where the isoflurane flow was MinVol: 29 mL/min. Through-and-through holes of 2-mm diameter were made in the ear pinna centre using a scissor-style ear punch (Hammacher Solingen; LOT FTC-15/8670/1). Prior to treatment, the animals were randomised into groups of six. Each group was given subcutaneous injections of sodium alginate solution (400 µl) with zebularine, retinoic acid, or both, or the *vehicle* alone immediately after wounding (d0) and on day 10 post-injury (d10). In the groups in which chitosan was tested as a carrier, the following were given analogously subcutaneous injections of chitosan solution (400 µl) with zebularine, retinoic acid, or both, or the *vehicle* alone immediately after wounding (d0) and on day 10 post-injury (d10). The protocol for animal experiments was approved by the Local Ethics Committee for Animal Experimentation in Bydgoszcz (approval no. 51/2020). The progress of wound closure was photographed weekly for 6 weeks, followed by the computer-assisted analysis of photographic documentation with ImageJ (ver. 1.52a) (Schneider, Rasband *et al*. 2012).

6.1.3 Ultrasound examination

An ultrasound examination was performed to check the degree and rate of degradation of the alginate under the skin of mice. The experiments were performed in the Department of Biochemistry (Faculty of Medicine, Medical University of Gdańsk) using Vinno6 VET (VINNO Technology, Suzhou, China) and a 21 MHz linear probe with the technical assistance of Msc. Oliwia Król and under the supervision of Prof. Ryszard T. Smoleński. During the measurements, the mice were anaesthetised with isoflurane. Measurements were performed immediately after injection of the tested formulations and on days 7, 14, 21, 28, 35 and 42. The experiment involved 3 mice that received zebularine (48 mg per 200 µl of sodium alginate solution) and retinoic acid (0.

8 per 200 µl of sodium alginate solution), 3 control mice that received 400 µl of the alginate vehicle alone, and 3 mice not subjected to injections as an additional reference. The ultrasound images from the area covering the nape and scapulae exported as tiff files were scaled and transformed to 8-bit format using ImageJ ver. 1.52a (Schneider, Rasband *et al*. 2012). Next, the images were converted to binary masks using the intensity auto threshold. The regions of interest for signal quantification were selected based on the images of non-injected controls to cut off the non-specific signals from the ultrasound probe. Five to eight images per mouse per time point were used for the computations. Image processing support was provided by Dr. Rafał Płatek from the Laboratory for Regenerative Biotechnology, Gdańsk University of Technology.

6.2 Molecular analyses

6.2.1 Tissue collection

The punched-out ear pinna discs were collected immediately after the injury. Prior to tissue collection, the animals were euthanised in a CO_2 chamber. Ear pinnae were collected at 7, 14, 21 and 42 days post-injury from 3 treatment mice and 3 mice of the control groups for each time point. Immediately after collection, the ear pinnae were placed in liquid nitrogen and stored at -80˚C. For RNA extraction, tissue samples were collected as follows: the rings surrounding wounds were excised with a 3-mm and 5-mm biopsy punch and discs from the uninjured part of the ear pinna were excised with 3-mm biopsy punch (Fig. 11).

6.2.2 Gene expression

6.2.2.1 Nucleic acid extraction

Total RNA from mouse ear pinna tissues was extracted using an RNeasy Mini Kit (Qiagen, Cat No. 74104) according to the manufacturer's instructions. The determination of RNA concentration in the tested samples was carried out using a spectrophotometer NanoDrop2000 (Thermo Scientific).

6.2.2.2 Determination of transcripts levels

The templates to determine transcript levels were obtained by cDNA synthesis performed in a reaction mix containing (80-120 ng of RNA), 100 picomoles of oligo dT_{20}, 4 µl of 5x reaction buffer (250 mM Tris-HCl, 375 mM KCl, 15 mM $MgCl_2$, 50 mM DTT), and 200 units of Maxima Reverse Transcriptase (ThermoScientific, Cat.No.

EP0742) in a final volume of 20 µl. Real-time PCR reactions were carried out in a final volume of 10 µl containing 5 µl of FastStart Essential DNA Green Master (Roche, Cat. No. 06402712001), 2 µl of cDNA, and 0.25 µl each of forward and reverse primers (10 µM) on a LightCycler LC96 (Roche). The temperature profiles of real-time PCR reactions are presented in Table 1. The transcript levels were calculated using the 2^{-dCt} method relative to reference genes *Tbp* and *Gapdh*. In the 2^{-dCt} formula, dCt is the difference between the cycle in which the amplification enters the exponential phase for the analysed transcript and the reference gene. The primer sequences are listed in Table 2. qPCR reactions were performed in triplicate.

Table 1 PCR temperature profile.

Reaction stage	Temperature [°C]	Time [s]	Number of cycles
Initial denaturation	95	600	1
Amplification	95	10	38
	70°C for the first 10 cycles, 60°C for the remaining cycles	10	
	72	10	
DNA melting	95	10	1
	65	60	
	97	1	

6.2.2.3 Primer design

The primer sequences were designed based on the nucleotide transcript sequences deposited in the National Center for Biotechnology Information database (https://www.ncbi.nlm.nih.gov/gene). The specificities of the primers were confirmed using the Primer-BLAST tool (https://www.ncbi.nlm.nih.gov/tools/primer-blast/), the secondary structures were analyzed using the Biosoft NetPrimer program (https://www.premierbiosoft.com/netprimer). The designed primer nucleotide sequences are listed in Table 2.

Table 2 PCR primer nucleotide sequences.

Gene	**Forward primer**	**Reverse primer**	**Amplicon size [bp]**
Acta2	AAGAGCTACGAACTGCCTGACG	GTTTCGTGGATGCCCGCTGA	119
Ccl11	GAATCACCAACAACAGATGCAC	ATCCTGGACCCACTTCTTCTT	98
Ccl3	GTGTAGAGCAGGGGCTTGAG	AGTCCCTCGATGTGGCTACT	97
Ccn2	TGAGGCTGAGTCCAGCTGTTCTTT	ACTTGCCACAAGCTGTCCAGTCTA	118
Egf	GCTCCGTCCGTCTTATCAGG	TGAGAAGTTCGGGGTCAGGA	249
Fbxo15	GCAGCGAGGGTCACTTCA	CTGCGTACTTCCTGACCCAA	317
Fgf1	ACACCGACGGGCTTTTATACG	CCCATTCTTCTTGAGGCCAAC	143
Gdnf	CGCCGCCAATATGCCTGAA	GCCGCTTGTTTATCTGGTGACCTTTT	105
Grem1	AAGGCACTTCCTGTTACTCTGC	TACGACTGAGATGTCAGGGAGA	256
Gsk3b	GAGCCACTGATTACACGTCCAG	CCAACTGATCCACACCACTGTC	111
Il13ra2	GAGGACCCATTCCACCAAGG	CATGGAGGCTCTTCCCAACA	223
Il4	CAACCCCCAGCTAGTTGTCA	TGTCGCATCCGTGGATATGG	71
Klf4	AAGGATCTCGGGCAATCTGG	CATGTCAGACTCGCCAGGTG	162
Lrp5	ACGTCCCGTAAGGTTCTCTTC	GCCAGTAAATGTCGGAGTCTAC	172
Lrp6	TGCAAACAGACGGGACTTGAG	CGGGGACAATAATCCAGAAACAA	217
Myc	CTTTCCCTACCCGCTCAAC	GCCTCTTCTCCACAGACACC	227
Nanog	TACCTCAGCCTCCAGCAGAT	CCAGATGCGTTCACCAGATA	221
Neurog1	AGATGAGCCCCTGAAGACGA	AATGCATGAAGCCCACTCCT	150
Pou5f1	GGAGAAGTGGGTGGAGGAAG	TGATTGGCGATGTGAGTGAT	186
Prrx1	CCCGGATGCTTTTGTTCGAGA	CATGTGGCAGAATAAGTAGCCAT	345
Reno1	GACACCCCTCTTTGGGATCG	CGTCCTGGGCTGGACATAAG	73
Sfrp2	CTAGTAGCGACCACCTCCTG	GCACGGATTTCTTCAGGTCC	243

Snai1	AAACCCACTCGGATGTGAAG	GAAGGAGTCCTGGCAGTGAG	184
Sox2	GGGAGAAAGAAGAGGAGAGAGA	CGATTGTTGTGATTAGTTTTTGGA	85
Tac1	ATGAAAATCCTCGTGGCCGT	GTTCTGCATCGCGCTTCTTT	327
Wnt10a	GAGAGAGTGCTTTCGCCTAC	ACCGCAAGCCTTCAGTTTA	92
Wnt11	CAGGATCCCAAGCCAATAAA	GACAGGTAGCGGGTCTTGAG	187
Reference genes			
Tbp	GAGAGCCACGGACAACTGCG	GGGAACTTCACATCACAGCTC	187
Gapdh	TGGCCTTCCGTGTTCCTAC	GAGTTGCTGTTGAAGTCGCA	178

6.2.2.4 Statistical analyses

Statistical significance for two-sample comparisons was determined using the two-tailed Mann-Whitney U test. The Kruskal-Wallis two-tailed test with *post hoc* pair-wise comparisons with the Conover-Iman test and the Bonferroni correction for multiple testing was used for three or more samples. The Friedman test with the post hoc pairwise Nemenyi tests was performed for paired comparisons. The single Grubbs test was applied to detect outliers. The two-tailed Fisher's exact test was carried out to examine the over-representation of positive signals from the *Fbxo15* transcript in tested samples. All computations were performed in XLSTAT (Addinsoft). A significance level of 0.05 was applied. Statistical significance was marked by one, two, or three asterisks indicating * $p < 0.05$, ** $p < 0.01$, or *** $p < 0.001$, respectively.

7. Results and discussion

Alginate formulations with zebularine and retinoic acid

Previous studies conducted in the Laboratory for Regenerative Biotechnology at the Gdańsk University of Technology demonstrated that zebularine activated complex tissue regeneration in adult mice in an ear pinna model. Further, it was shown that the synergistic action of an epigenetic drug (zebularine) and the transcriptional activator - retinoic acid even more effectively induced the regenerative response. The approach defined a new pharmacological regeneration strategy based on the concerted use of epigenetic derepression with transcriptional activation (Sass, Sosnowski *et al*. 2019). However, the treatment required multiple intraperitoneal injections, 7 of zebularine in saline and 6 of retinoic acid in oil, within 11 days. In order to develop treatment options, the regenerative drugs were combined with the potential of the alginate carrier. Specifically, the use of the alginate carrier was expected to allow for gradual drug release, simplify the administration schedule, and enable direct administration to the lesions localized in difficult-to-reach sites.

Hydrophilic zebularine mixed with 2% sodium alginate using a bead mill homogenizer formed a homogeneous suspension, even at very high zebularine contents of up to 240 mg of zebularine per 1 ml of 2% sodium alginate that exceeded almost fivefold the reported solubility of zebularine in aqueous solutions estimated at 50 mg/ml (Sass, Sosnowski *et al*. 2019). Microscopic examination did not reveal zebularine crystals in the alginate preparations (Fig. 5B). However, hydrophobic retinoic acid did not dissolve in sodium alginate solutions. Mixing retinoic acid with 2% sodium alginate solution at a ratio of 4 mg retinoic acid per 1 ml of 2% sodium alginate using a bead mill homogenizer resulted in an even distribution of retinoic acid crystals throughout the mixture volume (Fig. 5C). Such content of retinoic acid in the formulation with sodium alginate by almost five orders of magnitude exceeded the achievable content in aqueous solutions limited by trace solubility of retinoic acid 6 x 10^{-5} mg/ml (Szuts and Harosi 1991).

While most studies report using Ca^{2+}-crosslinked hydrogels (Introduction, section 5.2), the preparations described above were not subjected to gelling. For comparison, tests were performed with Ca^{2+}-cross-linked alginate hydrogels. The preparations obtained

this way rapidly solidified (Fig. 5D) and were unsuitable for injections. Therefore, alginate solutions in water but not alginate hydrogels were applied as the carrier.

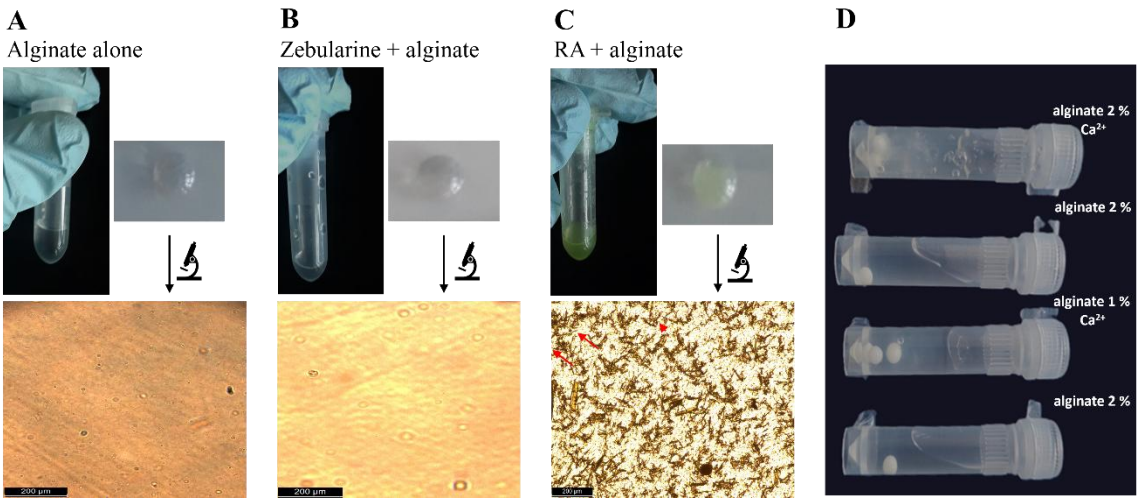

Figure 5 Alginate formulations of zebularine and retinoic acid. ***A*** *- pure 2% sodium alginate, a 200 µl drop placed on a plastic dish (lower) in a tube (higher) and observed under a microscope (bottom);* ***B*** *- zebularine in 2% sodium alginate (240 mg per 1 ml), a 200 µl drop placed on a plastic dish (lower) in a tube (higher); and observed under a microscope (bottom);* ***C*** *- retinoic acid (RA) in 2% sodium alginate (4 mg per 1 ml), a 200 µl drop placed on a plastic dish (lower), in a tube (higher); and observed under a microscope (bottom, red arrows indicate tiny crystals of retinoic acid); calibrator 200 µm;* ***D*** *- comparison of solidified Ca^{2+} crosslinked hydrogels with non-crosslinked injectable solutions of sodium alginate that were used to prepare the formulations with zebularine and retinoic acid (the solidified hydrogels do not flow down).*

Testing the regenerative effect of zebularine and retinoic acid administered subcutaneously in alginate formulations using an ear punch wound model in mice

In order to evaluate the pro-regenerative effect of the alginate formulation of the active substances zebularine and retinoic acid, a series of experiments in an ear pinna punch wound model was performed. It was assumed that the degree of closing the ear pinna punch wounds corresponds to the regenerative effect of the tested preparation (Sosnowski, Sass *et al*. 2022).

The alginate preparations of zebularine and retinoic acid were administered subcutaneously to mice. For comparison, analogous treatments were performed with sodium alginate alone, sodium alginate with zebularine alone, and sodium alginate with retinoic acid alone. The administration was performed immediately after the injury and repeated on the 10th day after the injury. The second injection was applied to sustain the drug level. Each of the drugs tested improved the closure of the excisional through-and-through wound in the ear pinna compared to the control of sodium alginate alone (Fig. 6).

Statistically significant improvements in ear hole closure were determined for three tested formulations. On day 21 post-injury, maximal wound closure was observed for the combination of zebularine and retinoic acid (71.1%, $p = 0.0005$ vs alginate control), while for zebularine alone, the closure reached (64.8%, $p = 0.03$ vs alginate control). The treatment with retinoic acid alone achieved a statistically significant effect on day 14 (62.4%, $p = 0.006$ vs. alginate control), followed by a decline in the subsequent time points (Fig. 6A). The combined treatment of zebularine and retinoic acid showed statistically significant effects at all time points. The effect of retinoic acid alone was significant only on days 7 and 14, while that of zebularine alone on days 14, 21, 28 and 42 compared to the control. These observations demonstrate that retinoic acid synergistically enhances the regenerative effect of zebularine. Doubling the dose of zebularine increased the regenerative response to 73.35%±8.06% (Fig. 7).

The experiments in an ear pinna model showed that 2% sodium alginate was an effective carrier for both the hydrophilic zebularine, which dissolved, forming a homogeneous mixture, and the hydrophobic retinoic acid, which is practically insoluble in aqueous solutions.

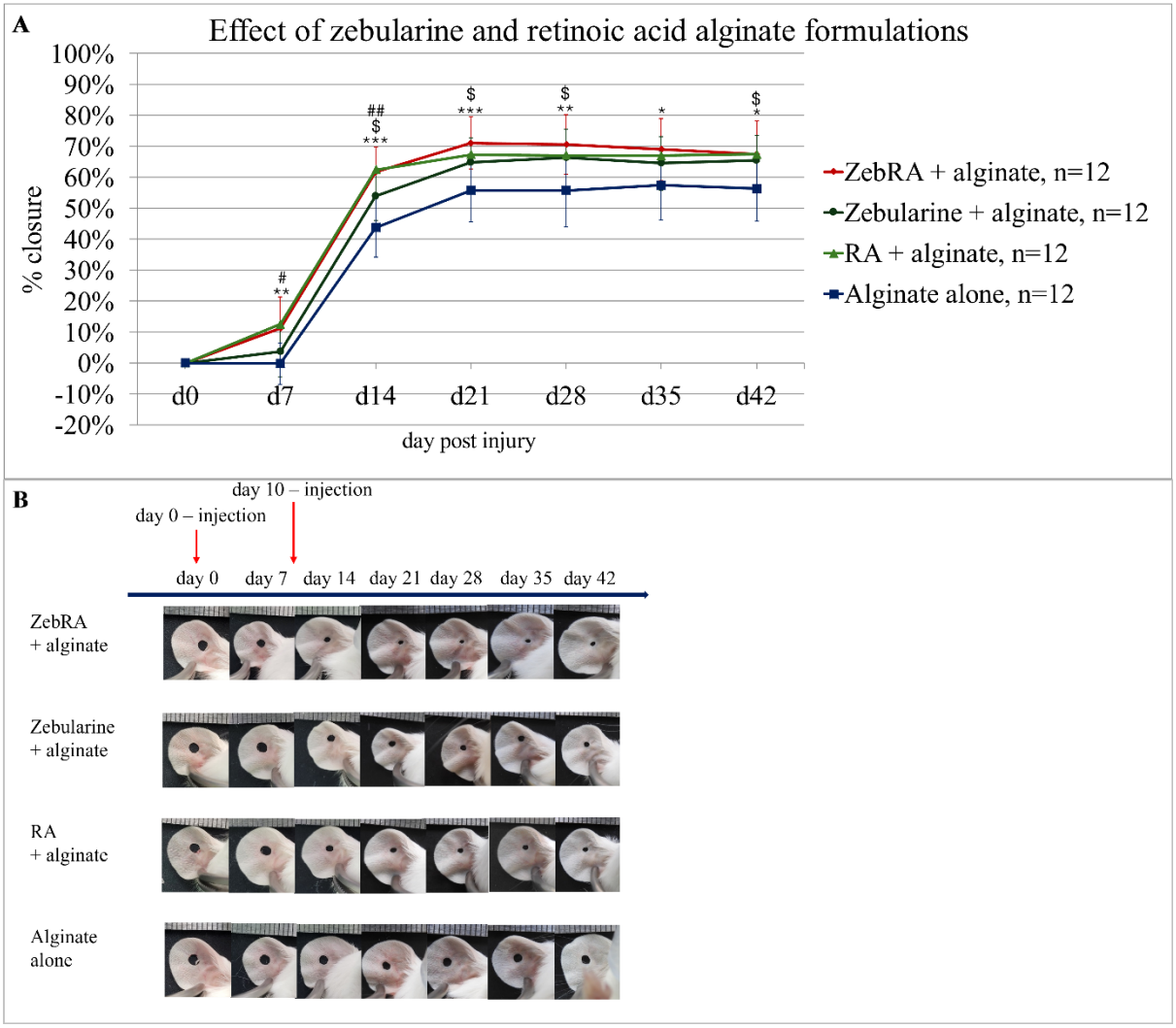

*Figure 6 Progress of ear pinna hole closure in mice treated with the formulations of zebularine and retinoic acid in 2% sodium alginate – **A** - mean percentages of ear hole closure for six-mice experimental groups (n=12 ears) receiving subcutaneous injections of alginate formulations on days 0 and 10 post-injury; error bars represent standard deviation. **B** - representative photographs of ear pinnae. The treatments were designated as follows: ZebRA + alginate - 48 mg of zebularine in 200 µl of 2% sodium alginate + 0.8 mg of retinoic acid in 200 µl of 2% sodium alginate; Zebularine + alginate - 48 mg of zebularine in 200 µl of 2% sodium alginate + 200 µl of 2% sodium alginate; RA + alginate 0.8 mg of retinoic in 200 µl of 2% sodium alginate + 200 µl of 2% sodium alginate; Alginate alone - two 200 µl portions of 2% sodium alginate. Statistically significant differences were determined with the two-tailed Mann-Whitney U test and indicated as follows: with asterisks * for ZebRA vs alginate alone, dollar signs $ for zebularine vs alginate alone, hashtags # for RA vs alginate alone. Single, double, and triple signs denote $p < 0.05$, $p < 0.001$, and $p < 0.001$, respectively.* The ruler scale is 1 mm.

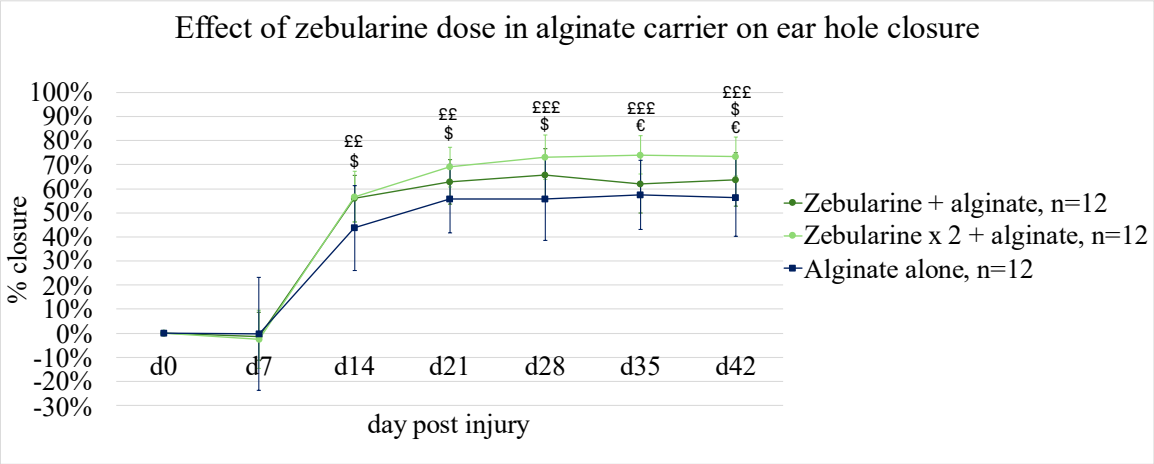

Figure 7 Comparison of different doses of zebularine on ear hole closure. Mean percentages of ear hole closure for six-mice treatment groups (n=12 ears) receiving subcutaneous injections of alginate formulations on days 0 and 10 post-injury; error bars represent standard deviation. The treatments were designated as follows: Zebularine + alginate - 48 mg of zebularine in 200 µl of 2% sodium alginate + 200 µl of 2% sodium alginate; Zebularine x 2 + alginate - doubled zebularine dose, two 200 µl portions of 2% sodium alginate each containing 48 mg of zebularine each; Alginate alone - two 200 µl portions of 2% sodium alginate; Statistically significant differences were determined with the two-tailed Mann-Whitney U test and indicated as follows: with dollar signs $ for Zebularine vs Alginate alone, euro signs € for Zebularine x 2 vs Zebularine (doubled vs single dose), and pound signs £ for Zebularine x 2 vs Alginate alone. Single, double, and triple signs denote $p < 0.05$, $p < 0.001$, and $p < 0.001$, respectively.

Testing the regenerative effect of zebularine and retinoic acid administered subcutaneously in chitosan formulations using an ear punch wound model in mice

A series of experiments were also carried out in which 0.75% chitosan saturated with carbon dioxide was used as a carrier. The preparations were analogous to the formulation with alginate. For comparison, analogous treatments were performed with chitosan alone, chitosan with zebularin alone, and chitosan with retinoic acid alone. The administration was performed immediately after the injury and repeated on the 10th day after the injury. Each of the tested drugs improved the closure of the ear pinna compared to the control group in which chitosan alone was used, similar to the sodium alginate formulation. On day 42-post-injury, statistically significant improvements in ear hole closure were determined for three tested formulations, with zebularine alone (67.9%±5.9%, $p = 0.05$ vs chitosan control), with retinoic acid alone (76.0%±12.5%, $p = 0.007$ vs chitosan control) and with their combination (84.5%±6.5%, $p = 0.00003$ vs chitosan control) compared to the chitosan carrier control (59.0%±12.9%) (Fig. 8).

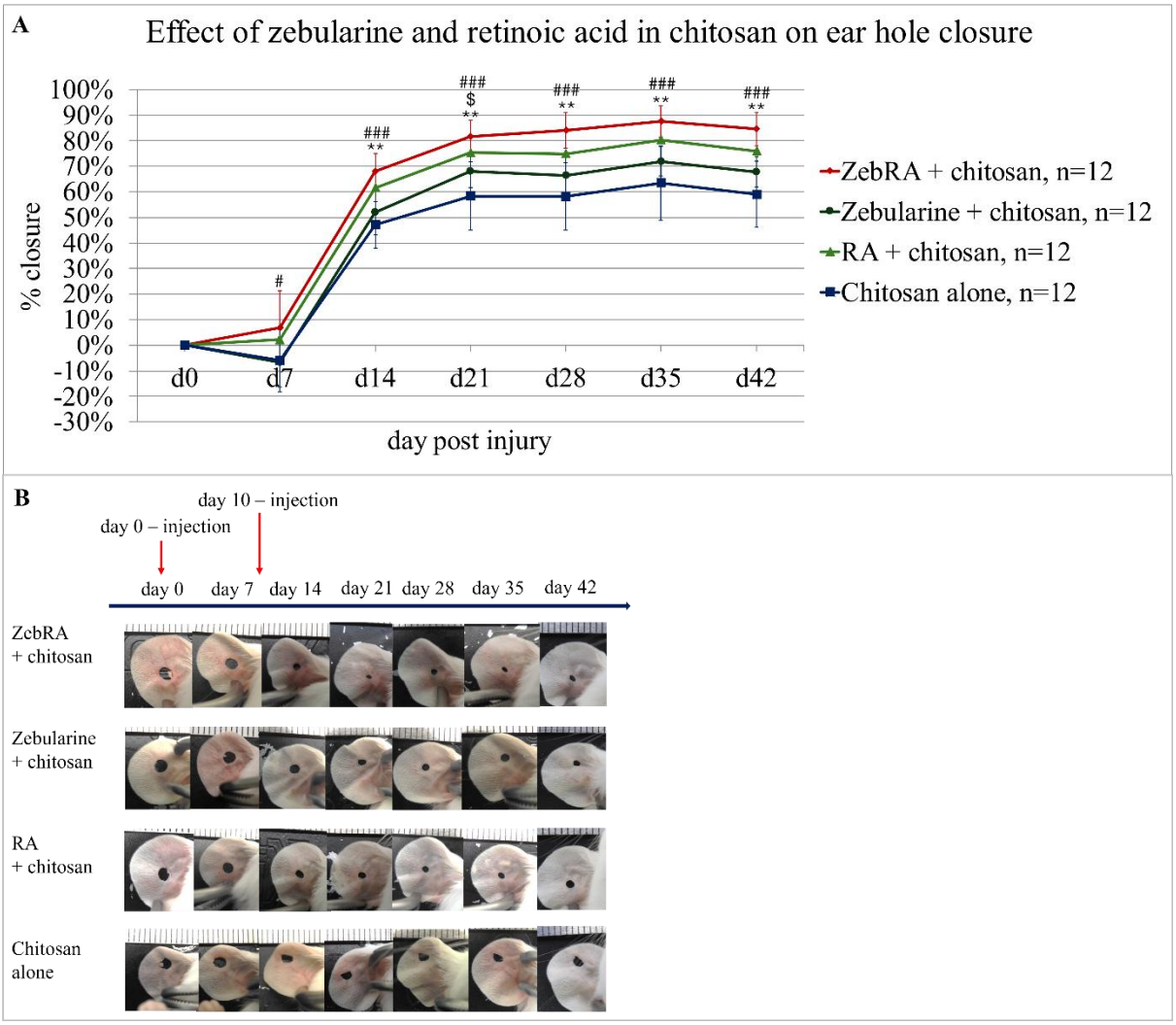

Figure 8 Progress of ear pinna hole closure in mice treated with the formulations of zebularine and retinoic acid in 0.75% chitosan – **A** - mean percentages of ear hole closure for six-mice experimental groups (n=12 ears) receiving subcutaneous injections of chitosan formulations on days 0 and 10 post-injury; error bars represent standard deviation. **B** - representative photographs of ear pinnae. The treatments were designated as follows: ZebRA + chitosan - 48 mg of zebularine in 200 µl of 0.75% chitosan + 0.8 mg of retinoic acid in 200 µl of 0.75% chitosan; Zebularine + alginate - 48 mg of zebularine in 200 µl of 0.75% chitosan + 200 µl of 0.75% chitosan; RA + 0.75% chitosan 0.8 mg of retinoic in 200 µl of 0.75% chitosan + 200 µl of 0.75% chitosan; 0.75% chitosan alone - two 200 µl portions of 0.75% chitosan. Statistically significant differences were determined with the two-tailed Mann-Whitney U test and indicated as follows: with asterisks * for ZebRA vs 0.75% chitosan alone, dollar signs $ for zebularine vs 0.75% chitosan alone, hashtags # for RA vs 0.75% chitosan alone. Single, double, and triple signs denote $p < 0.05$, $p < 0.001$, and $p < 0.001$, respectively. The ruler scale is 1 mm.

However, sodium alginate was chosen as the primary carrier for testing drugs for pro-regenerative properties. Compared to chitosan, sodium alginate presents no risk of

immune reactions that are typical for materials of animal origin, such as chitosan (Hoemann and Fong 2017) and better stability. Sodium alginate is dissolved in pure water and has a neutral pH, while chitosan requires dissolution in acid or saturation with carbon dioxide. Carbonated chitosan materials change their properties while releasing carbon dioxide, eventually solidifying. This may impair experimental repeatability. On the other hand, the pro-regenerative chitosan formulations effectively promoted ear pinna hole closure (Fig. 9). Remarkably, 0.75% chitosan demonstrated similar suitability for subcutaneous injections as 2% sodium alginate, and the smaller amount of carrier may be a crucial advantage depending on the applications.

Biocompatibility of subcutaneously injected alginate formulations

Both zebularine and retinoic acid in alginate formulations have shown pro-regenerative effects when injected subcutaneously. Despite being administered at relatively high doses, the mice did not show any adverse effects such as apathy, weakness, lethargy, isolation, excessive excitability and irritability, or changes in the fur appearance, the typical symptoms signalling adverse drug effects in laboratory animals (Burkholder, Foltz *et al*. 2012). Also, there was no decrease in body weight in response to the treatment (Fig. 9), which indicates that the animals were in good condition during the treatment. No necrosis or irritation was observed at the injection site, confirming that the preparations were well tolerated under the skin. Necropsies performed on day 42 after injury did not reveal any residue of the injected preparation (Fig. 10C) in 4 of 6 animals. The above observations confirm the biocompatibility of the tested alginate formulations.

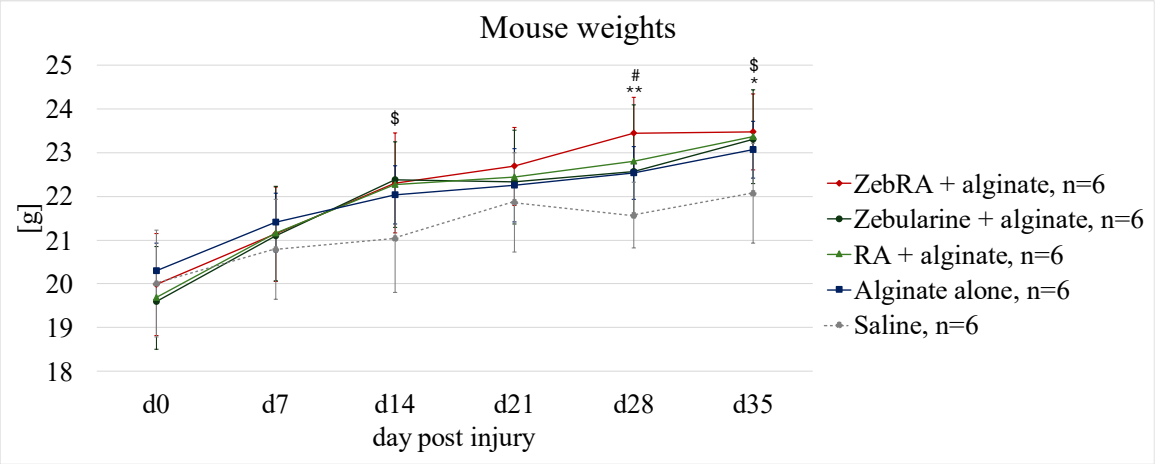

*Figure 9 Mouse weights in the course of the treatment with alginate formulations of zebularine and retinoic acid, n - number of mice, error bars represent the standard deviation (Cerneckis, Cai et al. 2024). Statistically significant differences were determined with the Kruskal-Wallis test and indicated as follows: with asterisks * for ZebRA vs saline, dollar signs $ for zebularine vs saline, and hashtags # for RA vs saline. Single, double, and triple signs denote p < 0.05, p < 0.001, and p < 0.001, respectively.*

Ultrasound examination of subcutaneously injected alginate formulations

Although necropsies did not reveal any remains of the alginate preparations under the skin, it was not known whether they were absorbed rapidly or gradually and slowly. Performing mouse necropsies to examine the amounts of remaining preparations at several time points would involve sacrificing a vast number of animals. Moreover, at each time point, the observation would concern a different animal and injection of the preparation, which could distort the results. I carried out live tracking of alginate preparations injected under the skin of mice using ultrasound. The presence of the injected preparation was determined by a comparative examination with mice that did not receive injections. The analysis showed a gradual decrease in ultrasound signals from alginate preparations under the skin (Fig. 10AB). To accurately visualize the results, based on selected ultrasound frames, a qualification was performed to measure the intensity of the signal coming from alginate (Fig. 10B). These results suggest a gradual absorption of the alginate formulations, leading to complete elimination, confirmed by necropsies on day 42 post-injury, as described above. The effect may explain the activity of retinoic acid, resulting in improved ear hole closure, as the compound is hydrophobic and thus unlikely to be released from the alginate carrier by diffusion, as demonstrated in *in vitro* release studies (Słonimska, Baczyński-Keller *et al.* 2024).

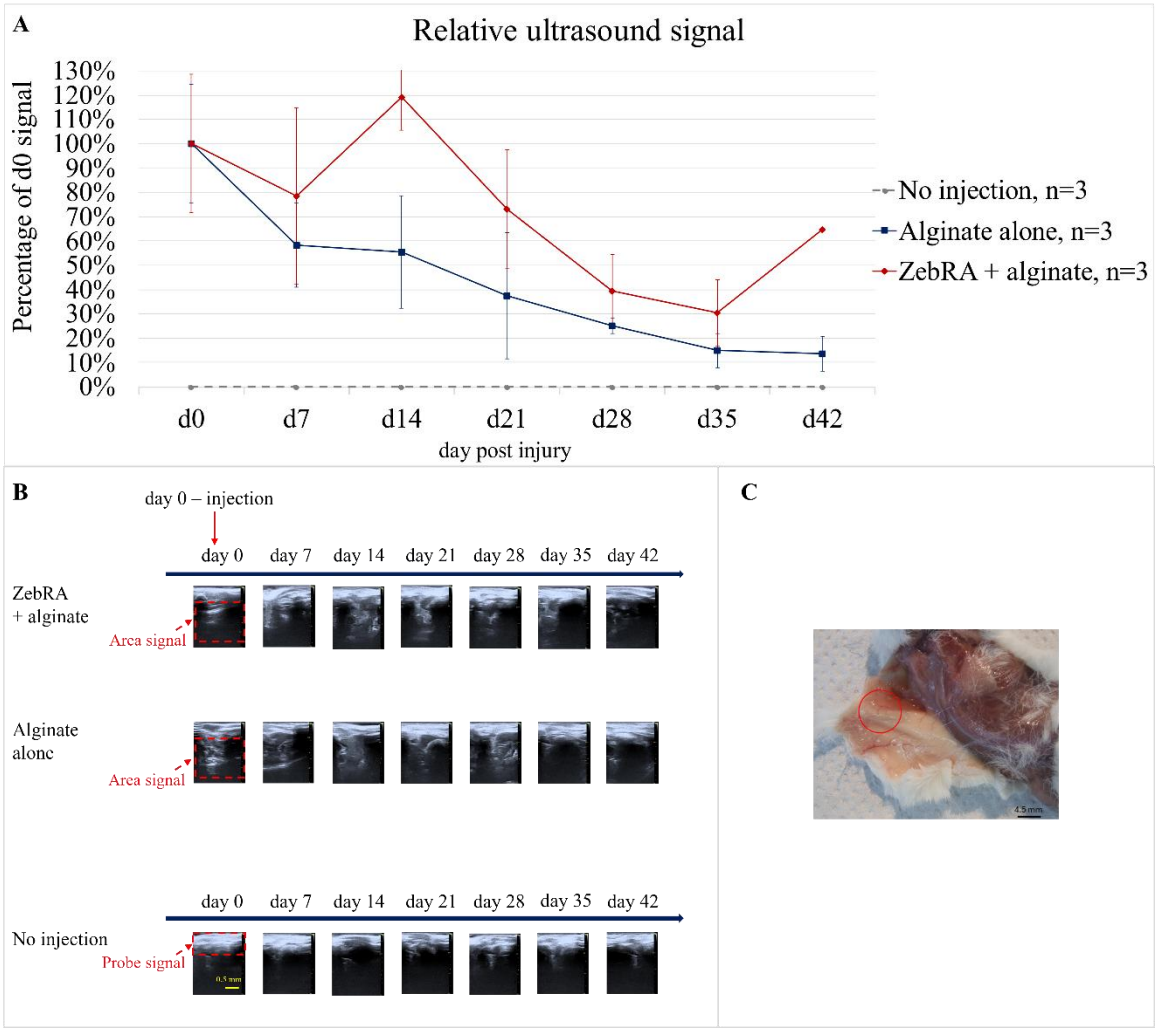

*Figure 10 Live-imaging of subcutaneously-injected alginate-based formulations – **A** - ultrasound signal from subcutaneous alginate formulations determined weekly from the day of injection with 400 µl of 2% sodium alginate and its formulations with zebularine (48 mg in 200 µl of 2% alginate sodium alginate and of retinoic acid 0.8 mg in 200 µl of 2% sodium alginate) compared with non-injected mice. Data for each mouse and each time point was calculated from 5-8 images. Each treatment was conducted for three mice (n=3); error bars represent the. No significant differences between the groups were determined. **B** - representative ultrasound images. **C** - Necropsy of a mouse that received subcutaneous injections of zebularine and retinoic acid formulations in 2% sodium alginate. Sacrifice and post-mortem examinations were performed on day 42 post-injury. The injection site is indicated with a red circle.*

Transcriptional responses of genes with potential importance in regenerative processes in the ear pinna

In order to investigate the effects of alginate formulation with zebularine and retinoic acid at the molecular level, the transcriptional activities of selected markers were analyzed in the regenerating ear pinna of mice. A panel of 27 transcripts included markers of pluripotency, neurogenesis, Wnt signalling, pro-fibrotic activity and growth factors essential in tissue regeneration and wound healing. The genes were chosen based

on literature analysis. A short description of the markers and the source literature are presented in Table 3. The importance of the chosen pathways for regeneration processes is explained further (in the following parts of a given chapter).

The tissues were collected from three sites of ear pinna: a 3-mm ring immediately around the 2-mm wound, i.e., the regenerating area; a 5-mm ring surrounding the 3-mm one, i.e., adjacent to the regenerating area; and a 3-mm circle from a non-injured area, distant from the wound (Fig. 11). In order to investigate the dynamism of transcriptional responses, the tissue samples were collected on day 7, 14, 21 and 42 post-injury.

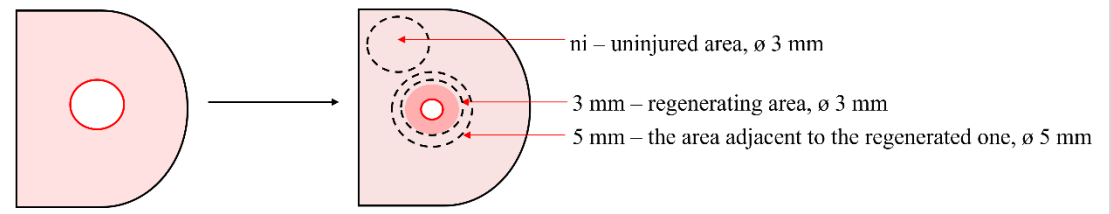

Figure 11 Scheme of tissue samples collection from ear pinna - 3-mm ring (3mm) of the regenerating area directly contacting the 2-mm excisional wound, 5-mm ring (5mm) adjacent to the regenerating area around the 3-mm ring, 3-mm ring excised from the non-injured (ni) area distant from the wound.

The expression levels of selected transcripts were determined with quantitative PCR (qPCR). This approach enables the quantification of multiple markers, but not the whole transcriptome, as RNA-Seq does. However, qPCR is helpful when the examination involves multiple samples representing several time points and several tissue types, as in the present study design. For a thorough analysis, it was necessary to analyze the changes in each ear of the three mice in the experimental group separately. Pooling can be considered not an adequate approach due to the biological variance of the animals. For such a large number of samples as included in this study, qPCR would be affordable, unlike the RNA-Seq. What is more, the regenerating tissues are available in scarce amounts. Therefore, the quantity and quality of a template obtained from an individual mouse may not be sufficient for RNA-seq requirements.

Table 3 Markers of potential importance for wound healing and tissue regeneration selected for transcriptional profiling.

Gene	Full name	Group	Short characteristics
Fbxo15	F-box protein 15	Pluripotency marker	Fbxo15 is a stem cell-specific protein. The *Fbxo15* activity signalled pluripotency induction in the pioneering experiments by Yamanaka and Takahashi (Takahashi and Yamanaka 2006). It is preferentially expressed in undifferentiated cells and is used as a marker of induced pluripotent stem cells (Werner and Rape 2017). Inactivation of Oct3/4 in embryonic stem cells has led to rapid quenching of *Fbxo15* expression (Tokuzawa, Kaiho *et al*. 2003).
Klf4	Kruppel-like factor 4	Pluripotency marker, one of the reprogramming factors of the "Yamanaka cocktail" (Takahashi and Yamanaka 2006)	A transcription factor, Kruppel-like factor 4 (*Klf4*), is an evolutionarily conserved zinc finger-containing transcription factor that regulates various cellular processes such as cell growth, proliferation, and differentiation. It is one of the four factors involved in the induction of pluripotent stem cells (Cerneckis, Cai *et al*. 2024). *Klf4* acts as a direct early regulator of adipogenesis (Birsoy, Chen *et al*. 2008). *Klf4* is highly expressed in the gastrointestinal tract and other epithelial tissues, including skin. *Klf4* deficiency was found to delay skin wound healing in mice, during which *Klf4*-expressing multipotent cells migrated toward the wound area (Li, Zheng *et al*. 2012).
Myc	Myc	Pluripotency marker, one of the reprogramming factors of the "Yamanaka cocktail" (Takahashi and Yamanaka 2006)	The transcription factor regulates genes involved in hepatocyte growth, proliferation, metabolism, and differentiation (Sanders, Schorl *et al*. 2012). Experiments with cultured human keratinocytes suggest that *c-Myc* promotes epidermal and stem cell differentiation (Arnold and Watt 2001). *c-Myc* can induce epidermal stem cell differentiation *in vitro*. Dysregulated *c-Myc* expression in stem cells has been shown to reduce the expression of β1 integrin, which is

			essential for both keratinocyte migration and stem cell maintenance (Waikel, Kawachi *et al*. 2001).
Nanog	Nanog Homeobox	Pluripotency marker	A transcription factor is a highly divergent homeodomain-containing protein widely assigned a central position in the pluripotency transcriptional network. The Nanog transcription factor is essential for dedifferentiated intermediates to transition to ground-state pluripotency (Silva, Nichols *et al*. 2009). NANOG also regulates the reprogramming of induced pluripotent stem cells, binds to the OCT4 promoter, and enhances the self-renewal of embryonic stem cells (ES). Numerous studies have reported that NANOG is a key transcription factor (Yin, Zhang *et al*. 2022).
Pou5f1	Octamer binding transcription factor 4	Pluripotency marker, one of the reprogramming factors of the "Yamanaka cocktail" (Takahashi and Yamanaka 2006)	The POU domain transcription factor is an essential regulator of pluripotency in embryonic stem (ES) cells and induced pluripotent stem (Cerneckis, Cai *et al*. 2024) cells. *Oct4* expression may identify somatic stem cell populations with inherent multipotency or a propensity for facilitated reprogramming (Fong, Hohenstein *et al*. 2008, Limbourg, Schnabel *et al*. 2014).
Sox2	SRY-Box Transcription Factor 2	Pluripotency marker, one of the reprogramming factors of the "Yamanaka cocktail" (Takahashi and Yamanaka 2006)	A high mobility group DNA-binding domain transcription factor is expressed in a pluripotent mouse embryonic line. *Sox2* is expressed in multipotent cells of the extraembryonic ectoderm and precursor cells of the developing central nervous system, suggesting a role for *Sox2* in maintaining developmental potential (Fong, Hohenstein *et al*. 2008). In the skin, *Sox2* is expressed in cells around the bulge area of hair follicles, dermal papillae, Merkel cells, and neural crest precursor cells but was not detected in epidermal keratinocytes. It plays an essential role in skin repair. *Sox2* expression has been

			shown to promote cutaneous wound healing in mice (Uchiyama, Nayak *et al*. 2019).
Egf	Epidermal growth factor	Growth factor	Epidermal growth factor (*Egf*) can reduce skin scarring by suppressing inflammatory responses, reducing TGF-b1 expression, and mediating collagen formation (Kim, Lew *et al*. 2010).
Fgf1	Fibroblast growth factor 1	Growth factor	Fibroblast growth factor *Fgf1* was originally identified as an endothelial cell mitogen and subsequently for various mesenchymal- and neuroectoderm-derived cells. It is a potent angiogenic factor *in vivo*. It is expressed in multiple developing and adult tissues and cultured cells, promoting cell proliferation, division, spreading, and migration (Zhang, Madiai *et al*. 2001).
Gdnf	Glial cell-derived neurotrophic factor	Neurogenesis	The glial cell line-derived neurotrophic factor *Gdnf* was originally identified as a midbrain dopaminergic survival factor. It promotes survival and regulates the differentiation of many peripheral neurons, including sympathetic, parasympathetic, and sensory neurons (Sariola and Saarma 2003).
Neurog1	Neurogenin 1	Neurogenesis	*Neurog1* is one of the critical regulators of neuronal differentiation (Kameda, Imamura *et al*. 2018) and can also promote neuronal proliferation (Song, Jadali *et al*. 2017).
Reno1	Regulator of early neurogenesis	Neurogenesis	*Reno1* is a regulator of early neurogenesis (Seal, Tweedie *et al*. 2023). Loss of *Reno1* leads to an early arrest in neuronal engagement, failure to induce the neuronal gene expression program, and a global reduction in chromatin accessibility in regions marked with the H3K4me3 chromatin marker at the onset of differentiation (Hezroni, Ben-Tov Perry *et al*. 2020).
Tac1	Tachykinin precursor 1	Neurogenesis	Substance P (SP) is an 11-amino-acid neuropeptide on unmyelinated primary sensory

			neurons' peripheral and central terminals. SP is encoded by the tachykinin 1 (*Tac1*) gene, which also encodes neurokinin A (Goenka, Sant *et al*.). SP activity is mediated via interactions with the G protein-coupled neurokinin receptors (NKRs) found on blood vessels and lymphatics endothelial cells, immune cells, fibroblasts, and neurons. SP plays vital roles in multiple life processes, including inflammation, angiogenesis, and wound healing (Graefe and Mohiuddin 2020).
Prrx1	Paired-related homeobox gene 1	Blastema marker (in amphibians)	Prrx1 – blastema marker gene in amphibians – is expressed throughout the developing limb bud mesenchyme (Satoh, Hirata *et al*. 2011); Prrx1 is a transcription factor that plays a crucial role in limb development. During limb regeneration in amphibians, Prrx1 is specifically expressed in migrating fibroblasts. Prrx1-positive fibroblasts have been demonstrated in the dermis of adult mice, located in perivascular and hair follicle niches, which can expand in response to injury (Leavitt, Hu *et al*. 2020). Prrx1 is also identified as a negative regulator of adipogenesis. It is decreased during adipogenesis *in vitro* and *in vivo* (Du, Cawthorn *et al*. 2013).
Gsk3b	Glycogen synthase kinase-3 beta	Wnt signalling pathway; Canonical pathway; Negative regulation	*Gsk3b* is a β-catenin inhibitory factor. *Gsk3b* is involved in tissue repair and fibrogenesis. It plays a key role in connecting Wnt adenosine I receptor signalling pathways, potentially promoting tissue remodelling during wound healing (Kapoor, Liu *et al*. 2008).
Lrp5	Low-density lipoprotein receptor-related protein 5	Wnt signalling pathway; Canonical pathway; Positive regulation	As endocytotic receptors on the cell surface, *Lrp5* and *Lrp6* are essential in the canonical Wnt signalling pathway. When Wnt signalling occurs, β-catenin is a significant component of the Wnt/β-catenin signalling pathway and

			promotes the transcription of target genes, thereby regulating cell proliferation. The Wnt signalling pathway can regulate several molecules that play essential roles in developing fibroblasts, epidermal stem cells, and hair follicle stem cells (Bai, Guo *et al*. 2023).
Lrp6	Low-density lipoprotein receptor-related protein 6	Wnt signalling pathway; Canonical pathway; Positive regulation	
Sfrp2	Secreted frizzled-related protein 2	Wnt signalling pathway; Canonical pathway; Negative regulation	*Sfrp2* is a modulator of Wnt signalling. It is a potent signalling molecule recognized for its ability to modulate Wnt/β-catenin signalling. It plays many biological roles in a variety of cellular processes, including tissue development and tissue homeostasis. It is involved in the proliferation and energy metabolism in cardiac fibroblasts and regulates cell proliferation, survival, and the regenerative phenotype of mesenchymal stem cells (Ledwon, Vaca *et al*. 2022).
Wnt10a	wingless-type MMTV integration site family, member 10A	Wnt signalling pathway; Canonical pathway; Positive regulation	*Wnt10a* plays a crucial role in the growth of fibroblasts/myofibroblasts and microvascular endothelial cells. Wnt10a-deficient mice were shown to have significantly more significant areas of damage and delayed wound healing, which was associated with fewer fibroblasts/myofibroblasts and microvessels and more reduced collagen expression and synthesis compared to mice with intact *Wnt10a* expression. These observations indicate that *Wnt10a* signalling may play a key role *in vivo* in wound healing by regulating the expression and synthesis of collagen as one of the fibrogenic factors (Wang, Li *et al*. 2025).
Wnt11	wingless-type MMTV integration site family, member	Wnt signalling pathway; Non-canonical pathway;	*Wnt-11* is expressed in the mouse embryonic dermis. When reviewing the temporal expression of preselected Wnt genes during wound healing, increased expression of *Wnt11* was consistently observed (Fathke, Wilson *et al*.

	11	Positive regulation	2006).
Acta2	Actin alpha 2	Pro-fibrotic marker	The α-smooth muscle actin gene *Acta2* is a myofibroblast marker gene (Wietecha, Pensalfini *et al*. 2020). It has been shown to be increased in expression during the healing of burn wounds. *Acta2* expression increases significantly soon after human skin burns. It is believed that Tgfb1 is one of the main factors involved in the regulation of *Acta2* and, thus, the development of hypertrophic scars. In the skin, Tgfb1 binds as an inactive precursor molecule to the extracellular matrix of the dermis via latency-related peptide and latent Tgfb-binding protein. After tissue damage, active Tgfb1 is released, activating fibroblasts to differentiate into myofibroblasts, producing large amounts of *Acta2* (Hofmann, Fink *et al*. 2021). Active fibroblasts (myofibroblasts) that are positive for *Acta2* contribute to wound healing by regulating the secretion of extracellular matrix (ECM), matrix metalloproteinases, tissue inhibitors of metalloproteinases, growth factors, and cytokines necessary for wound healing (Qiang, Yang *et al*. 2021).
Ccl3	C-C motif chemokine ligand 3	Pro-fibrotic marker	*Ccl3* is a chemokine known as macrophage inflammatory protein1α (Heinrichs, Berres *et al*. 2013). During wound healing, lymphocytes enter the wound to modulate the immune response. *Ccl3* attracts lymphocytes to the wound. T cells produce essential cytokines and interact with antigen-presenting cells for host defence (Johnson, Mahoney *et al*. 2019).
Ccl11	C-C motif chemokine ligand 11	Pro-fibrotic marker	*Ccl11* promotes endothelial cell migration, weak proliferation, and angiogenesis (Park, Kang *et al*. 2017). Stimulation with *Ccl11* ligands has enhanced wound repair in cultured endothelial

			cells (Bünemann, Hoff *et al*. 2018).
Ccn2	Cellular communication network 2	Pro-fibrotic marker	The CCN family of cell-matrix proteins, including CCN2, is thought to play a significant role in controlling tissue morphogenesis and repair *in vivo*. In adult skin, *Ccn2* levels increase during fibrosis and wound healing. It has been shown that the loss of *Ccn2* results in impaired recruitment of pericyte-like cells (essential in wound healing) to the wound area. Therefore, *Ccn2* may represent a specific antifibrotic target (Liu, Thompson *et al*. 2014).
Grem1	Gremlin 1	Pro-fibrotic marker	*Grem1* positively affects angiogenesis (Saraswati, Marrow *et al*. 2019).
Il4	Interleukin 4	Pro-fibrotic marker	The cytokine *Il4* affects the differentiation of keratinocytes. *Il4* has been shown to impair the wound-healing response of keratinocytes by reducing fibronectin production (Serezani, Bozdogan *et al*. 2017).
Il13ra2	Interleukin 13 receptor subunit alpha 2	Pro-fibrotic marker	When *Il13ra2* expression is low or absent, IL13-dependent fibrosis is exacerbated. Ectopic overexpression of *Il13ra2* attenuates keloid fibrogenesis by inducing apoptosis and inhibiting myofibroblast migration, invasion, and collagen synthesis *in vivo* and *in vitro* (Chao, Zheng *et al*. 2023).
Snai1	Snail family transcriptional repressor 1	Pro-fibrotic marker	Overexpression of *Snai1* accelerates wound healing (Aomatsu, Arao *et al*. 2012). During embryonic development, Snai1 is essential for gastrulation, mesoderm, and neural crest formation (Galvagni, Lentucci *et al*. 2015).

Pluripotency markers and growth factors

The ultimate goal of regenerative processes is to replace lost or damaged cells. This can be done by dedifferentiation, transdifferentiation or reprogramming. Many regenerative processes involve dedifferentiation (Jopling, Boue *et al*. 2011). Dedifferentiation is a reverse developmental process in which differentiated cells with specialized functions become undifferentiated progenitor cells. Dedifferentiation and subsequent proliferation are the basis for tissue regeneration and the creation of new stem cell lines (Eguizabal, Montserrat *et al*. 2013). Studies show that adding a group of genes can not only restore pluripotency in a fully differentiated cell (reprogramming) but can also induce cell proliferation (dedifferentiation) or even transition to another cell type (transdifferentiation) (Jopling, Boue *et al*. 2011). The transcription factors *Oct4*, *Sox2*, *Klf4*, and *c-Myc* enable the reprogramming of somatic cells into induced pluripotent cells (Aguirre, Escobar *et al*. 2023). The transcription factor Nanog is essential for the dedifferentiation of intermediates for the transition to ground-state pluripotency (Silva, Nichols *et al*. 2009). Also, it regulates the reprogramming of induced pluripotent stem cells (Yin, Zhang *et al*. 2022). Another example is *c-Myc*, which is involved in self-renewal processes and induces epigenetic changes that promote dedifferentiation or block cell differentiation. Overexpression of *Oct4*, necessary for establishing and maintaining cellular pluripotency, induces cellular differentiation (Aguirre, Escobar *et al*. 2023).

Wound healing requires cell proliferation and cellular interactions between fibroblasts, myofibroblasts, keratinocytes, smooth muscle cells, endothelial cells, and immune cells. Growth factors mediate these processes. Epidermal growth factor *Egf* and fibroblast growth factor *Fgf* are listed among those critical in proper skin wound healing (Balakrishnan and Jayakrishnan 2005).

The transcription profiles for the pluripotency and growth factors genes are presented in Fig. 12 and 13, respectively; the fold changes between the treatment and control groups are listed in Tables 4 5.

In the 3 mm zone, i.e. within the tissues immediately contacting the injury and regenerating area, increases in the expression of almost all pluripotency markers and growth factors were observed in the treatment compared to the control animals. However, statistically significant increases between the treatment and control groups

were determined only on day 42 for *Nanog, Klf4 and Oct4*. Although the differences showed remarkable at other time points, they were statistically insignificant when comparing the treatment and control groups. Nevertheless, in contrast to the controls, the treatment group tends to demonstrate more marked changes over time. This was especially accentuated when comparing day 7 post-injury, i.e., the early phase of regenerative response when the inflammatory phase is still ongoing, but tissue restoration is minimal, if any (Fig. 4), and day 42, the last day of the experiment, when ear hole closure plateaus with the intermediate time points, days 14 and 21, where the tissue growth is the most intensive. The exception is *Myc*, which on day 7 shows lower, but statistically insignificant, expression in the treatment group relative to the alginate-only control. The treatment and control groups exhibit relatively low changes between days 14 and 21 post-injury compared to the preceding and subsequent time points. However, the changes between days 14 and 21 showed statistically significant for *Myc* and *Oct4*. To sum up, in 3-mm rings comprising the regenerating tissues, the highest expression levels of most of the pluripotency markers and growth factors tested occur on day 7 after wounding (Balakrishnan and Jayakrishnan 2005). On days 14-21, the curve flattens out over time, and on day 42, there is a sharp increase in the treatment groups' expression level, statistically significant compared to day 21, contrasting with slight and insignificant changes in the controls.

In the 5 mm rings surrounding but not directly contacting the area of wound and regeneration, no significant differences between the control and treatment groups were determined. However, most of the analysed genes tend to decrease expression at time points following day 7, but the changes were insignificant except for *Oct4* in the control and *Fgf1* for the treatment groups. In contrast, *Myc5* and *Klf4* showed statistically significant increases in the expression on day 42 compared to earlier time points, but only in the treatment groups.

In the non-injured area (ni), distant from the site of damage, the expression kinetics were similar to those observed in the regenerating area (3mm) and surrounding tissues (5mm) for the genes of pluripotency but not the growth factors genes. The differences between the control and treatment groups were insignificant, whereas significant changes between time points were found almost exclusively in the latter.

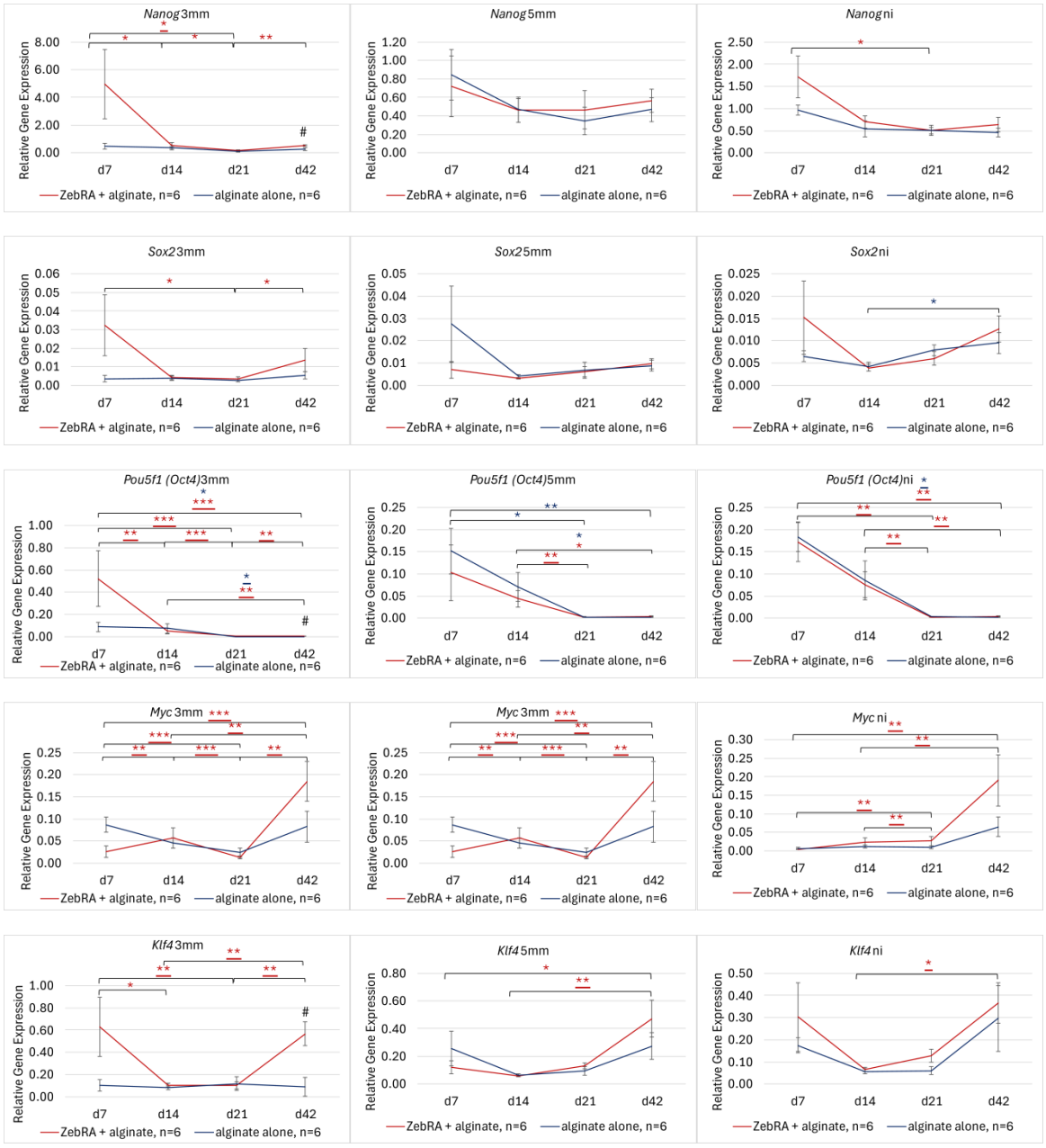

Figure 12 Transcriptomic responses of pluripotency in regenerating ear pinnae following subcutaneous injections of zebularine and retinoic acid in alginate carrier.

*Statistically significant differences between time points were determined using the Kruskal-Wallis test and denoted with asterisks: *<0.05, **<0.01, ***<0.001, marked red (*) for the treatment groups receiving zebularine and retinoic acid (**ZebRA**) and navy blue (*) for the controls injected with 2%* ***alginate alone****; the results significant after the Bonferroni correction are underlined. Statistically significant differences between the treatment and control groups were calculated using the Mann-Whitney U test and indicated with a hash sign (#<0.05). The error bars represent SEM; n=6 (six ear pinnae representing three mice).* The examined sites of ear pinna directly are indicated as follows: **3mm** – immediate to the wound, regenerating area; **5mm** – adjacent to the regenerating area, **ni** (non-injured) - distant to the wound.

Table 4 Expression fold changes of pluripotency genes following subcutaneous injections of zebularine and retinoic acid in 2% sodium alginate in regenerating ear pinnae. Statistically significant differences between the treatment group (ZebRA + alginate) and the control group (alginate alone) were determined using the Mann-Whitney U test and denoted: #<0.05; red and green fonts mark increase and decrease in expression in response to ZebRA treatment, respectively.

Gene	Fold change ZebRA/alginate											
	Area: 3 mm				Area: 5 mm				Area: ni			
	day 7	day 14	day 21	day 42	day 7	day 14	day 21	day 42	day 7	day 14	day 21	day 42
Nanog	10.747	1.480	1.159	**2.061 #**	0.854	0.987	1.352	1.205	1.779	1.304	1.016	1.391
Sox2	8.949	1.024	1.231	2.569	0.254	0.799	0.904	1.096	2.321	0.948	0.767	1.328
Pou5f1	6.004	0.672	1.629	**2.916 #**	0.678	0.627	1.115	2.376	0.943	0.881	0.878	2.463
Myc	0.304	1.238	0.571	2.240	0.189	0.768	0.930	3.277	0.689	2.021	2.637	2.966
Klf4	6.300	1.266	0.848	**6.231 #**	0.467	0.911	1.416	1.719	1.741	1.148	2.099	1.240

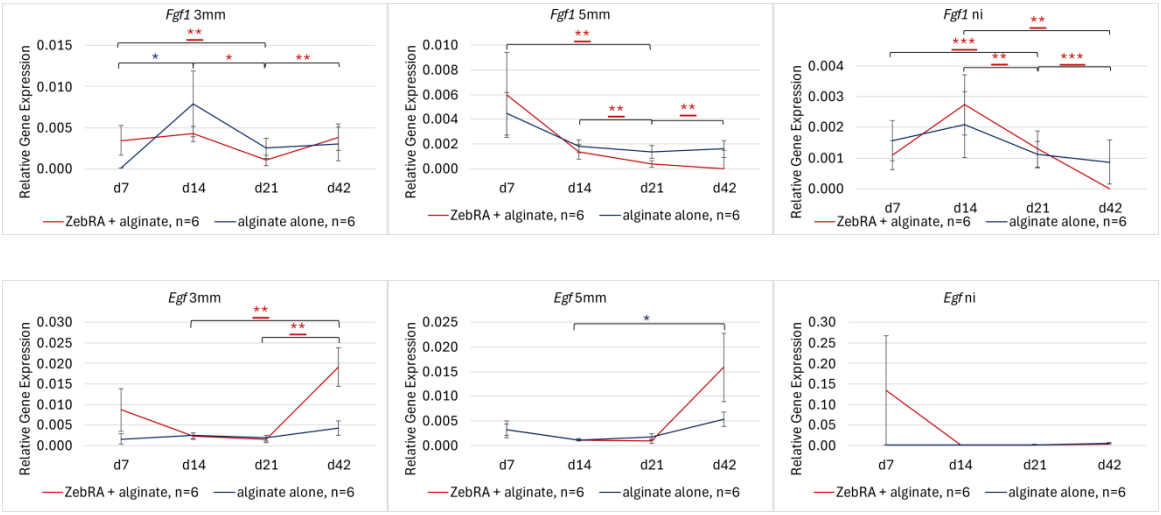

Figure 13 Transcriptomic responses of growth factor, Fgf1 and Egf, in regenerating ear pinnae following subcutaneous injections of zebularine and retinoic acid in alginate carrier.

*Statistically significant differences between time points were determined using the Kruskal-Wallis test and denoted with asterisks: *<0.05, **<0.01, ***<0.001, marked red (*) for the treatment groups receiving zebularine and retinoic acid (**ZebRA**) and navy blue (*) for the controls injected with 2% **alginate alone**; the results significant after the Bonferroni correction are underlined. Statistically significant differences between the treatment and control groups were calculated using the Mann-Whitney U test and indicated with a hash sign (#<0.05). The error bars represent SEM; n=6 (six ear pinnae representing three mice).* The examined sites of ear pinna directly are indicated as follows: **3mm** – immediate to the wound, **5mm** – adjacent to the regenerating area, **ni** (non-injured) - distant to the wound.

Table 5 Expression fold changes of growth factors following subcutaneous injections of zebularine and retinoic acid in 2% sodium alginate in regenerating ear pinnae. Statistically significant differences between the treatment group (ZebRA + alginate) and the control group (alginate alone) were determined using the Mann-Whitney U test and denoted: #<0.05; Red and green fonts mark increase and decrease in expression in response to ZebRA treatment, respectively. If ZebRA (numerator) was not determined, the fold change was assumed <0.001.

Gene	Fold change ZebRA/alginate											
	Area: 3 mm				Area: 5 mm				Area: ni			
	day 7	day 14	day 21	day 42	day 7	day 14	day 21	day 42	day 7	day 14	day 21	day 42
Fgf1	49.290	0.535	0.408	1.269	1.338	0.748	0.269	<0.001	0.700	1.305	1.160	<0.001
Vegfa	6.329	1.102	1.292	289.440	0.467	0.858	1.353	2.837	4.109	0.966	1.430	0.686
Egf	5.384	0.939	0.877	**4.482 #**	0.973	1.038	0.510	2.967	124.681	1.459	1.039	0.701

Zebularine with retinoic acid in alginate had a pro-regenerative effect, as demonstrated by the degree of closure of the holes in the ear pinna of mice (Fig. 6). Molecular experiments showed an increase in the expression of pluripotency markers and growth factors in the group treated with the tested formulation compared to the control group. These increases were observed in 3-mm rings comprising the regenerating tissue. This may indicate that the tested formulation stimulated regenerative processes by activating some genes related to pluripotency and growth factors. However, these results are not statistically significant, possibly linked to biological variance. Time-dependent changes were observed, especially on day 7, the initial phase of response to injury, preceding rapid ear hole closure observed between days 7 and 14 (Fig. 6A) On days 14-21, a flattening of the curve is observed, indicating lower marker activity at this time. Interestingly, a significant increase in the expression level of markers occurs on day 42, compared to day 21. Looking at the kinetics of the wound closure in the ear pinna, no significant progress has been observed between these time points (Fig. 6A); however, increased levels of pluripotency markers and growth factors gene expression were recorded.

Fbxo15 - the first marker of cellular reprogramming

Fbxo15 encodes F-box protein 15, which is most often referred to as Fbx15. Fbx15 is a part of the protein-ubiquitin ligase complex, which interacts with ubiquitinylation targets. Its activity is characteristic of undifferentiated embryonic cells; also, it plays a suppressive role in breast cancer progression (Tekcham, Chen *et al.* 2020). Fbx15 serves as the first marker of fibroblast reprogramming into pluripotent

stem cells (Takahashi and Yamanaka 2006), signalling co-expression of Oct4 and Sox2 (Tokuzawa, Kaiho *et al*. 2003). In adults, its expression is observed in the fallopian tubes and testes.

The regenerating mouse ear pinna showed an absence of expression in most ear pinnae in control groups treated with alginate alone. Positive signals were observed after treatment with zebularine with retinoic acid in the alginate formulation. Although the expression levels were low, they indicated activation of *Fbxo15* in response to the epigenetic treatment. This is particularly visible on day 7 post-injury in both wound area and noninjured tissues, as demonstrated by statistically significant overrepresentation of *Fbxo15* transcript detections using the Fisher's-exact test (p = 0.004) (Fig. 14).

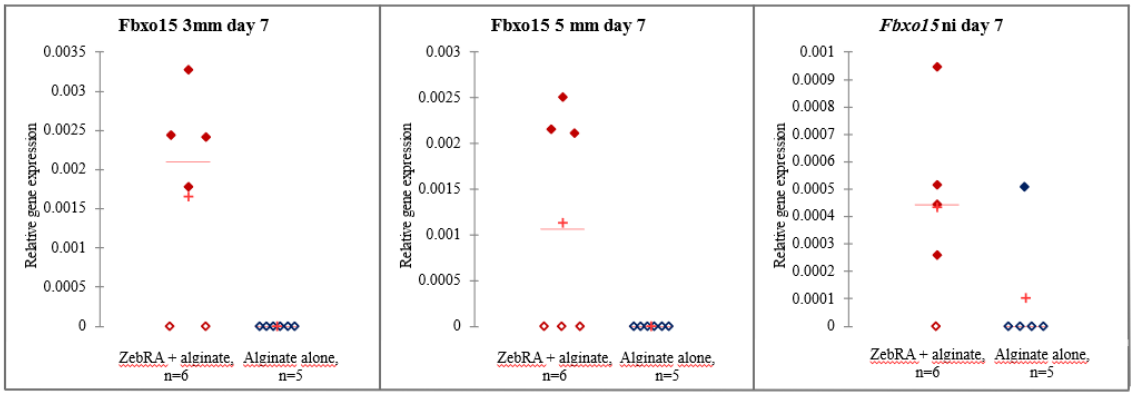

Figure 14 Transcriptomic responses of Fbxo15 in regenerating ear pinnae following subcutaneous injections of zebularine and retinoic acid in alginate carrier; in ZebRA + alginate group n=6 (six ear pinnae representing three mice, in Alginate alone group n=5 (five ear pinnae representing two mice ang one ear pinna in third mouse). The examined sites of ear pinna are indicated as follows: ***3mm*** *– immediate to the wound,* ***5mm*** *– adjacent to the regenerating area,* ***ni*** *(non-injured) - distant to the wound. Red and black markers indicate ZebRA-treated and control tissues, respectively. Empty markers represent the samples where Fbxo15 transcripts were undetected (zero signals). The Fbxo15 transcript signals are significantly overrepresented (p= 0.004) for assembled ZebRA-treated tissues (n=18) vs controls (n=15), as assessed with the Fisher's exact test.*

Nerve growth markers

Nerve dependence in tissue regeneration is spectacular in the studies on amphibians, where stump denervation prevents limb regeneration (Kumar and Brockes 2012). Experimental evidence indicates that innervation is essential in tissue regeneration in mammals (Ackermann and Hart 2013, Pagella, Jiménez-Rojo *et al*. 2014, Laverdet, Danigo *et al*. 2015, Alapure, Lu *et al*. 2018, Rink, Bendella *et al*. 2019).

The studies attracted my attention to the genes involved in nerve growth and development and encouraged me to examine their activity in regenerating ear pinnae. The selected markers included *Reno1*, which is a regulator of early neurogenesis; *Neurog1*, which is one of the critical regulators of neuronal differentiation; *Gdnf*, regulating the differentiation of peripheral neurons as well as *Tac1* encoding the neuropeptide - substance P expressed in central and peripheral nervous system and playing vital roles many life processes, including wound healing (Sariola and Saarma 2003, Matak, Tékus *et al*. 2017, Song, Jadali *et al*. 2017, Seal, Tweedie *et al*. 2023).

The transcription profiles for the neurogenesis genes are presented in Fig. 15; the fold changes between the treatment and control groups are listed in Table 6. In the 3-mm rings of the regenerating tissues and the 5-mm rings surrounding this area, higher expression of *Reno* and *Neurog1* was observed on day 7 compared to the following days, but the results were statistically significant only for *Reno* in the treatment group. *Gdnf* shows significant increases in expression with time in both treatment and control groups. Similar kinetics of *Reno*, *Neurog1* and *Gdnf* were observed in the non-injured (ni) parts of the ear pinna. No significant difference between the treatment and control groups was determined for these three genes, except for *Reno* on day 42 (3mm).

Tac1 expression profiles are inconsistent with those of the remaining genes of this group. Elevated *Tac1* transcript levels were observed in the treatment group on day 42 in 3-mm rings and on day 7 in 5-mm rings adjacent and non-injured tissues, but the changes were not statistically significant. In the controls, *Tac1* displayed higher expression on day 14 in 5-mm rings, and this result was statistically significant.

The regenerative effect is associated with the growth of nerve fibres. The interdependence of nerves during regeneration has long been known in amphibians, but in mammals, it is not yet well understood (Słonimska, Baczyński-Keller *et al*. 2024). The transcriptional changes demonstrated here suggest the activity of neurogenesis pathways during the regenerative response, especially in the initial phase of ear pinna hole closure, as indicated by elevated expression levels of *Reno* and *Neurog1* on day 7 post-injury. The results are consistent with the previously reported transcriptomic data pointing to the activation of neurodevelopmental genes in response to the epigenetic regenerative treatment (Sass, Sosnowski *et al*. 2019, Słonimska, Baczyński-Keller *et al*.

2024) and the development of nerve fibre networks in regenerating ear pinnae (Sosnowski, Sass *et al*. 2022, Słonimska, Baczyński-Keller *et al*. 2024).

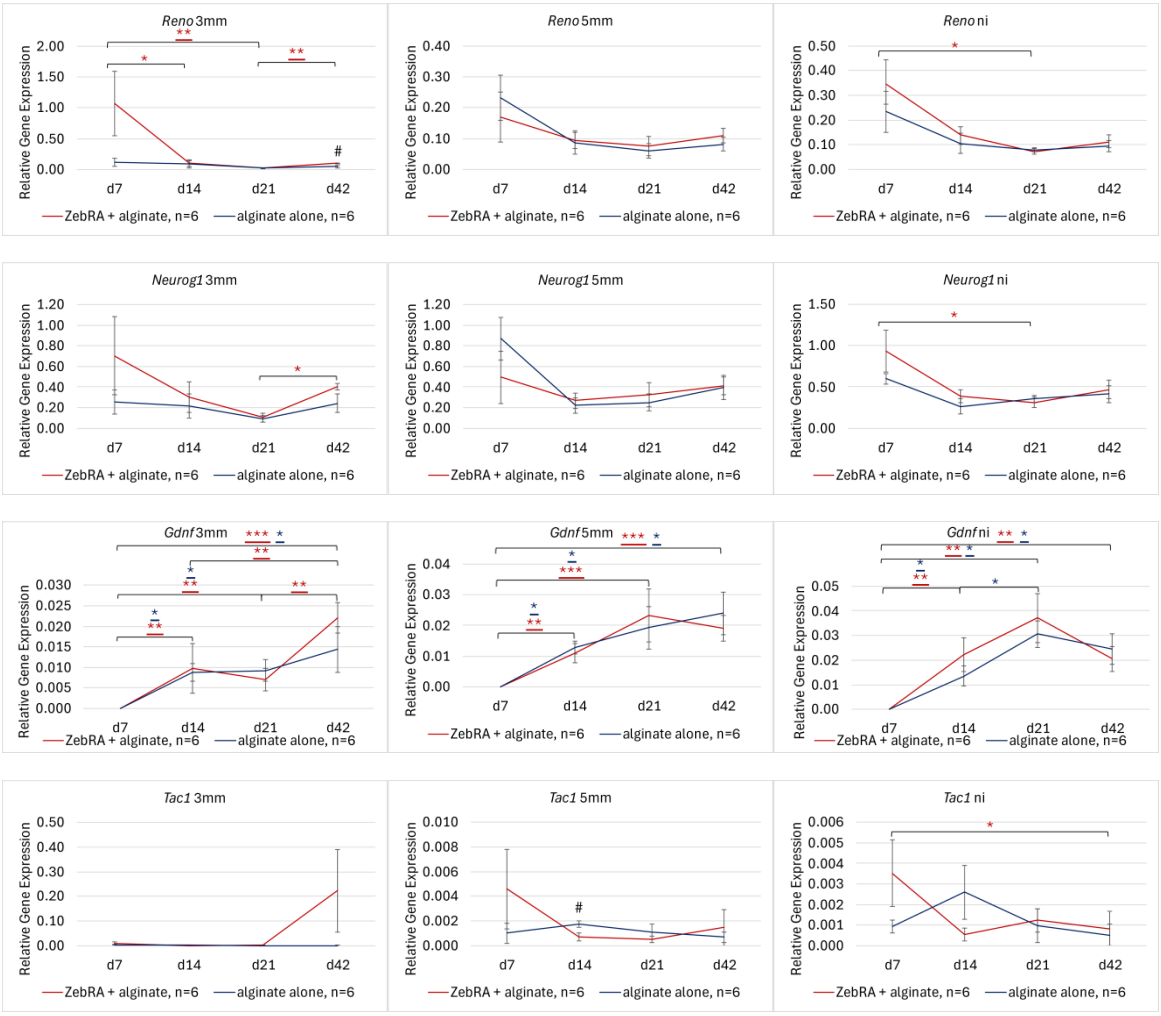

Figure 15 Transcriptomic responses of neurogenesis markers in regenerating ear pinnae following subcutaneous injections of zebularine and retinoic acid in alginate carrier.

*Statistically significant differences between time points were determined using the Kruskal-Wallis test and denoted with asterisks: *<0.05, **<0.01, ***<0.001, marked red (*) for the treatment groups receiving zebularine and retinoic acid (**ZebRA**) and navy blue (*) for the controls injected with 2% **alginate alone**; the results significant after the Bonferroni correction are underlined. Statistically significant differences between the treatment and control groups were calculated using the Mann-Whitney U test and indicated with a hash sign (#<0.05). The error bars represent SEM; n=6 (six ear pinnae representing three mice). The examined sites of ear pinna directly are indicated as follows: **3mm** – immediate to the wound, **5mm** – adjacent to the regenerating area, **ni** (non-injured) - distant to the wound.*

Table 6 Expression fold changes of neurogenesis genes following subcutaneous injections of zebularine and retinoic acid in 2% sodium alginate in regenerating ear pinnae. Statistically significant differences between the treatment group (ZebRA + alginate) and the control group (alginate alone) were determined using the Mann-Whitney U test and denoted: #<0.05; red and green fonts mark increase and decrease in expression in response to ZebRA treatment, respectively; ND - expression below the limit of determination.

Gene	Fold change ZebRA/alginate											
	Area: 3 mm				Area: 5 mm				Area: ni			
	day 7	day 14	day 21	day 42	day 7	day 14	day 21	day 42	day 7	day 14	day 21	day 42
Reno	8.954	1.194	1.047	**2.037 #**	0.732	1.087	1.251	1.353	1.478	1.316	0.903	1.179
Neurog1	2.793	1.400	1.145	1.674	0.567	1.211	1.300	1.034	1.562	1.470	0.886	1.131
Gdnf	ND	1.104	0.769	1.537	<0.001	0.858	1.209	0.802	ND	1.651	1.215	0.838
Tac1	5.866	0.336	1.499	305.259	4.515	**0.406 #**	0.458	2.176	3.814	0.207	1.261	1.605

Assessment of Prrx1 expression as a potential blastema marker

Blastema is a mass of undifferentiated cells forming in the lesion site during epimorphic regeneration, which gives a beginning to the regenerating organs. A canonical example is the blastema formed in the stumps after limb amputation in amphibians and then develops into a functional limb (Seifert and Muneoka 2018). In mammals, blastema-like structures are reported in amputated digit tips and injured ear pinna (Seifert and Muneoka 2018). *Prrx1* encoding one of homeobox proteins can be regarded as a blastema marker in amphibians (Suzuki, Satoh *et al*. 2007, Satoh, Hirata *et al*. 2011, Hayashi, Tamura *et al*. 2020), where it was shown to be expressed throughout the developing limb bud mesenchyme (Nohno, Koyama *et al*. 1993, Leussink, Brouwer *et al*. 1995, Martin and Olson 2000). Blastema cells derived from skin fibroblasts exhibit multipotency within the connective tissue lineage. *Prrx1* is expressed in multipotent blastema cells but is not detectable in fully differentiated fibroblasts. Therefore, Prrx1 is considered an ideal marker gene for tracking the activation of skin fibroblasts in the early phase of regeneration (Satoh, Hirata *et al*. 2011). In mammals, no canonical blastema marker has been established (Seifert and Muneoka 2018). Therefore, I decided to evaluate the expression of this homeobox gene during ear pinna regeneration in mice.

Prrx1 shows similar expression profiles in the 3-mm rings of regenerating tissue and in the 5-mm adjacent rings. The expression levels do not change markedly between days 7, 14, and 21. A substantial increase in expression occurs on day 42 post-injury in both treatment and control groups but is more pronounced in the first one. The kinetics in the non-injured area (ni) look different in the treatment and control mice. Compared to the control group, there is an increased *Prrx1* expression in the treatment group on days 7 and 14, and the result is statistically significant on the latter time point (Fig. 16, Table 7).

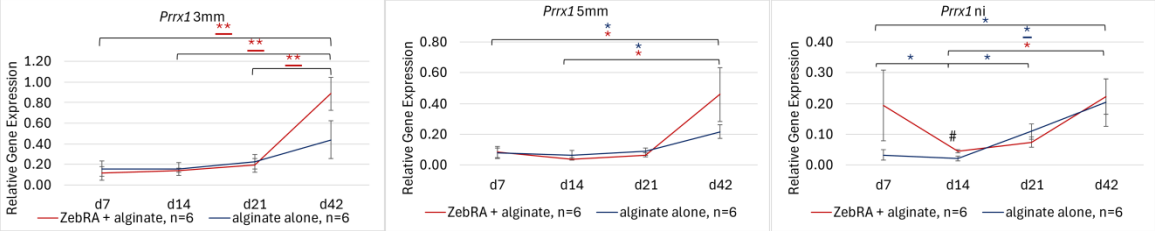

Figure 16 Transcriptomic responses of blastema marker in regenerating ear pinnae following subcutaneous injections of zebularine and retinoic acid in alginate carrier.

*Statistically significant differences between time points were determined using the Kruskal-Wallis test and denoted with asterisks: *<0.05, **<0.01, marked red (*) for the treatment groups receiving zebularine and retinoic acid (**ZebRA**) and navy blue (*) for the controls injected with 2% **alginate alone**; the results significant after the Bonferroni correction are underlined. Statistically significant differences between the treatment and control groups were calculated using the Mann-Whitney U test and indicated with a hash sign (#<0.05). The error bars represent SEM; n=6 (six ear pinnae representing three mice). The examined sites of ear pinna directly are indicated as follows: **3mm** – immediate to the wound, **5mm** – adjacent to the regenerating area, **ni** (non-injured) - distant to the wound.*

Table 7 Expression fold changes of blastema marker following subcutaneous injections of zebularine and retinoic acid in 2% sodium alginate in regenerating ear pinnae. Statistically significant differences between the treatment group (ZebRA + alginate) and the control group (alginate alone) were determined using the Mann-Whitney U test and denoted: #<0.05; red and green fonts mark increase and decrease in expression in response to ZebRA treatment, respectively.

Gene	Fold change ZebRA/alginate											
	Area: 3 mm				Area: 5 mm				Area: ni			
	day 7	day 14	day 21	day 42	day 7	day 14	day 21	day 42	day 7	day 14	day 21	day 42
Prrx1	0.704	0.925	0.849	2.020	1.104	0.639	0.742	2.103	5.803	**1.986 #**	0.686	1.093

A significant increase in *Prrx1* activity on day 42 may indicate an ongoing fibroblast differentiation process in the remodelling phase. This is a different relationship than in the case of amphibian limb regeneration, where the most significant fibroblast activity occurs at the earliest stage of regeneration, immediately after the injury (Yokoyama 2008).

Wnt signalling pathway

Wnt signalling plays a crucial role in regulating skin cells' proliferation, differentiation, and motility during their morphogenesis (Widelitz 2008). Wnts are a large family of secreted signalling molecules homologous to the Wingless protein. Signalling is mediated by binding to transmembrane receptors, the Frizzled (Fz) proteins. Fz proteins have 10 family members. There are also many secreted Wnt inhibitory molecules, such as *Sfrp2*. Without Wnt signalling, β-catenin is phosphorylated by a degradation complex containing axin and *Gsk3b*, signifying its proteasomal degradation. When Wnt binds to Fz receptors and low-density lipoprotein receptor-related protein (*Lrp5, Lrp6*), the β-catenin degradation complex is inhibited. This enables the accumulation of β-catenin in the cell and translocation into the nucleus, leading to transcriptional induction (Widelitz 2008). There is also β-catenin-independent, non-canonical Wnt signalling (Sarabia-Sánchez and Robles-Flores 2024).

The canonical Wnt pathway is mainly involved in regulating cell proliferation and maintaining stem cell pluripotency. In contrast, non-canonical Wnt pathways, such as the planar cell polarity pathway and the Wnt/Ca2+ pathway, control cell migration, polarity, and morphogenesis (Komiya and Habas 2008). Canonical Wnt signalling has been implicated as being active in regeneration processes in mammals (Takeo, Chou *et al*. 2013, Girardi and Le Grand 2018, Gao, Fan *et al*. 2021).

Typically, Wnt signalling studies focus on cellular models and analyse markers on the protein level. In order to analyze the activity of a panel of genes involved in Wnt signalling in scarce amounts of regenerating tissues with high sensitivity, I decided to examine transcriptional responses using qPCR.

Except for *Wnt11*, the Wnt signalling genes under the analysis tend to show higher activity in the treatment than the control groups on days 7 and 42 post-injury in all analysed ear pinna sites. Of note, statistically significantly elevated expression levels in the treatment group were determined for *Lrp6, Wnt10a*, and *Sfrp2* in the regenerating tissues in 3-mm rings immediate to the wounds and for *Gsk3b* in the 5-mm ring adjacent to the regenerating area (Fig. 17, Table 8). Notably, there is a nearly 50-fold elevation of the *Sfrp2* transcript in response to the epigenetic treatment on day 14 post-injury in the tissue immediately contacting the wound (3mm).

The transcriptional responses indicate induction of Wnt signalling in the group treated with the tested formulation of zebularine and retinoic acid observed in regenerating ear pinnae both in the wound vicinity and the noninjured parts. However, many results were not statistically significant, possibly linked to biological variance.

Marked differences are visible for *Gsk3b* in the 3 mm and 5 mm rings (statistically significant) on day 42 post-injury. *Gsk3b* is known to regulate angiogenesis (Wang, Li *et al*. 2025). The significant activity of *Gsk3b* may correlate with the intensive reconstruction of vessels, which is characteristic of the remodelling stage.

In the Wnt signalling, regulation can be positive or negative. Positive Wnt regulation stimulates regenerative processes, wound healing, and angiogenesis. Negative Wnt regulation has opposite effects, such as inhibiting cell proliferation, which may delay wound healing. Positive regulation includes *Lrp5, Lrp6, Wnt10a, Wnt11*. The highest activity of these markers was demonstrated on days 7 and 42, both in 3 mm and 5 mm rings. On days 14-21, the curve flattens, indicating a decreasing activity of these markers. The transcript kinetics may reflect the dynamics of wound closure, the most rapid between days 7 and 14 and slowing down between days 14 and 21 (Fig. 6A).

In principle, *Sfrp2* is connected with the negative regulation of Wnt, specifically the canonical Wnt, while in non-canonical Wnt, its role depends on the context (Hou, Tan *et al*. 2004). Therefore, interpreting the almost 50-fold increased *Sfrp2* transcript level at day 14 under zebularine and retinoic acid treatment may be ambiguous. Furthermore, following day 14, *Sfrp2* expression increases much faster in the control than in the treatment mice. Similarly, as for the positive regulators, these *Sfrp2* transcriptional profiles seem to correspond with intensive tissue regrowth manifested by rapid ear hole closure between days 7 and 14, preceded and followed by markedly lower closure rates (Fig. 6A).

The transcriptional responses of Wnt markers observed during ear pinna hole closure show the dynamism of Wnt signalling in the regeneration process and the significant effects of the epigenetic treatment.

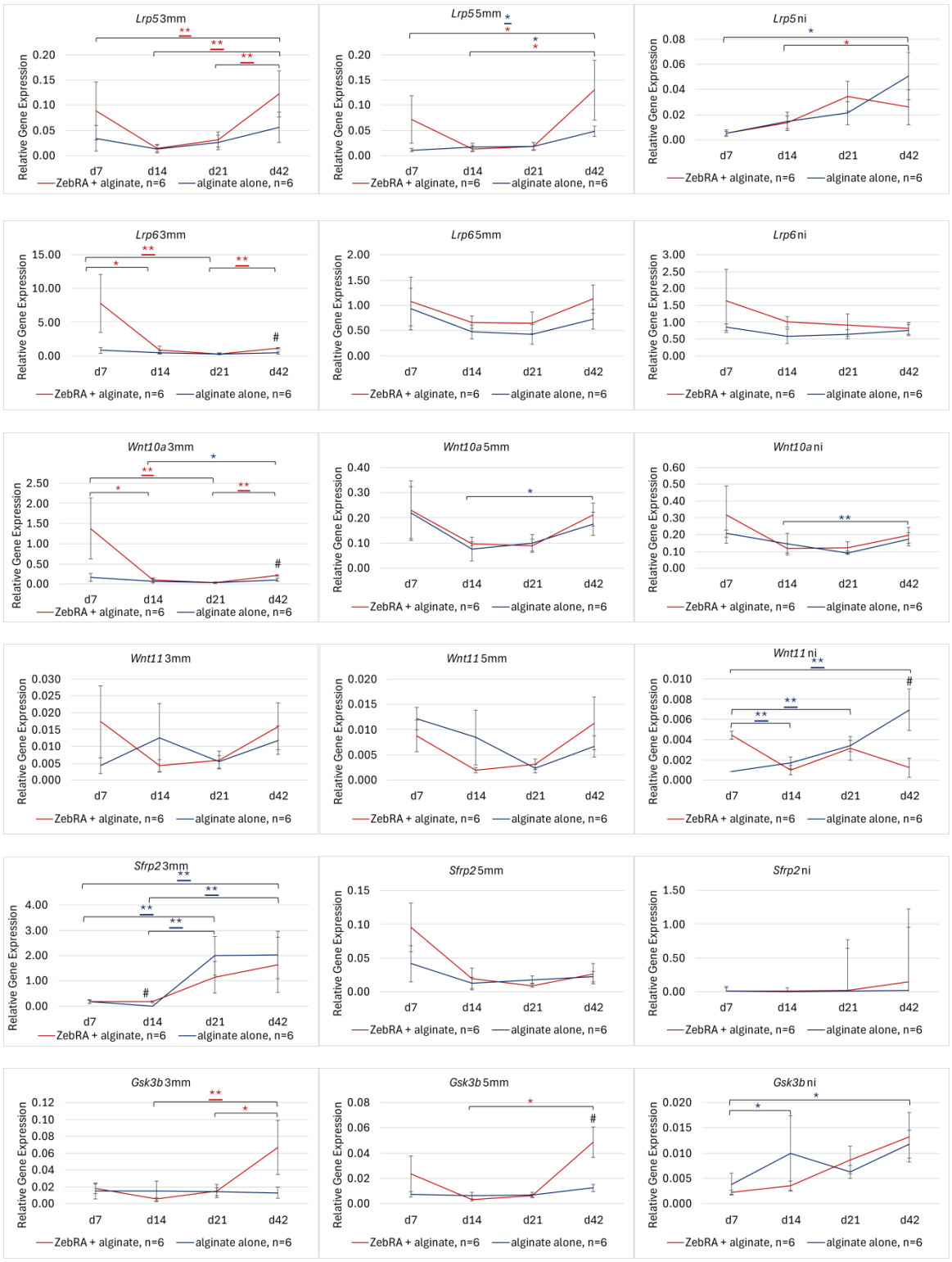

*Figure 17 Transcriptomic responses of Wnt signalling pathway markers in regenerating ear pinnae following subcutaneous injections of zebularine and retinoic acid in alginate carrier. Statistically significant differences between time points were determined using the Kruskal-Wallis test and denoted with asterisks: *<0.05, **<0.01, marked red (*) for the treatment groups receiving zebularine and retinoic acid (**ZebRA**) and navy blue (*) for the controls injected with 2% **alginate alone**; the results significant after the Bonferroni correction are underlined. Statistically significant differences between the treatment and control groups were calculated using the Mann-Whitney U test and indicated with a hash sign (#<0.05). The error bars represent SEM; n=6 (six ear pinnae representing three mice). The examined sites of ear pinna directly are indicated as follows: **3mm** – immediate to the wound, **5mm** – adjacent to the regenerating area, **ni** (non-injured) - distant to the wound.*

Table 8 Expression fold changes of Wnt signalling pathway markers following subcutaneous injections of zebularine and retinoic acid in 2% sodium alginate in regenerating ear pinnae. Statistically significant differences between the treatment group (ZebRA + alginate) and the control group (alginate alone) were determined using the Mann-Whitney U test and denoted: #<0.05; red and green fonts mark increase and decrease in expression in response to ZebRA treatment, respectively.

Gene	Fold change ZebRA/alginate											
	Area: 3mm				Area: 5mm				Area: ni			
	day 7	day 14	day 21	day 42	day 7	day 14	day 21	day 42	day 7	day 14	day 21	day 42
Lrp5	2.587	1.122	1.200	2.172	6.555	0.804	1.029	2.696	1.037	0.952	1.636	0.512
Lrp6	9.596	1.776	1.035	**2.379 #**	1.153	1.396	1.509	1.538	1.924	1.722	1.414	1.062
Wnt10a	8.415	1.434	1.091	**2.071 #**	1.041	1.272	0.892	1.205	1.536	0.828	1.325	1.133
Wnt11	3.994	0.349	1.097	1.346	0.720	0.232	1.341	1.680	5.208	0.574	0.930	**0.176 #**
Sfrp2	0.958	**48.466 #**	0.569	0.801	2.314	1.638	0.499	1.177	1.029	4.750	2.099	6.967
Gsk3b	1.223	0.383	1.069	5.084	3.193	0.501	0.880	**3.908 #**	0.578	0.354	1.369	1.116

Pro-fibrotic markers

Fibrosis is the process associated with scar formation, i.e., the replacement of normal tissue with non-functional fibrous connective tissue within the wound. On the one hand, the increased expression of pro-fibrotic marker genes may indicate scar formation; on the other hand, their induction may mark the increased activity of fibroblasts, which is necessary for wound healing and tissue regeneration (Bainbridge 2013). As previously mentioned, fibroblasts play a crucial role in tissue repair and fibrosis. In the wound healing process, fibroblasts transmit signals to other key types of wound cells and directly close and fill the defect site. However, they appear only at a later stage of wound healing, approximately 5-7 days after the injury. The early recruitment and activity of inflammatory cells and platelets activates their migration to the wound. Then, fibroblasts are responsible for synthesizing and depositing new extracellular matrix to repair the skin's structural skeleton. Fibroblasts recruited to the wound differentiate into myofibroblasts under mechanical tension and cytokines. Myofibroblasts are responsible for wound contracture after injury. In the case of postnatal wound healing, profound activation of fibroblasts by cytokines and the inflammatory environment of the wound leads to the detachment of excess poorly ordered matrix, which leads to fibrosis. Fibrocytes, i.e., circulating fibroblasts, are a group of mesenchymal progenitor cells originating from the bone marrow. They migrate to the injury bed responding to cytokine stimuli and differentiate into contractile fibroblasts under interleukin (IL)-4, IL-13, and interferon (IFN)-ɣ. However, they constitute a small minority of all fibroblasts involved in wound healing in the skin, liver, lungs, heart, blood vessels, and eye cornea. During remodelling, i.e., in the last phase of wound healing, fibroblasts cross-link and reverse the partially deposited extracellular matrix. They replace part of the type III collagen with type I collagen and structurally modify the initially deposited granulation tissue, causing the extracellular matrix to strengthen and stiffen over time, ultimately forming a mature scar (Talbott, Mascharak *et al*. 2022).

Fibroblasts show functional specialization depending on their origin, body location, and spatial position. Connective tissues of mesenchymal origin, including the heart, lungs, gastrointestinal tract, muscles, and nerves, contain specialized fibroblasts. Differences in gene expression have been demonstrated between dermal and nondermal fibroblasts. Fibroblasts from different anatomical sites have different developmental

origins, including neural crest, lateral plate mesoderm, and dermatomyome. There are also significant differences in the architecture of the *dermis* in different parts of the body, which is associated with different potential for disease processes, such as the formation of keloid scars. Differences in the behaviour of fibroblasts from different body sites likely reflect a combination of intrinsic differences and the role of factors such as mechanical loading that vary among body regions. The bone marrow-derived fibroblast population has the ability to differentiate into multiple lineages. At first, it was suggested that they could contribute to the development of the *dermis*, but subsequent research did not confirm this conjecture. Pericytes - fibroblasts associated with blood vessels - are considered the *in vivo* equivalent of stromal stem cells. Pericytes are associated with and surround vascular channels in most tissues. Within muscles, pericytes appear to be able to differentiate into muscle fibres.

The results show a trend for a decrease in pro-fibrotic gene expression levels on days 14 and 21 in the treatment compared to the control group. The decrease contrasts with the increased expression of the pro-fibrotic genes in the initial phase of wound closure on day 7 and on day 42, corresponding to the remodelling phase in the treatment compared to the control group. The trends can be observed in all analysed sites of ear pinna, i.e., 3- and 5-mm rings surrounding the wound and non-injured tissues distant to the wound. The increased expression of pro-fibrotic genes in the treatment relative to the control group reached statistical significance 42 for *Acta2* and *Ccn2* on day 42, while the decrease for *Snai* on day 14.

The decreases in the expression of pro-fibrotic genes following day 7 post-injury (Fig. 18, Table 9) correlate with the highest rate of wound closure between days 7 and 14 (Fig. 6A). The effect of zebularine and retinoic acid treatment on the kinetics of pro-fibrotic transcripts levels may be associated not only with enhanced wound closure but also the restoration of tissue architecture with a characteristic cartilage layer resembling that in the non-injured ear pinna and the absence of scarring demonstrated by histological analysis (Słonimska, Baczyński-Keller *et al*. 2024). The histological results obtained for subcutaneous administration of zebularine and retinoic acid in alginate formulations are consistent with earlier observations for intraperitoneal delivery reported by Sass *et al.* (Sass, Sosnowski *et al*. 2019).

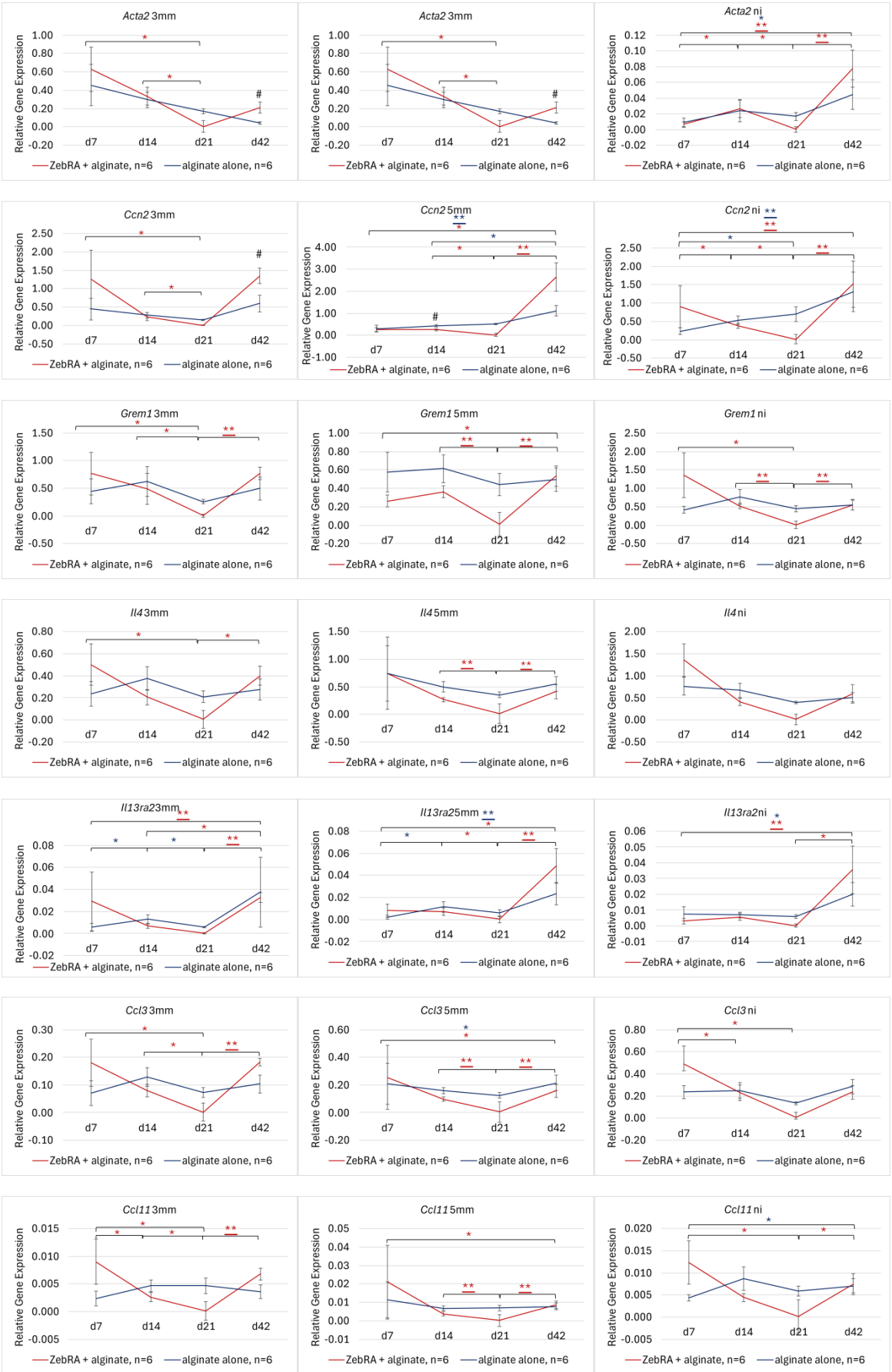
Acta2 3mm
Acta2 3mm
Acta2 ni
Ccn2 3mm
Ccn2 5mm
Ccn2 ni
Grem1 3mm
Grem1 5mm
Grem1 ni
Il4 3mm
Il4 5mm
Il4 ni
Il13ra2 3mm
Il13ra2 5mm
Il13ra2 ni
Ccl3 3mm
Ccl3 5mm
Ccl3 ni
Ccl11 3mm
Ccl11 5mm
Ccl11 ni
Relative Gene Expression
d7
d14
d21
d42
ZebRA + alginate, n=6
alginate alone, n=6

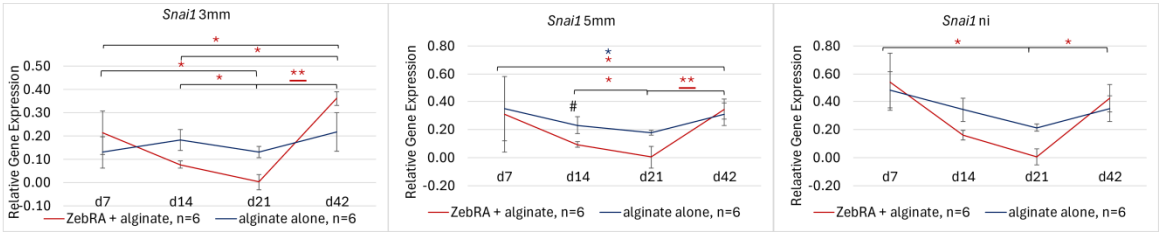

Figure 18 Transcriptomic responses of pro-fibrotic markers in regenerating ear pinnae following subcutaneous injections of zebularine and retinoic acid in alginate carrier.

*Statistically significant differences between time points were determined using the Kruskal-Wallis test and denoted with asterisks: *<0.05, **<0.01, marked red (*) for the treatment groups receiving zebularine and retinoic acid (**ZebRA**) and navy blue (*) for the controls injected with 2% **alginate alone**; the results significant after the Bonferroni correction are underlined. Statistically significant differences between the treatment and control groups were calculated using the Mann-Whitney U test and indicated with a hash sign (#<0.05). The error bars represent SEM; n=6 (six ear pinnae representing three mice). The examined sites of ear pinna directly are indicated as follows:* **3mm** – immediate to the wound, **5mm** – adjacent to the regenerating area, **ni** (non-injured) - distant to the wound.

Table 9 Expression fold changes of pro-fibrotic markers marker following subcutaneous injections of zebularine and retinoic acid in 2% sodium alginate in regenerating ear pinnae. Statistically significant differences between the treatment group (ZebRA + alginate) and the control group (alginate alone) were determined using the Mann-Whitney U test and denoted: #<0.05; red and green fonts mark increase and decrease in expression in response to ZebRA treatment, respectively.

Gene	Fold change ZebRA/alginate											
	Area: 3mm				Area: 5mm				Area: ni			
	day 7	day 14	day 21	day 42	day 7	day 14	day 21	day 42	day 7	day 14	day 21	day 42
Acta2	1.374	1.129	0.022	**5.183 #**	1.569	0.296	0.022	**6.107 #**	0.700	1.108	0.020	1.738
Ccn2	2.825	0.866	0.021	**2.263 #**	0.853	**0.585 #**	0.024	2.384	3.792	0.726	0.020	1.164
Grem1	1.716	0.785	0.018	1.558	0.454	0.590	0.026	1.079	3.268	0.672	0.024	1.018
Il4	2.122	0.545	0.022	1.457	1.004	0.535	0.035	0.752	1.786	0.613	0.029	1.151
Il13ra2	5.242	0.507	0.014	0.873	3.484	0.613	0.028	2.107	0.395	0.827	0.022	1.776
Ccl3	2.537	0.621	0.029	1.772	1.213	0.607	0.042	0.736	2.055	0.919	0.037	0.830
Ccl11	3.774	0.559	0.018	1.901	1.853	0.552	0.028	1.101	2.855	0.509	0.031	1.055
Snai1	1.642	0.428	0.022	1.656	0.882	**0.409 #**	0.031	1.111	1.117	0.466	0.027	1.213

Notably, the anti-fibrotic activity of zebularine treatment has been reported in other models. Zebularine has significantly alleviated renal tubular fibrosis (Koh, Kim *et al.* 2022, Lyu, Xiao *et al.* 2023). In the treatment of fibrosis, zebularine inhibits TGF-β1-induced differentiation of epithelial cells into myofibroblasts, thereby reducing the occurrence of fibrosis (Zhou, Lu *et al.* 2011). Research by Huang *et al.* showed that zebularine increases PGE2 reactivity in fibroblasts. PGE2 is prostaglandin E2 - a lipid mediator - that can limit fibrosis by inhibiting numerous functions of fibroblasts

characterized by excessive proliferation, including in pulmonary fibrosis disease (Huang, Fisher *et al*. 2010).

In addition to the effect of zebularine on fibrosis, that of retinoic acid, the other drug administered, should be considered. Current research shows that treatment with retinoic acid may influence various processes related to the occurrence and progression of fibrotic disease (Zhou, Drummen *et al*. 2012). However, several reports indicate that retinoic acid positively affects the progression of fibrosis and alleviates the accumulation of extracellular matrix. Other sources report that retinoic acid exacerbates fibrosis and induces the accumulation of extracellular matrix. Retinoic acid has been shown to have a protective role in fibrotic diseases, such as liver and renal fibrosis. This is justified by the observations that retinoic acid effectively inhibits the expression of various collagens, including collagen III, collagen 1A1, and procollagen I, as well as numerous other biomolecules, such as α-SMA, TNF-α, IL-6 (Zhou, Drummen *et al*. 2012). However, at a concentration of 0.5 μg/ml, retinoic acid stimulated, but at 2.5 μg/ml, inhibited the production of collagen I (Varani, Mitra *et al*. 1990). Different doses of retinoic acid may have different effects on cell signalling and, therefore, the degree to which components of signalling pathways are up or down-regulated (Zhou, Drummen *et al*. 2012). Retinoic acid is involved in a myriad of signalling pathways in the pathogenesis of fibrotic diseases; therefore, the potential mechanisms leading to its occurrence and progression are complex and involve the dose, the isoform used, and the time point analysed (Zhou, Drummen *et al*. 2012). In addition, retinoic acid promotes exfoliation of the *epidermis*, reducing *stratum corneum* thickness (Maia Campos, Gaspar *et al*. 2015). The exfoliating properties of retinoic acid are utilized in treating *acne* scars (Gozali and Zhou 2015), and they may be involved in the tissue regenerative outcomes observed in ear pinnae.

Cellular models can provide additional insights into the possible actions of zebularine and retinoic acid on fibrosis. Zebularine slightly stimulated the viability of 46BR.1N fibroblast after 72 hours of cultivation at low concentrations (0.1 and 1.0 μg/ml), while at a concentration of 0.01 μg/ml, it exerted an inhibitory effect, potentiated at 10-150 μg/ml (Sass, Sosnowski *et al*. 2019). Retinoic acid promoted fibroblast proliferation at concentrations ranging from 0.5 to 2.0 μg/ml in the MRC-5 fibroblast cell line; no stimulation was observed at higher or lower concentrations. As mentioned above, dependent on concentrations, retinoic acid stimulated (0.5 μg/ml) or

inhibited (over 2.5 μg/ml) collagen I production in fibroblasts. These data indicate that *in vitro* retinoic acid can induce proliferation and extracellular matrix production, mimicking the major changes observed in the *dermis* after topical treatment with this drug (Varani, Mitra *et al*. 1990), but the outcomes are dose-dependent.

The increased expression level of selected pro-fibrotic transcripts may be related to other functions that are not directly connected with fibrosis. For example, *Grem1* has a positive effect on angiogenesis, the *Il4* cytokine (anti-inflammatory cytokine) influences the differentiation of keratinocytes, *Ccl3* attracts T lymphocytes to the wound, producing cytokines necessary for wound healing, and *Ccl11* promotes the migration of endothelial cells and angiogenesis, *Snai1* is necessary for the formation of neural crest. *Il13ra2* is a pro-fibrotic factor, but its overexpression attenuates keloid fibrogenesis (Galvagni, Lentucci *et al*. 2015, Park, Kang *et al*. 2017, Serezani, Bozdogan *et al*. 2017, Johnson, Mahoney *et al*. 2019, Mahmoudi, Mancini *et al*. 2019, Saraswati, Marrow *et al*. 2019, Chao, Zheng *et al*. 2023). *Acta2*-encoded αSMA-stimulated fibroblast proliferation also delays their ageing (Mahmoudi, Mancini *et al*. 2019).

Transcriptional responses of genes with potential importance in regenerative processes in ear pinna depending on the tissue location relative to the wound

Transcriptional responses to injury and the epigenetic treatment in the tissues immediately contacting the wound (3-mm ring), the surrounding area (5-mm ring), and the distal non-injured ear pinna parts allowed the analyses in the spatial context presented as fold changes in Tables 10-13.

Among pluripotency and growth factors, statistically significant changes in transcript levels are shown by *Nanog*, *Sox2*, *Pou5f1* (*Oct4*), *Myc*, and *Vegfa* (Table 10). A significant decrease in *Nanog* expression is observed on day 21 in the 3-mm rings (3mm), i.e. within the tissues immediately contacting the injury and regenerating area relative to both the 5-mm rings surrounding but not directly contacting the area of wound and regeneration (5mm) and the distal non-injured ear pinna parts (ni) in both the treatment and control groups. For *Sox2*, similar effects were determined but proved statistically significant in the control group only. In the 3-mm rings, *Myc*, showed significantly elevated expression compared to 5-mm rings on day 14, with an almost 5-fold increase in response to zebularine and retinoic acid treatment. Also, on day 14, a statistically significant increase in *Vegfa* expression was noted in the 3-mm ring in the treatment group (Table 10).

In the case of neurogenesis genes, statistically significant spatial differences in expression were recorded on day 21. In the treatment and control groups, significantly lower *Reno*, *Neurog1*, and *Gdnf* expression levels were observed in the 3-mm compared to the 5-mm rings and noninjured part of the ear pinnae (Table 11).

Among the genes of the Wnt signalling pathway, marked changes were observed for *Sfrp2*, *Gsk3b*, and *Lrp5*, manifested as an increased expression in the wound vicinity (3mm) compared to the distal parts relative to the wound (5mm, ni) in response to zebularine and retinoic acid. (Table 13) The changes were statistically significant on day 7, and *Sfrp2* reached almost a 50-fold increase.

A statistically significant change in response to zebularine and retinoic acid was also observed for the putative blastema marker *Prrx1* on day 42 post-injury. Increased expression of this gene was demonstrated in the immediate wound vicinity (3mm) compared to the distal, noninjured parts of ear pinnae (ni) (Table 12).

Among the profibrotic markers, worth noting is the elevated expression of *Acta2* in the peri-wound area compared to the noninjured part of ear pinnae (ni) on day 7 post-injury in response to zebularine and retinoic acid, reaching a nearly 18-fold statistically significant increase within the 5-mm ring surrounding (Table 14).

In summary, significant transcriptional differences were observed both between the immediate vicinity of the wound and the surrounding ring (3mm vs 5mm) and between the peri-wound and noninjured part of ear pinnae (3mm and 5mm vs ni). These differences were recorded on days 7, 14, and 21 but not on day 42, except for *Prrx1*. Of note are markedly elevated expression levels in response to zebularine and retinoic acid on day 7 post-injury in the wound area compared to the noninjured ear pinna parts for the Wnt signalling genes *Sfrp2*, *Lrp5*, and *Gsk3b* and a significant induction of *Acta2*, encoding alpha-smooth muscle actin connected with increased cellular motility and contractility in myofibroblasts during wound healing.

Table 10 Changes in the expression of pluripotency markers and growth factors depending on the location relative to the wound in response to subcutaneous injections of zebularine and retinoic acid in 2% sodium alginate into the regenerating ear pinnae. Statistically significant differences between the ear pinna locations were determined using the Friedman test and marked: *<0.05.

Gene	Day	Treatment	Relative expression			Fold change		
			3 mm	5 mm	ni	3 mm/5 mm	5 mm/ni	3 mm/ni
Nanog	d7	ZebRA + alginate	4.966	0.724	1.718	6.859	0.421	2.891
		Alginate alone	0.460	0.850	0.970	0.541	0.876	0.474
	d14	ZebRA + alginate	0.520	0.461	0.710	1.128	**0.649 ***	0.732
		Alginate alone	0.351	0.467	0.537	0.752	0.870	0.654
	d21	ZebRA + alginate	0.147	0.466	0.509	**0.315 ***	0.916	**0.289 ***
		Alginate alone	0.126	0.344	0.501	**0.366 ***	0.687	**0.251 ***
	d42	ZebRA + alginate	0.541	0.565	0.635	0.958	0.890	0.852
		Alginate alone	0.262	0.469	0.456	0.559	1.029	0.575
Sox2	d7	ZebRA + alginate	0.032	0.007	0.015	4.641	0.458	2.127
		Alginate alone	0.004	0.027	0.007	0.132	4.191	0.552
	d14	ZebRA + alginate	0.004	0.003	0.004	1.261	0.811	1.023
		Alginate alone	0.004	0.004	0.004	0.984	0.964	0.948
	d21	ZebRA + alginate	0.003	0.006	0.006	0.540	0.996	0.537
		Alginate alone	0.003	0.007	0.008	**0.396 ***	0.845	**0.335 ***
	d42	ZebRA + alginate	0.014	0.010	0.013	1.407	0.768	1.080
		Alginate alone	0.005	0.009	0.010	0.600	0.930	0.558
Pou5f1	d7	ZebRA + alginate	0.521	0.103	0.172	5.069	0.597	3.025
		Alginate alone	0.087	0.152	0.183	0.572	0.830	0.475
	d14	ZebRA + alginate	0.051	0.044	0.075	1.153	**0.586 ***	0.676
		Alginate alone	0.076	0.071	0.086	1.076	0.824	0.886
	d21	ZebRA + alginate	0.002	0.003	0.003	0.536	1.042	0.559
		Alginate alone	0.001	0.003	0.003	**0.367 ***	0.821	**0.301 ***
	d42	ZebRA + alginate	0.004	0.004	0.005	0.846	0.931	0.787
		Alginate alone	0.000	0.002	0.002	0.189	0.965	0.183
Myc	d7	ZebRA + alginate	0.026	0.007	0.004	3.859	1.571	6.063
		Alginate alone	0.028	0.036	0.006	0.768	5.721	4.392
	d14	ZebRA + alginate	0.057	0.012	0.023	**4.770 ***	0.514	2.450
		Alginate alone	0.046	0.016	0.012	**2.958 ***	1.352	**3.999 ***
	d21	ZebRA + alginate	0.014	0.013	0.027	1.068	0.479	0.511
		Alginate alone	0.024	0.014	0.010	1.741	1.357	2.363
	d42	ZebRA + alginate	0.185	0.175	0.191	1.052	0.920	0.968
		Alginate alone	0.082	0.054	0.064	1.539	0.833	1.281
Klf4	d7	ZebRA + alginate	0.630	0.120	0.303	5.260	0.396	2.082
		Alginate alone	0.100	0.257	0.174	0.390	1.475	0.575
	d14	ZebRA + alginate	0.104	0.058	0.066	1.804	0.874	1.577
		Alginate alone	0.082	0.063	0.057	1.298	1.102	1.430
	d21	ZebRA + alginate	0.099	0.132	0.127	0.755	1.035	0.781
		Alginate alone	0.117	0.093	0.061	1.261	1.534	1.934
	d42	ZebRA + alginate	0.566	0.472	0.367	1.198	1.288	1.543
		Alginate alone	0.091	0.275	0.296	0.331	0.929	0.307

Fgf1	d7	ZebRA + alginate	0.003	0.006	0.001	0.576	5.430	3.125
		Alginate alone	0.000	0.004	0.002	0.016	2.842	0.044
	d14	ZebRA + alginate	0.004	0.001	0.003	3.114	0.499	1.553
		Alginate alone	0.008	0.002	0.002	4.349	0.870	3.786
	d21	ZebRA + alginate	0.001	0.000	0.001	2.751	0.283	0.779
		Alginate alone	0.002	0.001	0.001	1.815	1.221	2.216
	d42	ZebRA + alginate	0.004	ND	ND	ND	ND	ND
		Alginate alone	0.003	0.002	0.001	1.899	1.838	3.491
Vegfa	d7	ZebRA + alginate	0.054	0.007	0.022	7.292	0.335	2.440
		Alginate alone	0.008	0.016	0.005	0.538	2.942	1.584
	d14	ZebRA + alginate	0.007	0.003	0.002	**2.550 ***	1.206	**3.074 ***
		Alginate alone	0.006	0.003	0.002	1.986	1.357	2.694
	d21	ZebRA + alginate	0.006	0.004	0.003	1.302	1.448	1.886
		Alginate alone	0.004	0.003	0.002	1.363	1.531	2.087
	d42	ZebRA + alginate	0.082	0.053	0.019	1.534	2.798	4.290
		Alginate alone	0.000	0.019	0.028	0.015	0.676	0.010
Egf	d7	ZebRA + alginate	0.009	0.003	0.135	2.721	0.024	0.065
		Alginate alone	0.002	0.003	0.001	0.492	3.049	1.499
	d14	ZebRA + alginate	0.002	0.001	0.001	1.983	0.920	1.825
		Alginate alone	0.002	0.001	0.001	2.191	1.293	2.833
	d21	ZebRA + alginate	0.002	0.001	0.002	1.775	0.472	0.838
		Alginate alone	0.002	0.002	0.002	1.032	0.961	0.993
	d42	ZebRA + alginate	0.019	0.016	0.004	1.210	4.079	4.937
		Alginate alone	0.004	0.005	0.006	0.801	0.964	0.772

Table 11 Changes in the expression of neurogenesis genes depending on the location relative to the wound in response to subcutaneous injections of zebularine and retinoic acid in 2% sodium alginate into the regenerating ear pinnae. Statistically significant differences between the ear pinna locations were determined using the Friedman test and marked: *<0.05.

Gene	Day	Treatment	Relative expression			Fold change		
			3 mm	5 mm	ni	3 mm/5 mm	5 mm/ni	3 mm/ni
Reno	d7	ZebRA + alginate	1.070	0.170	0.347	6.290	0.491	3.087
		Alginate alone	0.119	0.232	0.234	0.514	0.991	0.510
	d14	ZebRA + alginate	0.104	0.095	0.139	1.102	0.679	0.749
		Alginate alone	0.087	0.087	0.106	1.003	0.822	0.825
	d21	ZebRA + alginate	0.022	0.076	0.071	**0.285 ***	1.070	**0.305 ***
		Alginate alone	0.021	0.060	0.078	**0.341 ***	0.772	**0.263 ***
	d42	ZebRA + alginate	0.100	0.110	0.112	0.910	0.980	0.891
		Alginate alone	0.049	0.081	0.095	0.604	0.853	0.516
Neurog1	d7	ZebRA + alginate	0.702	0.494	0.934	1.421	0.529	0.752
		Alginate alone	0.251	0.871	0.598	0.289	1.457	0.420
	d14	ZebRA + alginate	0.300	0.267	0.389	1.123	0.687	0.772
		Alginate alone	0.214	0.221	0.265	0.972	0.834	0.810
	d21	ZebRA + alginate	0.104	0.324	0.314	**0.321 ***	1.034	**0.332 ***
		Alginate alone	0.091	0.250	0.354	**0.364 ***	0.705	0.257
	d42	ZebRA + alginate	0.402	0.409	0.469	0.981	0.874	0.857
		Alginate alone	0.240	0.396	0.414	0.606	0.956	0.579
Gdnf	d7	ZebRA + alginate	ND	ND	ND	ND	ND	ND
		Alginate alone	ND	ND	ND	ND	ND	ND
	d14	ZebRA + alginate	0.010	0.011	0.022	0.881	0.496	0.437
		Alginate alone	0.009	0.013	0.013	0.685	0.953	0.653
	d21	ZebRA + alginate	0.007	0.023	0.037	**0.303 ***	0.627	**0.190 ***
		Alginate alone	0.009	0.019	0.031	**0.476 ***	0.631	**0.300 ***
	d42	ZebRA + alginate	0.022	0.019	0.021	1.150	0.933	1.073
		Alginate alone	0.014	0.024	0.025	0.600	0.974	0.585
Tac1	d7	ZebRA + alginate	0.011	0.005	0.004	2.303	1.308	3.013
		Alginate alone	0.002	0.001	0.001	1.772	1.105	1.959
	d14	ZebRA + alginate	0.001	0.001	0.001	1.303	1.329	1.733
		Alginate alone	0.003	0.002	0.003	1.573	0.678	1.067
	d21	ZebRA + alginate	0.001	0.001	0.001	2.655	0.412	1.093
		Alginate alone	0.001	0.001	0.001	0.812	1.132	0.919
	d42	ZebRA + alginate	0.223	0.001	0.001	151.661	1.781	270.115
		Alginate alone	0.001	0.001	0.001	1.081	1.314	1.420

Table 12 Changes in the expression of potential blastema marker depending on the location relative to the wound in response to subcutaneous injections of zebularine and retinoic acid in 2% sodium alginate into the regenerating ear pinnae. Statistically significant differences between the ear pinna locations were determined using the Friedman test and marked: *<0.05.

Gene	Day	Treatment	Relative expression			Fold change		
			3 mm	5 mm	ni	3 mm/5 mm	5 mm/ni	3 mm/ni
Prrx1	d7	ZebRA + alginate	0.111	0.086	0.193	1.291	0.447	0.576
		Alginate alone	0.158	0.078	0.033	2.023	2.347	4.748
	d14	ZebRA + alginate	0.143	0.041	0.045	3.501	0.900	3.153
		Alginate alone	0.154	0.064	0.023	2.419	2.799	6.771
	d21	ZebRA + alginate	0.192	0.067	0.075	2.853	0.896	2.557
		Alginate alone	0.226	0.091	0.109	**2.495 ***	0.828	2.066
	d42	ZebRA + alginate	0.887	0.459	0.222	1.931	2.065	**3.987 ***
		Alginate alone	0.439	0.218	0.203	2.010	1.074	2.158

Table 13 Changes in the expression of Wnt signalling pathway markers depending on the location relative to the wound in response to subcutaneous injections of zebularine and retinoic acid in 2% sodium alginate into the regenerating ear pinnae. Statistically significant differences between the ear pinna locations were determined using the Friedman test and marked: *<0.05.

Gene	Day	Treatment	Relative expression			Fold change		
			3 mm	5 mm	ni	3 mm/5 mm	5 mm/ni	3 mm/ni
Lrp5	d7	ZebRA + alginate	0.088	0.072	0.005	1.234	13.392	**16.522** *
		Alginate alone	0.034	0.011	0.005	3.126	2.119	6.625
	d14	ZebRA + alginate	0.014	0.014	0.014	1.057	0.995	1.052
		Alginate alone	0.013	0.017	0.014	0.758	1.177	0.892
	d21	ZebRA + alginate	0.032	0.019	0.035	1.702	0.541	0.922
		Alginate alone	0.027	0.018	0.021	1.460	0.860	1.256
	d42	ZebRA + alginate	0.123	0.130	0.026	0.945	5.009	4.735
		Alginate alone	0.057	0.048	0.051	1.173	0.951	1.116
Lrp6	d7	ZebRA + alginate	7.759	1.075	1.636	7.217	0.657	4.743
		Alginate alone	0.809	0.932	0.850	0.867	1.096	0.951
	d14	ZebRA + alginate	0.877	0.662	1.005	1.325	0.658	0.872
		Alginate alone	0.494	0.474	0.584	1.041	0.812	0.845
	d21	ZebRA + alginate	0.303	0.649	0.910	0.467	0.713	0.333
		Alginate alone	0.293	0.430	0.643	0.680	0.668	0.455
	d42	ZebRA + alginate	1.127	1.124	0.812	1.003	1.384	1.389
		Alginate alone	0.474	0.731	0.764	0.649	0.956	0.620
Wnt10a	d7	ZebRA + alginate	1.378	0.229	0.318	6.005	0.723	4.339
		Alginate alone	0.164	0.220	0.207	0.743	1.066	0.792
	d14	ZebRA + alginate	0.093	0.097	0.119	0.961	0.817	0.785
		Alginate alone	0.065	0.076	0.144	0.852	0.531	0.453
	d21	ZebRA + alginate	0.037	0.090	0.121	0.414	0.742	0.307
		Alginate alone	0.034	0.101	0.091	0.338	1.102	0.373
	d42	ZebRA + alginate	0.217	0.212	0.197	1.024	1.074	1.100
		Alginate alone	0.105	0.176	0.174	0.596	1.010	0.602
Wnt11	d7	ZebRA + alginate	0.017	0.009	0.004	1.977	1.970	3.896
		Alginate alone	0.004	0.012	0.001	0.357	14.248	5.080
	d14	ZebRA + alginate	0.004	0.002	0.001	2.227	2.001	4.455
		Alginate alone	0.013	0.008	0.002	1.482	4.949	7.334
	d21	ZebRA + alginate	0.006	0.003	0.003	1.903	0.998	1.899
		Alginate alone	0.005	0.002	0.003	2.327	0.692	1.610
	d42	ZebRA + alginate	0.016	0.011	0.001	1.416	9.196	13.020
		Alginate alone	0.012	0.007	0.007	1.767	0.964	1.704
Sfrp2	d7	ZebRA + alginate	0.166	0.096	0.003	1.733	27.496	**47.645** *
		Alginate alone	0.174	0.041	0.003	4.185	12.224	51.160
	d14	ZebRA + alginate	0.164	0.020	0.013	8.301	1.557	12.929
		Alginate alone	0.003	0.012	0.003	0.281	4.517	1.267
	d21	ZebRA + alginate	1.132	0.009	0.018	127.672	0.501	63.981
		Alginate alone	1.987	0.018	0.008	111.947	2.106	235.815
	d42	ZebRA + alginate	1.629	0.026	1.119	62.106	0.023	1.456
		Alginate alone	2.034	0.022	0.020	91.208	1.110	101.203

Gsk3b	d7	ZebRA + alginate	0.018	0.024	0.002	0.773	10.678	**8.256 ***
		Alginate alone	0.015	0.007	0.004	2.019	1.932	3.901
	d14	ZebRA + alginate	0.006	0.003	0.004	1.747	0.922	1.612
		Alginate alone	0.015	0.006	0.010	2.288	0.652	1.491
	d21	ZebRA + alginate	0.015	0.006	0.009	2.443	0.720	1.759
		Alginate alone	0.014	0.007	0.006	**2.011 ***	1.120	**2.252 ***
	d42	ZebRA + alginate	0.067	0.049	0.013	1.373	3.705	5.087
		Alginate alone	0.013	0.012	0.012	1.055	1.058	1.116

Table 14 Changes in the expression of profibrotic markers depending on the location relative to the wound in response to subcutaneous injections of zebularine and retinoic acid in 2% sodium alginate into the regenerating ear pinnae. Statistically significant differences between the ear pinna locations were determined using the Friedman test and marked: *<0.05.

Gene	Day	Treatment	Relative expression			Fold change		
			3 mm	5 mm	ni	3 mm/5 mm	5 mm/ni	3 mm/ni
Acta2	d7	ZebRA + alginate	0.626	0.116	0.007	5.382	**17.851** *	96.079
		Alginate alone	0.456	0.074	0.009	6.147	7.968	48.979
	d14	ZebRA + alginate	0.335	0.032	0.026	10.309	1.227	12.653
		Alginate alone	0.296	0.110	0.024	2.701	4.595	12.411
	d21	ZebRA + alginate	0.163	0.039	0.014	4.215	2.827	11.915
		Alginate alone	0.168	0.047	0.017	3.553	2.839	10.087
	d42	ZebRA + alginate	0.213	0.276	0.077	0.774	3.564	2.759
		Alginate alone	0.041	0.045	0.044	0.912	1.014	0.925
Ccn2	d7	ZebRA + alginate	1.333	0.257	0.894	5.182	0.288	1.491
		Alginate alone	0.445	0.302	0.236	1.475	1.280	1.888
	d14	ZebRA + alginate	0.239	0.248	0.384	0.967	0.645	0.623
		Alginate alone	0.276	0.423	0.529	0.653	0.800	0.522
	d21	ZebRA + alginate	0.152	0.462	0.541	0.329	0.854	0.280
		Alginate alone	0.150	0.508	0.702	0.295	0.724	0.213
	d42	ZebRA + alginate	1.351	2.644	1.515	0.511	1.745	0.892
		Alginate alone	0.041	0.045	0.044	0.912	1.014	0.925
Grem1	d7	ZebRA + alginate	0.764	0.261	1.356	2.930	0.192	0.563
		Alginate alone	0.445	0.574	0.415	0.776	1.383	1.073
	d14	ZebRA + alginate	0.490	0.361	0.514	1.357	0.702	0.953
		Alginate alone	0.624	0.612	0.766	1.020	0.799	0.815
	d21	ZebRA + alginate	0.239	0.407	0.446	0.587	0.912	0.536
		Alginate alone	0.258	0.440	0.446	0.587	0.987	0.580
	d42	ZebRA + alginate	0.772	0.533	0.553	1.447	0.965	1.397
		Alginate alone	0.597	1.109	1.301	0.538	0.852	0.459
Il4	d7	ZebRA + alginate	0.502	0.746	1.193	0.673	0.626	0.421
		Alginate alone	0.237	0.743	0.759	0.318	0.979	0.312
	d14	ZebRA + alginate	0.206	0.267	0.410	0.772	0.650	**0.502** *
		Alginate alone	0.378	0.498	0.669	**0.758** *	0.745	**0.564** *
	d21	ZebRA + alginate	0.254	0.443	0.499	0.574	0.888	0.510
		Alginate alone	0.210	0.355	0.392	0.591	0.907	0.536
	d42	ZebRA + alginate	0.401	0.415	0.588	0.967	0.705	0.681
		Alginate alone	0.495	0.494	0.543	1.002	0.910	0.912
Il13ra2	d7	ZebRA + alginate	0.096	0.008	0.003	12.001	2.697	32.365
		Alginate alone	0.006	0.002	0.008	2.427	0.306	0.742
	d14	ZebRA + alginate	0.007	0.007	0.006	0.957	1.235	1.182
		Alginate alone	0.013	0.011	0.007	1.156	1.666	1.926
	d21	ZebRA + alginate	0.004	0.006	0.005	0.725	1.143	0.828
		Alginate alone	0.006	0.006	0.006	1.006	0.997	1.003
	d42	ZebRA + alginate	0.033	0.049	0.036	0.674	1.374	0.926
		Alginate alone	0.275	0.552	0.511	0.499	1.079	0.539

Ccl3	d7	ZebRA + alginate	0.180	0.254	0.487	0.711	0.521	0.370
		Alginate alone	0.071	0.209	0.237	0.340	0.882	0.300
	d14	ZebRA + alginate	0.080	0.096	0.229	0.825	0.420	**0.347 ***
		Alginate alone	0.128	0.159	0.250	0.806	0.637	**0.513 ***
	d21	ZebRA + alginate	0.112	0.187	0.211	0.603	0.886	0.534
		Alginate alone	0.073	0.124	0.135	0.590	0.918	0.542
	d42	ZebRA + alginate	0.183	0.157	0.237	1.162	0.664	0.772
		Alginate alone	0.038	0.023	0.020	1.625	1.159	1.883
Ccl11	d7	ZebRA + alginate	0.009	0.021	0.012	0.428	1.712	0.733
		Alginate alone	0.002	0.011	0.004	0.210	2.638	0.555
	d14	ZebRA + alginate	0.003	0.004	0.004	0.698	0.846	**0.591 ***
		Alginate alone	0.005	0.007	0.009	0.689	0.780	**0.538 ***
	d21	ZebRA + alginate	0.005	0.007	0.009	0.716	0.767	0.549
		Alginate alone	0.005	0.007	0.006	0.677	1.163	0.787
	d42	ZebRA + alginate	0.007	0.009	0.007	0.783	1.164	0.912
		Alginate alone	0.004	0.008	0.007	0.454	1.115	0.506
Snai1	d7	ZebRA + alginate	0.214	0.310	0.541	0.689	0.574	0.395
		Alginate alone	0.130	0.352	0.484	0.370	0.727	0.269
	d14	ZebRA + alginate	0.078	0.095	0.160	0.822	**0.594 ***	**0.488 ***
		Alginate alone	0.182	0.232	0.343	0.786	0.676	0.532
	d21	ZebRA + alginate	0.152	0.202	0.253	0.755	0.797	0.602
		Alginate alone	0.131	0.180	0.216	0.728	0.836	0.608
	d42	ZebRA + alginate	0.361	0.347	0.425	1.042	0.815	0.850
		Alginate alone	0.218	0.312	0.350	0.699	0.891	0.622

FINAL COMMENTS

Development of alginate-based pro-regenerative formulations

Previous research by the Laboratory for Regenerative Biotechnology team has proven that the demethylating agent zebularine and the transcription activator retinoic acid induce complex tissue regeneration in an ear punch wound model in mice (Sass, Sosnowski *et al*. 2019). My research aimed to develop the potential of this regenerative treatment by introducing a carrier of the active substances. After preliminary testing of several formulations based on chitosan and sodium alginate, 2% sodium alginate was chosen as the leading carrier. The carrier in the form of a sol, i.e. non-crosslinked 2% sodium alginate solution in water, allowed for the administration of both hydrophilic zebularine and hydrophobic retinoic acid. Zebularine is well dissolved in 2% sodium alginate. The hydrophobic retinoic acid in the alginate solution dispersed, forming evenly distributed fine crystals. An innovative methodological improvement was the application of a bead mill homogenizer for efficient mixing compounds poorly soluble in aqueous solutions with the alginate carrier. The method allows for obtaining homogenous alginate-based preparations of substances practically insoluble in water, like retinoic acid. It is worth noting that the retinoic acid content in the alginate formulation (4000 μg/ml) exceeded its water solubility (0.25 μM, 0.075 μg/ml, (Szuts and Harosi 1991) by five orders of magnitude. Both zebularine-alginate and retinoic acid-alginate formulations proved injectable.

Both zebularine and retinoic acid administered separately promoted the closure of the ear pinnae punch wounds compared to the control of alginate alone; however, the differences were not significant at all time points. Doubling the dose of zebularine improved the closure. The combined administration of zebularine and retinoic acid accelerated the process and resulted in statistically significant effects at all time points tested. Therefore, downstream transcriptomic experiments were performed for the combined treatment. Moreover, the synergism of zebularine and retinoic acid action in ear pinna regeneration demonstrated previously for intraperitoneal injections in saline (zebularine) and oil (retinoic acid) (Sass, Sosnowski *et al*. 2019) encouraged me to concentrate on the combined treatment. Nevertheless, the significant activity of the drugs applied separately deserves attention. The results may provide clues for

researchers interested in administering zebularine alone or retinoic acid alone in the alginate carrier, not necessarily in regenerative applications.

It should be noted that increased ear pinna hole closure signals tissue growth, but it does not warrant enhanced regenerative response. Additional analyses are necessary to assess the structure of restored tissues. A histological examination of the regenerated ear pinnae was performed on day 42 after the injury. The structure of the regrowing tissue resembled that of a normal ear pinna, and regenerating cartilage was observed after treatment with zebularine and retinoic acid. Immunofluorescence examinations demonstrated the formation of blood vessels and nerve fibres in the regenerated areas of ear pinnae (Słonimska, Baczyński-Keller *et al*. 2024).

An ultrasound examination was performed to check the degree and speed of alginate degradation under the skin of mice. This method allowed the remaining preparations to be checked at several time points without sacrificing many animals. The analysis showed a gradual decrease in ultrasonic signals from the alginate preparations under the skin, indicating a gradual absorption of the alginate carrier. Additionally, *in vitro* release studies showed no diffusion-mediated release of hydrophobic retinoic acid from the alginate carrier (Słonimska, Baczyński-Keller *et al*. 2024). Ultrasound live imaging and *in vitro* release studies indicate that alginate carrier absorption under the skin is responsible for the pro-regenerative effects of retinoic acid formulations manifested in improved ear pinna hole closure. The alginate carrier has proven to be safe, even though administered subcutaneously in significant amounts. Two subcutaneous injections of zebularine and retinoic acid in the alginate carrier were sufficient to induce the regenerative effect compared to multiple intraperitoneal injections in saline (Sass, Sosnowski *et al*. 2019). The mice did not show any side effects - they did not behave apathetically, they were not irritated. Their fur was in good condition, and their weight did not change. There were no signs of necrosis, irritation, or inflammation at the injection site or its surroundings. This proves the toleration of the tested preparations under the skin.

Transcriptomic responses to alginate-based formulations of zebularine and retinoic acid in regenerating ear pinnae

Sustained release from alginate-based formulations extends tissue exposure to the tested drugs, thus opening exciting insights into examining transcriptomic responses

in regenerating animal organs. The investigations focussed on the activity of selected gene panels of potential importance in wound healing and tissue regeneration, including pluripotency and growth factors, nerve growth, Wnt pathway markers, pro-fibrotic genes and a putative blastema marker. The analyses were scheduled for days 7, 14, 21, and 42 post-injury to address the dynamism of the regeneration process. The transcriptional responses of the alginate-based formulations of zebularine and retinoic acid on gene expression were examined both in the regenerated tissue (3-m rings) and the area adjacent to the regenerated area (5-mm rings), as well as in the noninjured tissue (ni), i.e., in the e ear pinna part distal to the wound. The use of quantitative PCR allowed the sensitive determination of 27 transcripts of interest in multiple tissue samples, representing 6 mice of control and 6 mice of the treatment group, in 4 time points and 3 different tissue sites.

Zebularine with retinoic acid administered in the alginate carrier significantly changed expression levels of several genes related to tissue regeneration, such as pluripotency markers, growth factors, neurogenesis, and those of Wnt signalling. Even more pronounced changes were observed in the kinetics of transcript levels, and most of them showed statistically significant. Such results may be explained by dramatic gene expression changes over time during the regeneration process and the relatively moderate effect of the epigenetic treatment on the transcript levels, although the changes can be consequential regarding tissue regeneration outcomes.

In general, the highest levels of expression of pluripotency markers and growth factors, Wnt neurogenesis, and pro-fibrotic genes were recorded on day 7, i.e., at the beginning of the regeneration process; then, they decreased on days 14 and 21 and increased again on day 42. The increases on days 7 and 42 tend to be higher in response to the treatment than the carrier alone. One of the most remarkable differences was the activation of *Fbxo15*, an embryonic stem cell marker used by Takahashi and Yamanaka in their Nobel prize-winning work (Yamanaka 2013) to determine pluripotency induction. My experiments showed transcriptional activation of *Fbxo15* almost exclusively in response to the epigenetic treatment on day 7 post-injury. Day 7, the earliest time point examined, corresponds to the late inflammatory and early growth phase of ear pinna hole closure. At this time point, the closure is minimal, if any. Day 42, when the ear hole closure plateaus, corresponds to the remodelling phase. Days 14 and 21 are time points when the most rapid ear hole closure is recorded (Fig. 6A). For a large group of

the examined genes, including *Nanog*, *Sox2*, *Pou5f1* (Aguirre, Escobar *et al*. 2023), *Klf4*, *Fgf1*, *Neurog1*, *Lrp5*, *Ccn2* the transcriptional activity tends to decrease when tissue regrowth is most intensive. The induction of pluripotency and neurogenesis genes corresponds with earlier observations in ear pinna following treatment with zebularine (Sass, Sosnowski *et al*. 2019). The induction of Wnt and neurogenesis genes is consistent with genome-wide methylome changes and transcriptome changes in response to zebularine and retinoic acid a day 7 post-injury (Słonimska, Baczyński-Keller *et al*. 2024). The activity of neurogenesis genes can also be associated with the formation of new nerve networks demonstrated in the restored tissues (Słonimska, Baczyński-Keller *et al*. 2024). Pro-fibrotic gene activation appears unexpected, considering that ear pinna wounds did not show scarring on day 42 post-injury, as demonstrated by histological examination (Słonimska, Baczyński-Keller *et al*. 2024). The elevated levels of pro-fibrotic transcripts may reflect the enhanced activity of fibroblasts in the early phase of ear hole closure and tissue remodelling. The transcriptional activation of Wnt, pluripotency and neurogenesis genes in ear pinnae regenerating in response to zebularine-mediated treatment is consistent with previous observations (Sass, Sosnowski *et al*. 2019, Słonimska, Baczyński-Keller *et al*. 2024). Specificaly, increases in activity of Wnt genes in reponse to zebularine and retinoic acid administered in alginate formulations were observed in independent experiments also on day 7 and 42 post-injury (Skowron 2024).

Critical remarks

The presented research used a model of ear pinna punch wound. Thanks to the complexity of this organ, it is possible to monitor regeneration in various types of tissues, such as skin, cartilage, nerves, vessels, and muscles. The issue of recognizing the ear pinna injury model as a skin wound-healing model remains debatable. A fundamental difference exists between the selected model and wounds after full-thickness skin excision. In an excision dosrsal skin wound model, the entire exposed surface deprived of skin can be considered an open wound, while only the edges around the holes can be regarded as wounds in the ear pinna. A remarkable advantage of the ear pinna model is the absence of wound contraction, a typical complication in mice experiments on excisional dorsal skin wounds. However, the ear pinna model goes

beyond dermal wound healing. Some studies indicate that regenerative responses in ear pinnae are connected with enhanced regeneration capability in other organs (Gawronska-Kozak 2004, Seifert, Monaghan *et al*. 2012, Sosnowski, Sass *et al*. 2022). The ear pinna tissue's complexity, the experiment's simplicity and convenient quantitation based on the progress of the ear hole closure make the model attractive for testing regenerative drug candidates and their combinations with different carriers.

Significance and novelty

An innovative solution was using a bead mill homogenizer to mix poorly soluble compounds in aqueous solutions with the alginate carrier. This method allows for obtaining homogeneous preparations based on alginates, which contain substances practically insoluble in water, like retinoic acid. This is important information because many drugs are hydrophobic and for mixing with aqueous carriers, and they are often initially dissolved in dimethyl sulfoxide (DMSO). However, the use of DMSO is associated with an undesirable effect related to its harmful interference with fundamental life processes (Santos, Figueira-Coelho *et al*. 2003, Verheijen, Lienhard *et al*. 2019). The exceptional advantage of the approach lies in safety and simplicity. The alginate carrier of non-animal origin is known for excellent biocompatibility and stability. Unlike multi-component carriers and covalently modified polymers, the simplicity of composition and preparation provides a fundamental basis for reproducibility. The method presented here was successfully applied, testing other hydrophobic small molecules with promising pro-regenerative potentials, specifically subcutaneous administration of flavonoids (the aglycon forms) in large doses (Słonimska 2022).

In the context of therapeutical development, subcutaneous injection is decisively more attractive than intraperitoneal administration. Few drugs are administered intraperitoneally, requiring trained personnel, and the approach is burdensome for animals and patients. Subcutaneous injections may be safely self-administered, e.g., Ozempic, one of the best-selling drugs currently, which translates into this route's growing popularity (Dubbelboer and Sjögren 2022).

Another methodological improvement worth noting is using the ultrasound approach for live imaging of subcutaneously injected alginate formulations in mice. Although image

interpretation may seem challenging compared to fluorescent or radioactive methods, the protocol saves animals and does not require expensive and inconvenient labelling.

To date, the *Fbxo15* gene has been well characterized in the context of stem cells, especially embryonic stem cells in mice. Previous studies have focused mainly on its role in pluripotency and early embryonic development (Tokuzawa, Kaiho *et al*. 2003, Cerneckis, Cai *et al*. 2024). A review of the currently available literature does not provide evidence that *Fbxo15* has been investigated strictly in the context of tissue regeneration in animal models. Therefore, the analysis of the expression level of *Fbxo15* in the regenerating mouse ear pinna is a new and vital contribution to the investigation of the role of *Fbxo15* in regeneration.

FUTURE PROSPECTS

The work has shown that subcutaneously administered formulations of zebularine and retinoic acid in 2% sodium alginate induced the regeneration of the ear pinna and did not cause adverse effects in animals. This formulation can be tested for various types of different tissues and injuries. The safety of subcutaneous injections of pro-regenerative alginate formulations with zebularine and retinoic acid warrants further studies involving site administration to surface and internal lesions, e.g. peripheral nerve injuries. Efficient and straightforward preparing alginate-based formulations can be applied to test other small-molecule pro-regenerative drug candidates, which may be particularly helpful for hydrophobic compounds.

The transcriptomic analysis provided a wealth of information about the regeneration process at the molecular level. As many genes involved in regenerative responses represent very low expression levels, the application of digital PCR should be considered to improve detection and accuracy.

Fbx15, a member of F-box proteins known to participate in signal transduction and cell-cycle regulation, encoded by the *Fbxo15* gene, is known to play an essential role in maintaining stem cell pluripotency. However, there is currently no evidence that it is directly involved in animal tissue regeneration processes. *Fbxo15* transcripts were detected in regenerating ear pinnae. Although the levels were low, they indicated the activation of *Fbxo15* in response to epigenetic therapy and stimulation of regeneration. Further insights into *Fbxo15* are needed to determine its role in tissue regeneration beyond the context of cell pluripotency.

LIST OF MAJOR ABBREVIATIONS AND SYMBOLS

BDNF – brain-derived neurotrophic factor

BMMSC - bone marrow-derived mesenchymal stem cells

DMSO – dimethyl sulfoxide

DMD - Duchenne muscular dystrophy

DNMT – DNA methyltransferase

DRG – dorsal root ganglion

ECM – extracellular matrix

EET - epoxyeicosatreic acids

EGF - epidermal growth factor

EPCs – endothelial progenitor cells

ES - embryonic stem

ESC - epidermal stem cells

EZH2 – enhancer of zest homolog 2

FGF - fibroblast growth factor

Fz – Frizzled protein

HATs - histone acetyltransferases

HDACs – histone-lysine deacetylases

HFSCs – hair follicle stem cells

IGF - insulin-like growth factor

iPSCs - induced pluripotent stem cells

ISWI – Imitation SWI

KAT – lysine acetyltransferases

KDMs – lysine demethylases

KGF - keratinocyte growth factor

KMT – lysine methyltransferases

lncRNA – long non-coding RNA

MSCs – mesenchymal stem cells

ncRNA – non-coding RNA

NKA - neurokinin A

NuRD/MI-2/CHD - Nucleosome Remodeling and Deacetylase/Mi-2/Chromodomain Helicase DNA-binding

PcG - Polycomb group proteins

PCNA – proliferation cell nuclear antigen

PDGF - platelet-derived growth factors

PGE2 – prostaglandin E2

SAH - S-adenosylhomocysteine levels

SAM - S-adenosylmethionine

SWI/SNF – Switch/Sucrose Non-Fermentable

TETs – translocation enzymes

TGF - transforming growth factors

TGF-β - transforming growth factor beta

TREGs - regulatory T cells

TrkB – tropomyosin B receptor

TrxG - Trithorax group proteins

VEGF - vascular endothelial growth factor

BIBLIOGRAPHY

1. Abarca-Buis, R. F. and E. Krötzsch (2023). "Proximal ear hole injury heals by limited regeneration during the early postnatal phase in mice." Journal of Anatomy **242**(3): 402-416.
2. Ackermann, P. W. and D. A. Hart (2013). "Influence of comorbidities: neuropathy, vasculopathy, and diabetes on healing response quality." Advances in wound care **2**(8): 410-421.
3. Aguirre, M., M. Escobar, S. Forero Amézquita, D. Cubillos, C. Rincón, P. Vanegas, M. P. Tarazona, S. Atuesta Escobar, J. C. Blanco and L. G. Celis (2023). "Application of the Yamanaka transcription factors Oct4, Sox2, Klf4, and c-Myc from the laboratory to the clinic." Genes **14**(9): 1697.
4. Al-Shamkhani, A. and R. Duncan (1995). "Radioiodination of alginate via covalently-bound tyrosinamide allows monitoring of its fate in vivo." Journal of bioactive and compatible polymers **10**(1): 4-13.
5. Alapure, B. V., Y. Lu, H. Peng and S. Hong (2018). "Surgical denervation of specific cutaneous nerves impedes excisional wound healing of small animal ear pinnae." Molecular neurobiology **55**: 1236-1243.
6. Anisha, T. B. K. (2024). "A review on the teratogenic effects of isotretinoin."
7. Aomatsu, K., T. Arao, K. Abe, A. Kodama, K. Sugioka, K. Matsumoto, K. Kudo, H. Kimura, Y. Fujita and H. Hayashi (2012). "Slug is upregulated during wound healing and regulates cellular phenotypes in corneal epithelial cells." Investigative ophthalmology & visual science **53**(2): 751-756.
8. Arnold, I. and F. M. Watt (2001). "c-Myc activation in transgenic mouse epidermis results in mobilization of stem cells and differentiation of their progeny." Current biology **11**(8): 558-568.
9. Arora, C. K., S. K. Chaudhury and P. S. Chauhan (1968). "Sodium-alginate toxicity in mice." Indian J Physiol Pharmacol **12**(3): 129-130.
10. Augst, A. D., H. J. Kong and D. J. Mooney (2006). "Alginate hydrogels as biomaterials." Macromolecular bioscience **6**(8): 623-633.
11. Baddour, J. A., K. Sousounis and P. A. Tsonis (2012). "Organ repair and regeneration: an overview." Birth Defects Research Part C: Embryo Today: Reviews **96**(1): 1-29.
12. Bai, R., Y. Guo, W. Liu, Y. Song, Z. Yu and X. Ma (2023). "The roles of WNT signaling pathways in skin development and mechanical-stretch-induced skin regeneration." Biomolecules **13**(12): 1702.
13. Bainbridge, P. (2013). "Wound healing and the role of fibroblasts." Journal of wound care **22**(8).
14. Balakrishnan, B. and A. Jayakrishnan (2005). "Self-cross-linking biopolymers as injectable in situ forming biodegradable scaffolds." Biomaterials **26**(18): 3941-3951.
15. Balnis, J., E. L. Jackson, L. A. Drake, D. V. Singer, R. B. Ramos, H. A. Singer and A. Jaitovich (2025). "Rapamycin improves satellite cells' autophagy and muscle regeneration during hypercapnia." JCI insight **10**(1): e182842.
16. Banach-Kopeć, A., S. Mania, J. Pilch, E. Augustin, I. Gabriel and R. Tylingo (2022). "A novel method of endotoxins removal from chitosan hydrogel as a potential bioink component obtained by CO2 saturation." International Journal of Molecular Sciences **23**(10): 5505.
17. Bartel, D. P. (2009). "MicroRNAs: target recognition and regulatory functions." cell **136**(2): 215-233.
18. Basso, J., A. Miranda, S. Nunes, T. Cova, J. Sousa, C. Vitorino and A. Pais (2018). "Hydrogel-based drug delivery nanosystems for the treatment of brain tumors." Gels **4**(3): 62.
19. Bastakoty, D., S. Saraswati, J. Cates, E. Lee, L. B. Nanney and P. P. Young (2015). "Inhibition of Wnt/β-catenin pathway promotes regenerative repair of cutaneous and cartilage injury." The FASEB Journal **29**(12): 4881.

20. Becker, T. A., M. C. Preul, W. D. Bichard, D. R. Kipke and C. G. McDougall (2007). "Preliminary investigation of calcium alginate gel as a biocompatible material for endovascular aneurysm embolization in vivo." Neurosurgery **60**(6): 1119-1128.
21. Bedelbaeva, K., B. Cameron, J. Latella, A. Aslanukov, D. Gourevitch, R. Davuluri and E. Heber-Katz (2023). "Epithelial–mesenchymal transition: an organizing principle of mammalian regeneration." Frontiers in Cell and Developmental Biology **11**: 1101480.
22. Ben-Kasus, T., Z. Ben-Zvi, V. E. Marquez, J. A. Kelley and R. Agbaria (2005). "Metabolic activation of zebularine, a novel DNA methylation inhibitor, in human bladder carcinoma cells." Biochemical pharmacology **70**(1): 121-133.
23. Bettica, P., S. Petrini, V. D'Oria, A. D'Amico, M. Catteruccia, M. Pane, S. Sivo, F. Magri, S. Brajkovic and S. Messina (2016). "Histological effects of givinostat in boys with Duchenne muscular dystrophy." Neuromuscular Disorders **26**(10): 643-649.
24. Birsoy, K., Z. Chen and J. Friedman (2008). "Transcriptional regulation of adipogenesis by KLF4." Cell metabolism **7**(4): 339-347.
25. Blaheta, R. A. and J. Cinatl Jr (2002). "Anti-tumor mechanisms of valproate: a novel role for an old drug." Medicinal research reviews **22**(5): 492-511.
26. Blankenhorn, E. P., S. Troutman, L. D. Clark, X.-M. Zhang, P. Chen and E. Heber-Katz (2003). "Sexually dimorphic genes regulate healing and regeneration in MRL mice." Mammalian genome **14**: 250-260.
27. Blum, N. and G. Begemann (2013). "The roles of endogenous retinoid signaling in organ and appendage regeneration." Cellular and Molecular Life Sciences **70**: 3907-3927.
28. Bosch, T. C. (2007). "Why polyps regenerate and we don't: towards a cellular and molecular framework for Hydra regeneration." Developmental biology **303**(2): 421-433.
29. Bouhadir, K. H., K. Y. Lee, E. Alsberg, K. L. Damm, K. W. Anderson and D. J. Mooney (2001). "Degradation of partially oxidized alginate and its potential application for tissue engineering." Biotechnology progress **17**(5): 945-950.
30. Brotzmann, K., S. E. Escher, P. Walker and T. Braunbeck (2022). "Potential of the zebrafish (Danio rerio) embryo test to discriminate between chemicals of similar molecular structure—A study with valproic acid and 14 of its analogues." Archives of toxicology **96**(11): 3033-3051.
31. Buckley, G., A. D. Metcalfe and M. W. Ferguson (2011). "Peripheral nerve regeneration in the MRL/MpJ ear wound model." Journal of anatomy **218**(2): 163-172.
32. Buckley, G., J. Wong, A. D. Metcalfe and M. W. Ferguson (2012). "Denervation affects regenerative responses in MRL/MpJ and repair in C57BL/6 ear wounds." Journal of anatomy **220**(1): 3-12.
33. Bünemann, E., N.-P. Hoff, B. A. Buhren, U. Wiesner, S. Meller, E. Bölke, A. Müller-Homey, R. Kubitza, T. Ruzicka and A. Zlotnik (2018). "Chemokine ligand–receptor interactions critically regulate cutaneous wound healing." European journal of medical research **23**: 1-17.
34. Burkholder, T., C. Foltz, E. Karlsson, C. G. Linton and J. M. Smith (2012). "Health evaluation of experimental laboratory mice." Current protocols in mouse biology **2**(2): 145-165.
35. Burnett, M. G. and E. L. Zager (2004). "Pathophysiology of peripheral nerve injury: a brief review." Neurosurgical focus **16**(5): 1-7.
36. Carlson, B. M. (2007). "Resource Review." Cell Stem Cell **1**.
37. Cattelan, G., A. Guerrero Gerbolés, R. Foresti, P. P. Pramstaller, A. Rossini, M. Miragoli and C. Caffarra Malvezzi (2020). "Alginate formulations: current developments in the race for hydrogel-based cardiac regeneration." Frontiers in bioengineering and biotechnology **8**: 414.
38. Cedar, H. and Y. Bergman (2012). "Programming of DNA methylation patterns." Annual review of biochemistry **81**(1): 97-117.

39. Cerneckis, J., H. Cai and Y. Shi (2024). "Induced pluripotent stem cells (iPSCs): molecular mechanisms of induction and applications." Signal Transduction and Targeted Therapy **9**(1): 112.
40. Chadwick, R. B., L. Bu, H. Yu, Y. Hu, J. E. Wergedal, S. Mohan and D. J. Baylink (2007). "Digit tip regrowth and differential gene expression in MRL/Mpj, DBA/2, and C57BL/6 mice." Wound Repair and Regeneration **15**(2): 275-284.
41. Chao, H., L. Zheng, P. Hsu, J. He, R. Wu, S. Xu, R. Zeng, Y. Zhou, H. Ma and H. Liu (2023). "IL-13RA2 downregulation in fibroblasts promotes keloid fibrosis via JAK/STAT6 activation." JCI insight **8**(6): e157091.
42. Chávez-Galán, L., M. L. Olleros, D. Vesin and I. Garcia (2015). "Much more than M1 and M2 macrophages, there are also CD169+ and TCR+ macrophages." Frontiers in immunology **6**: 263.
43. Chen, T.-H., F. E. Weber, J. Malina-Altzinger and C. Ghayor (2019). "Epigenetic drugs as new therapy for tumor necrosis factor-α-compromised bone healing." Bone **127**: 49-58.
44. Chen, Y., H. Sun, X. Yao, Y. Yu, T. Tian, W. Xu, Y. Zhou and H. Ouyang (2021). "Pharmaceutical therapeutics for articular regeneration and restoration: State-of-the-art technology for screening small molecular drugs." Cellular and Molecular Life Sciences **78**: 8127-8155.
45. Cheng, J. C., C. B. Matsen, F. A. Gonzales, W. Ye, S. Greer, V. E. Marquez, P. A. Jones and E. U. Selker (2003). "Inhibition of DNA methylation and reactivation of silenced genes by zebularine." Journal of the National Cancer Institute **95**(5): 399-409.
46. Cheng, J. C., C. B. Yoo, D. J. Weisenberger, J. Chuang, C. Wozniak, G. Liang, V. E. Marquez, S. Greer, T. F. Orntoft and T. Thykjaer (2004). "Preferential response of cancer cells to zebularine." Cancer cell **6**(2): 151-158.
47. Chenoweth, M. B. (1948). "The toxicity of sodium alginate in cats." Annals of surgery **127**(6): 1173.
48. Chuong, C.-M., V. A. Randall, R. B. Widelitz, P. Wu and T.-X. Jiang (2012). "Physiological regeneration of skin appendages and implications for regenerative medicine." Physiology **27**(2): 61-72.
49. Clapier, C. R. and B. R. Cairns (2009). "The biology of chromatin remodeling complexes." Annual review of biochemistry **78**(1): 273-304.
50. Clark, L. D., R. K. Clark and E. Heber-Katz (1998). "A new murine model for mammalian wound repair and regeneration." Clinical immunology and immunopathology **88**(1): 35-45.
51. Consalvi, S., V. Saccone, L. Giordani, G. Minetti, C. Mozzetta and P. L. Puri (2011). "Histone deacetylase inhibitors in the treatment of muscular dystrophies: epigenetic drugs for genetic diseases." Molecular medicine **17**: 457-465.
52. Coşkun, G., E. Karaca, M. Ozyurtlu, S. Özbek, A. Yermezler and İ. Çavuşoğlu (2014). "Histological evaluation of wound healing performance of electrospun poly (vinyl alcohol)/sodium alginate as wound dressing in vivo." Bio-Medical Materials and Engineering **24**(2): 1527-1536.
53. Cunningham, T. J. and G. Duester (2015). "Mechanisms of retinoic acid signalling and its roles in organ and limb development." Nature reviews Molecular cell biology **16**(2): 110-123.
54. Dai, W., Z. Liu, M. Yan, X. Nian, F. Hong, Z. Zhou, C. Wang, X. Fu, X. Li and M. Jiang (2024). "Nucleoporin Seh1 controls murine neocortical development via transcriptional repression of p21 in neural stem cells." Developmental Cell **59**(4): 482-495. e486.
55. Dalton, V. S., E. Kolshus and D. M. McLoughlin (2014). "Epigenetics and depression: return of the repressed." Journal of affective disorders **155**: 1-12.
56. De Carvalho, D. D., J. S. You and P. A. Jones (2010). "DNA methylation and cellular reprogramming." Trends in cell biology **20**(10): 609-617.

57. Delcuve, G. P., D. H. Khan and J. R. Davie (2012). "Roles of histone deacetylases in epigenetic regulation: emerging paradigms from studies with inhibitors." Clinical epigenetics **4**: 1-13.
58. Delcuve, G. P., M. Rastegar and J. R. Davie (2009). "Epigenetic control." Journal of cellular physiology **219**(2): 243-250.
59. Dettmar, P. W., V. Strugala and J. C. Richardson (2011). "The key role alginates play in health." Food Hydrocolloids **25**(2): 263-266.
60. Du, B., W. P. Cawthorn, A. Su, C. R. Doucette, Y. Yao, N. Hemati, S. Kampert, C. McCoin, D. T. Broome and C. J. Rosen (2013). "The transcription factor paired-related homeobox 1 (Prrx1) inhibits adipogenesis by activating transforming growth factor-β (TGFβ) signaling." Journal of Biological Chemistry **288**(5): 3036-3047.
61. Dubbelboer, I. R. and E. Sjögren (2022). "Physiological based pharmacokinetic and biopharmaceutics modelling of subcutaneously administered compounds–An overview of in silico models." International journal of pharmaceutics **621**: 121808.
62. Duester, G. (2008). "Retinoic acid synthesis and signaling during early organogenesis." Cell **134**(6): 921-931.
63. Eguizabal, C., N. Montserrat, A. Veiga and J. C. I. Belmonte (2013). Dedifferentiation, transdifferentiation, and reprogramming: future directions in regenerative medicine. Seminars in reproductive medicine, Thieme Medical Publishers.
64. Enoch, S. and D. J. Leaper (2008). "Basic science of wound healing." Surgery (Oxford) **26**(2): 31-37.
65. Estiragues, M., E. Morillo, C. Sarrasqueta and J. Olivas-Menayo (2023). Wound Care and Treatment of Scars. Post-maternity Body Changes: Obstetric Fundamentals and Surgical Reshaping, Springer**:** 197-229.
66. Evans, C. E., M. L. Iruela-Arispe and Y.-Y. Zhao (2021). "Mechanisms of endothelial regeneration and vascular repair and their application to regenerative medicine." The American journal of pathology **191**(1): 52-65.
67. Falanga, V. (2005). "Wound healing and its impairment in the diabetic foot." The Lancet **366**(9498): 1736-1743.
68. Fathke, C., L. Wilson, K. Shah, B. Kim, A. Hocking, R. Moon and F. Isik (2006). "Wnt signaling induces epithelial differentiation during cutaneous wound healing." BMC cell biology **7**: 1-9.
69. Fitzgerald, J., C. Rich, D. Burkhardt, J. Allen, A. S. Herzka and C. B. Little (2008). "Evidence for articular cartilage regeneration in MRL/MpJ mice." Osteoarthritis and cartilage **16**(11): 1319-1326.
70. Fong, H., K. A. Hohenstein and P. J. Donovan (2008). "Regulation of self-renewal and pluripotency by Sox2 in human embryonic stem cells." Stem cells **26**(8): 1931-1938.
71. Fu, X., L. Fang, H. Li, X. Li, B. Cheng and Z. Sheng (2007). "Adipose tissue extract enhances skin wound healing." Wound repair and regeneration **15**(4): 540-548.
72. Funakoshi, R., M. Irie and T. Ukita (1961). "Syntheses of unnatural pyrimidine nucleosides." Chemical and Pharmaceutical Bulletin **9**(5): 406-408.
73. Gaire, J., J. A. Varholick, S. Rana, M. D. Sunshine, S. Doré, W. B. Barbazuk, D. D. Fuller, M. Maden and C. S. Simmons (2021). "Spiny mouse (Acomys): an emerging research organism for regenerative medicine with applications beyond the skin." npj Regenerative Medicine **6**(1): 1.
74. Galvagni, F., C. Lentucci, F. Neri, D. Dettori, C. De Clemente, M. Orlandini, F. Anselmi, S. Rapelli, M. Grillo and S. Borghi (2015). "Snai1 promotes ESC exit from the pluripotency by direct repression of self-renewal genes." Stem Cells **33**(3): 742-750.
75. Ganesan, A., P. B. Arimondo, M. G. Rots, C. Jeronimo and M. Berdasco (2019). "The timeline of epigenetic drug discovery: from reality to dreams." Clinical epigenetics **11**: 1-17.
76. Gao, C., M. Liu, J. Chen and X. Zhang (2009). "Preparation and controlled degradation of oxidized sodium alginate hydrogel." Polymer degradation and stability **94**(9): 1405-1410.

77. Gao, J., L. Fan, L. Zhao and Y. Su (2021). "The interaction of Notch and Wnt signaling pathways in vertebrate regeneration." Cell Regeneration **10**: 1-17.
78. Gawriluk, T. R., J. Simkin, K. L. Thompson, S. K. Biswas, Z. Clare-Salzler, J. M. Kimani, S. G. Kiama, J. J. Smith, V. O. Ezenwa and A. W. Seifert (2016). "Comparative analysis of ear-hole closure identifies epimorphic regeneration as a discrete trait in mammals." Nature communications **7**(1): 11164.
79. Gawronska-Kozak, B. (2004). "Regeneration in the ears of immunodeficient mice: identification and lineage analysis of mesenchymal stem cells." Tissue Engineering **10**(7-8): 1251-1265.
80. Geiman, T. M. and K. D. Robertson (2002). "Chromatin remodeling, histone modifications, and DNA methylation—how does it all fit together?" Journal of cellular biochemistry **87**(2): 117-125.
81. Ghatak, S., E. V. Maytin, J. A. Mack, V. C. Hascall, I. Atanelishvili, R. Moreno Rodriguez, R. R. Markwald and S. Misra (2015). "Roles of proteoglycans and glycosaminoglycans in wound healing and fibrosis." International journal of cell biology **2015**(1): 834893.
82. Giannini, G., W. Cabri, C. Fattorusso and M. Rodriquez "Future Medicinal Chemistry-Targeted Oncology."
83. Gibelli, B., A. El-Fattah, G. Giugliano, M. Proh and E. Grosso (2009). "Thyroid stem cells–danger or resource?" Acta Otorhinolaryngologica Italica **29**(6): 290.
84. Girardi, F. and F. Le Grand (2018). "Wnt signaling in skeletal muscle development and regeneration." Progress in molecular biology and translational science **153**: 157-179.
85. Gobrecht, P., A. Andreadaki, H. Diekmann, A. Heskamp, M. Leibinger and D. Fischer (2016). "Promotion of functional nerve regeneration by inhibition of microtubule detyrosination." Journal of Neuroscience **36**(14): 3890-3902.
86. Godwin, J. W., A. R. Pinto and N. A. Rosenthal (2013). "Macrophages are required for adult salamander limb regeneration." Proceedings of the National Academy of Sciences **110**(23): 9415-9420.
87. Goenka, S., V. Sant and S. Sant (2014). "Graphene-based nanomaterials for drug delivery and tissue engineering." Journal of Controlled Release **173**: 75-88.
88. Gorroñogoitia, I., U. Urtaza, A. Zubiarrain-Laserna, A. Alonso-Varona and A. M. Zaldua (2022). "A study of the printability of alginate-based bioinks by 3D bioprinting for articular cartilage tissue engineering." Polymers **14**(2): 354.
89. Goss, R. J. and L. N. Grimes (1972). "Tissue interactions in the regeneration of rabbit ear holes." American Zoologist **12**(1): 151-157.
90. Gourevitch, D., L. Clark, P. Chen, A. Seitz, S. J. Samulewicz and E. Heber-Katz (2003). "Matrix metalloproteinase activity correlates with blastema formation in the regenerating MRL mouse ear hole model." Developmental dynamics: an official publication of the American Association of Anatomists **226**(2): 377-387.
91. Gozali, M. V. and B. Zhou (2015). "Effective treatments of atrophic acne scars." The Journal of clinical and aesthetic dermatology **8**(5): 33.
92. Górnikiewicz, B., A. Ronowicz, M. Krzemiński and P. Sachadyn (2016). "Changes in gene methylation patterns in neonatal murine hearts: Implications for the regenerative potential." BMC genomics **17**: 1-15.
93. Graefe, S. B. and S. S. Mohiuddin (2020). "Biochemistry, substance P."
94. Guo, S. a. and L. A. DiPietro (2010). "Factors affecting wound healing." Journal of dental research **89**(3): 219-229.
95. Halberstadt, C., C. Austin, J. Rowley, C. Culberson, A. Loebsack, S. Wyatt, S. Coleman, L. Blacksten, K. Burg and D. Mooney (2002). "A hydrogel material for plastic and reconstructive applications injected into the subcutaneous space of a sheep." Tissue engineering **8**(2): 309-319.
96. Hamidi, M., A. Azadi and P. Rafiei (2008). "Hydrogel nanoparticles in drug delivery." Advanced drug delivery reviews **60**(15): 1638-1649.

97. Hanh, N. T., P. T. N. Bich and H. T. T. Thao (2019). "Acute and subchronic oral toxicity assessment of calcium hydroxyapatite-alginate in animals." Vietnam Journal of Chemistry **57**(1): 16-20.
98. Hao, Y., T. Creson, L. Zhang, P. Li, F. Du, P. Yuan, T. D. Gould, H. K. Manji and G. Chen (2004). "Mood stabilizer valproate promotes ERK pathway-dependent cortical neuronal growth and neurogenesis." Journal of Neuroscience **24**(29): 6590-6599.
99. Hashemzadeh, M. R., N. Mahdavi-Shahri, A. R. Bahrami, M. Kheirabadi, F. Naseri and M. Atighi (2015). "Use of an in vitro model in tissue engineering to study wound repair and differentiation of blastema tissue from rabbit pinna." In Vitro Cellular & Developmental Biology-Animal **51**: 680-689.
100. Hattori, N., Y. Imao, K. Nishino, N. Hattori, J. Ohgane, S. Yagi, S. Tanaka and K. Shiota (2007). "Epigenetic regulation of Nanog gene in embryonic stem and trophoblast stem cells." Genes to Cells **12**(3): 387-396.
101. Hayashi, S., K. Tamura and H. Yokoyama (2020). Chromatin dynamics underlying the precise regeneration of a vertebrate limb–epigenetic regulation and cellular memory. Seminars in Cell & Developmental Biology, Elsevier.
102. Hayek, A., A. E. Kerstetter-Fogle, E. Sachlos and T. Bollenbach (2012). "Kartogenin: a game-changer in regenerative medicine." Regenerative Medicine **7**(4): 475-475.
103. He, S., H. Sun, L. Lin, Y. Zhang, J. Chen, L. Liang, Y. Li, M. Zhang, X. Yang and X. Wang (2017). "Passive DNA demethylation preferentially up-regulates pluripotency-related genes and facilitates the generation of induced pluripotent stem cells." Journal of Biological Chemistry **292**(45): 18542-18555.
104. Heinrichs, D., M.-L. Berres, A. Nellen, P. Fischer, D. Scholten, C. Trautwein, H. E. Wasmuth and H. Sahin (2013). "The chemokine CCL3 promotes experimental liver fibrosis in mice." PloS one **8**(6): e66106.
105. Henry, T. R. (2003). "The history of valproate in clinical neuroscience." Psychopharmacology bulletin **37**: 5-16.
106. Herranz, M., J. Martín-Caballero, M. F. Fraga, J. Ruiz-Cabello, J. M. Flores, M. Desco, V. Marquez and M. Esteller (2006). "The novel DNA methylation inhibitor zebularine is effective against the development of murine T-cell lymphoma." Blood **107**(3): 1174-1177.
107. Hezroni, H., R. Ben-Tov Perry, N. Gil, N. Degani and I. Ulitsky (2020). "Regulation of neuronal commitment in mouse embryonic stem cells by the Reno1/Bahcc1 locus." EMBO reports **21**(11): e51264.
108. Higgins, G. (1931). "Restoration of the liver of the white rat following partial surgical removal." AMA Arch Pathol **12**: 186-202.
109. Ho, A. D., W. Wagner and U. Mahlknecht (2005). "Stem cells and ageing: The potential of stem cells to overcome age-related deteriorations of the body in regenerative medicine." EMBO reports **6**(S1): S35-S38.
110. Ho, L. and G. R. Crabtree (2010). "Chromatin remodelling during development." Nature **463**(7280): 474-484.
111. Hodge, B. D., T. Sanvictores and R. T. Brodell (2018). "Anatomy, skin sweat glands."
112. Hoemann, C. D. and D. Fong (2017). Immunological responses to chitosan for biomedical applications. Chitosan Based Biomaterials Volume 1, Elsevier**:** 45-79.
113. Hofmann, E., J. Fink, A. Eberl, E.-M. Prugger, D. Kolb, H. Luze, S. Schwingenschuh, T. Birngruber, C. Magnes and S. I. Mautner (2021). "A novel human ex vivo skin model to study early local responses to burn injuries." Scientific reports **11**(1): 364.
114. Hou, X., Y. Tan, M. Li, S. K. Dey and S. K. Das (2004). "Canonical Wnt signaling is critical to estrogen-mediated uterine growth." Molecular endocrinology **18**(12): 3035-3049.

115. Hsu, X.-L., L.-C. Wu, J.-Y. Hsieh and Y.-Y. Huang (2021). "Nanoparticle-hydrogel composite drug delivery system for potential ocular applications." Polymers **13**(4): 642.
116. Hu, C., W. Lu, A. Mata, K. Nishinari and Y. Fang (2021). "Ions-induced gelation of alginate: Mechanisms and applications." International Journal of Biological Macromolecules **177**: 578-588.
117. Huang, S. K., A. S. Fisher, A. M. Scruggs, E. S. White, C. M. Hogaboam, B. C. Richardson and M. Peters-Golden (2010). "Hypermethylation of PTGER2 confers prostaglandin E2 resistance in fibrotic fibroblasts from humans and mice." The American journal of pathology **177**(5): 2245-2255.
118. Iismaa, S. E., X. Kaidonis, A. M. Nicks, N. Bogush, K. Kikuchi, N. Naqvi, R. P. Harvey, A. Husain and R. M. Graham (2018). "Comparative regenerative mechanisms across different mammalian tissues." NPJ Regenerative medicine **3**(1): 6.
119. Jambhekar, A., A. Dhall and Y. Shi (2019). "Roles and regulation of histone methylation in animal development." Nature reviews Molecular cell biology **20**(10): 625-641.
120. Jayant, R. D., M. J. McShane and R. Srivastava (2011). "In vitro and in vivo evaluation of anti-inflammatory agents using nanoengineered alginate carriers: Towards localized implant inflammation suppression." International journal of pharmaceutics **403**(1-2): 268-275.
121. Jiang, D. and K. Scharffetter-Kochanek (2020). "Mesenchymal stem cells adaptively respond to environmental cues thereby improving granulation tissue formation and wound healing." Frontiers in cell and developmental biology **8**: 697.
122. Jin, Y., T. Liu, H. Luo, Y. Liu and D. Liu (2022). "Targeting epigenetic regulatory enzymes for cancer therapeutics: novel small-molecule epidrug development." Frontiers in Oncology **12**: 848221.
123. Johnson, K., S. Zhu, M. S. Tremblay, J. N. Payette, J. Wang, L. C. Bouchez, S. Meeusen, A. Althage, C. Y. Cho and X. Wu (2012). "A stem cell–based approach to cartilage repair." Science **336**(6082): 717-721.
124. Johnson, Z. I., C. Mahoney, J. Heo, E. Frankel, D. R. Julian and C. C. Yates (2019). "The role of chemokines in fibrotic dermal remodeling and wound healing." Fibrosis in Disease: An Organ-Based Guide to Disease Pathophysiology and Therapeutic Considerations: 3-24.
125. Jopling, C., S. Boue and J. C. I. Belmonte (2011). "Dedifferentiation, transdifferentiation and reprogramming: three routes to regeneration." Nature reviews Molecular cell biology **12**(2): 79-89.
126. Kameda, T., T. Imamura and K. Nakashima (2018). "Epigenetic regulation of neural stem cell differentiation towards spinal cord regeneration." Cell and tissue research **371**: 189-199.
127. Kaminskas, E., A. T. Farrell, Y.-C. Wang, R. Sridhara and R. Pazdur (2005). "FDA drug approval summary: azacitidine (5-azacytidine, Vidaza™) for injectable suspension." The oncologist **10**(3): 176-182.
128. Kapoor, M., S. Liu, X. Shi-Wen, K. Huh, M. McCann, C. P. Denton, J. R. Woodgett, D. J. Abraham and A. Leask (2008). "GSK-3β in mouse fibroblasts controls wound healing and fibrosis through an endothelin-1–dependent mechanism." The Journal of clinical investigation **118**(10): 3279-3290.
129. Kato, Y., H. Onishi and Y. Machida (2003). "Application of chitin and chitosan derivatives in the pharmaceutical field." Current Pharmaceutical Biotechnology **4**(5): 303-309.
130. Kaucká, M. and I. Adameyko (2014). "Non-canonical functions of the peripheral nerve." Experimental cell research **321**(1): 17-24.
131. Kaur, G., S. S. S. Rathod, M. M. Ghoneim, S. Alshehri, J. Ahmad, A. Mishra and N. A. Alhakamy (2022). "DNA methylation: a promising approach in management of Alzheimer's disease and other neurodegenerative disorders." Biology **11**(1): 90.

132. Ketabforoush, A., F. Faghihi, F. Azedi, A. Ariaei, M. A. Habibi, M. Khalili, B. H. Ashtiani, M. T. Joghataei and W. D. Arnold (2024). "Sodium phenylbutyrate and tauroursodeoxycholic acid: a story of hope turned to disappointment in amyotrophic lateral sclerosis treatment." Clinical Drug Investigation **44**(7): 495-512.
133. Kim, C. H., V. E. Marquez, D. T. Mao, D. R. Haines and J. J. McCormack (1986). "Synthesis of pyrimidin-2-one nucleosides as acid-stable inhibitors of cytidine deaminase." Journal of medicinal chemistry **29**(8): 1374-1380.
134. Kim, Y. S., D. H. Lew, K. C. Tark, D. K. Rah and J. P. Hong (2010). "Effect of recombinant human epidermal growth factor against cutaneous scar formation in murine full-thickness wound healing." Journal of Korean medical science **25**(4): 589.
135. Koh, E. S., S. Kim, M. Son, J.-Y. Park, J. Pyo, W.-Y. Kim, M. Kim, S. Chung, C. W. Park and H.-S. Kim (2022). "The protective effect of zebularine, an inhibitor of DNA methyltransferase, on renal tubulointerstitial inflammation and fibrosis." International Journal of Molecular Sciences **23**(22): 14045.
136. Komiya, Y. and R. Habas (2008). "Wnt signal transduction pathways." Organogenesis **4**(2): 68-75.
137. Kooistra, S. M. and K. Helin (2012). "Molecular mechanisms and potential functions of histone demethylases." Nature reviews Molecular cell biology **13**(5): 297-311.
138. Kragl, M., D. Knapp, E. Nacu, S. Khattak, M. Maden, H. H. Epperlein and E. M. Tanaka (2009). "Cells keep a memory of their tissue origin during axolotl limb regeneration." Nature **460**(7251): 60-65.
139. Kumar, A. and J. P. Brockes (2012). "Nerve dependence in tissue, organ, and appendage regeneration." Trends in neurosciences **35**(11): 691-699.
140. Laflamme, M. A. and C. E. Murry (2011). "Heart regeneration." Nature **473**(7347): 326-335.
141. Lalley, A. L., N. A. Dyment, N. Kazemi, K. Kenter, C. Gooch, D. W. Rowe, D. L. Butler and J. T. Shearn (2015). "Improved biomechanical and biological outcomes in the MRL/MpJ murine strain following a full-length patellar tendon injury." Journal of Orthopaedic Research® **33**(11): 1693-1703.
142. Lamb, Y. N. (2024). "Givinostat: first approval." Drugs **84**(7): 849-856.
143. Lan, L., D. Cui, K. Nowka and M. Derwahl (2007). "Stem cells derived from goiters in adults form spheres in response to intense growth stimulation and require thyrotropin for differentiation into thyrocytes." The Journal of Clinical Endocrinology & Metabolism **92**(9): 3681-3688.
144. Landa, N., L. Miller, M. S. Feinberg, R. Holbova, M. Shachar, I. Freeman, S. Cohen and J. Leor (2008). "Effect of injectable alginate implant on cardiac remodeling and function after recent and old infarcts in rat." Circulation **117**(11): 1388-1396.
145. Langer, R. and N. A. Peppas (2003). "Advances in biomaterials, drug delivery, and bionanotechnology." AIChE Journal **49**(12): 2990-3006.
146. Laverdet, B., A. Danigo, D. Girard, L. Magy, C. Demiot and A. Desmoulière (2015). "Skin innervation: important roles during normal and pathological cutaneous repair."
147. Leavitt, T., M. S. Hu, M. R. Borrelli, M. Januszyk, J. T. Garcia, R. C. Ransom, S. Mascharak, U. M. Litzenburger, G. G. Walmsley and C. D. Marshall (2020). "Prrx1 fibroblasts represent a pro-fibrotic lineage in the mouse ventral dermis." Cell reports **33**(6).
148. Ledwon, J. K., E. E. Vaca, C. C. Huang, L. J. Kelsey, J. L. McGrath, J. Topczewski, A. K. Gosain and J. M. Topczewska (2022). "Langerhans cells and SFRP2/Wnt/beta-catenin signalling control adaptation of skin epidermis to mechanical stretching." Journal of cellular and molecular medicine **26**(3): 764-775.
149. Lee, R. J., A. Hinson, R. Bauernschmitt, K. Matschke, Q. Fang, D. L. Mann, R. Dowling, N. Schiller and H. N. Sabbah (2015). "The feasibility and safety of Algisyl-LVR™ as a method of left ventricular augmentation in patients with dilated

cardiomyopathy: initial first in man clinical results." International journal of cardiology **199**: 18-24.
150. Leferovich, J. M., K. Bedelbaeva, S. Samulewicz, X.-M. Zhang, D. Zwas, E. B. Lankford and E. Heber-Katz (2001). "Heart regeneration in adult MRL mice." Proceedings of the National Academy of Sciences **98**(17): 9830-9835.
151. Lehoczky, J. A., B. Robert and C. J. Tabin (2011). "Mouse digit tip regeneration is mediated by fate-restricted progenitor cells." Proceedings of the National Academy of Sciences **108**(51): 20609-20614.
152. Leussink, B., A. Brouwer, M. El Khattabi, R. E. Poelmann, A. C. Gittenberger-de Groot and F. Meijlink (1995). "Expression patterns of the paired-related homeobox genes MHox/Prx1 and S8/Prx2 suggest roles in development of the heart and the forebrain." Mechanisms of development **52**(1): 51-64.
153. Li, J., H. Zheng, J. Wang, F. Yu, R. J. Morris, T. C. Wang, S. Huang and W. Ai (2012). "Expression of Kruppel-like factor KLF4 in mouse hair follicle stem cells contributes to cutaneous wound healing." PLoS One **7**(6): e39663.
154. Li, Q., M. Frank, C. I. Thisse, B. V. Thisse and J. Uitto (2011). "Zebrafish: a model system to study heritable skin diseases." Journal of Investigative Dermatology **131**(3): 565-571.
155. Liang, C., G. Qiao, Y. Liu, L. Tian, N. Hui, J. Li, Y. Ma, H. Li, Q. Zhao and W. Cao (2021). "Overview of all-trans-retinoic acid (ATRA) and its analogues: Structures, activities, and mechanisms in acute promyelocytic leukaemia." European Journal of Medicinal Chemistry **220**: 113451.
156. Liberski, A. R. (2016). "Three-dimensional printing of alginate: From seaweeds to heart valve scaffolds." QScience Connect **2016**(2): 3.
157. Lillico, R., N. Stesco, T. Khorshid Amhad, C. Cortes, M. P. Namaka and T. M. Lakowski (2016). "Inhibitors of enzymes catalyzing modifications to histone lysine residues: structure, function and activity." Future medicinal chemistry **8**(8): 879-897.
158. Limbourg, A., S. Schnabel, V. J. Lozanovski, L. C. Napp, T.-C. Ha, T. Maetzig, J. Bauersachs, H. Y. Naim, A. Schambach and F. P. Limbourg (2014). "Genetic reporter analysis reveals an expandable reservoir of OCT4+ cells in adult skin." Cell Regeneration **3**: 1-6.
159. Lin, H.-R., K. Sung and W.-J. Vong (2004). "In situ gelling of alginate/pluronic solutions for ophthalmic delivery of pilocarpine." Biomacromolecules **5**(6): 2358-2365.
160. Lin, Y.-W., P.-S. Liu, K. A. Pook and L.-N. Wei (2018). "Glyburide and retinoic acid synergize to promote wound healing by anti-inflammation and RIP140 degradation." Scientific reports **8**(1): 834.
161. Liu, S., K. Thompson and A. Leask (2014). "CCN2 expression by fibroblasts is not required for cutaneous tissue repair." Wound repair and regeneration **22**(1): 119-124.
162. Londono, R., A. X. Sun, R. S. Tuan and T. P. Lozito (2018). "Tissue repair and epimorphic regeneration: an overview." Current pathobiology reports **6**: 61-69.
163. Longaker, M. T., D. J. Whitby, M. W. Ferguson, H. P. Lorenz, M. R. Harrison and N. S. Adzick (1994). "Adult skin wounds in the fetal environment heal with scar formation." Annals of surgery **219**(1): 65-72.
164. Lorden, E. R., H. M. Levinson and K. W. Leong (2015). "Integration of drug, protein, and gene delivery systems with regenerative medicine." Drug delivery and translational research **5**(2): 168-186.
165. Louie, K. a. W., E. H. Hasegawa, G. H. Farr III, A. Ignacz, A. Paguio, A. Maenza, A. G. Paquette, C. Henry and L. Maves (2025). "Epigenetic small molecule screening identifies a new HDACi compound for ameliorating Duchenne muscular dystrophy." bioRxiv: 2025.2001. 2024.634796.
166. Lucas, T., A. Waisman, R. Ranjan, J. Roes, T. Krieg, W. Müller, A. Roers and S. A. Eming (2010). "Differential roles of macrophages in diverse phases of skin repair." The Journal of Immunology **184**(7): 3964-3977.

167. Lyu, S.-Y., W. Xiao, G.-Z. Cui, C. Yu, H. Liu, M. Lyu, Q.-Y. Kuang, E.-H. Xiao and Y.-H. Luo (2023). "Role and mechanism of DNA methylation and its inhibitors in hepatic fibrosis." Frontiers in Genetics **14**: 1124330.
168. Maden, M. and M. Hind (2003). "Retinoic acid, a regeneration-inducing molecule." Developmental dynamics: an official publication of the American Association of Anatomists **226**(2): 237-244.
169. Mahmoudi, S., E. Mancini, L. Xu, A. Moore, F. Jahanbani, K. Hebestreit, R. Srinivasan, X. Li, K. Devarajan and L. Prélot (2019). "Heterogeneity in old fibroblasts is linked to variability in reprogramming and wound healing." Nature **574**(7779): 553-558.
170. Maia Campos, P. M. B. G., L. R. Gaspar, G. M. S. Gonçalves, L. H. T. R. Pereira, M. Semprini and R. A. Lopes (2015). "Comparative effects of retinoic acid or glycolic acid vehiculated in different topical formulations." BioMed Research International **2015**(1): 650316.
171. Mania, S., K. Partyka, J. Pilch, E. Augustin, M. Cieślik, J. Ryl, J.-R. Jinn, Y.-J. Wang, A. Michałowska and R. Tylingo (2019). "Obtaining and characterization of the PLA/chitosan foams with antimicrobial properties achieved by the emulsification combined with the dissolution of chitosan by CO2 saturation." Molecules **24**(24): 4532.
172. Martău, G. A., M. Mihai and D. C. Vodnar (2019). "The use of chitosan, alginate, and pectin in the biomedical and food sector—biocompatibility, bioadhesiveness, and biodegradability." Polymers **11**(11): 1837.
173. Martin, E. M. and R. C. Fry (2018). "Environmental influences on the epigenome: exposure-associated DNA methylation in human populations." Annual review of public health **39**(1): 309-333.
174. Martin, J. F. and E. N. Olson (2000). "Identification of a prx1 limb enhancer." genesis **26**(4): 225-229.
175. Matak, I., V. Tékus, Z. Lacković and Z. Helyes (2017). "Involvement of substance P in the antinociceptive effect of botulinum toxin type A: Evidence from knockout mice." Neuroscience **358**: 137-145.
176. Mathew-Steiner, S. S., S. Roy and C. K. Sen (2021). "Collagen in wound healing." Bioengineering **8**(5): 63.
177. McCusker, C., S. V. Bryant and D. M. Gardiner (2015). "The axolotl limb blastema: cellular and molecular mechanisms driving blastema formation and limb regeneration in tetrapods." Regeneration **2**(2): 54-71.
178. McGrath, J. A., R. Eady and F. Pope (2004). "Anatomy and organization of human skin." Rook's textbook of dermatology **1**: 3.2-3.80.
179. Merkel, F. (1875). "Tastzellen und Tastkörperchen bei den Hausthieren und beim Menschen." Archiv für mikroskopische Anatomie **11**(Suppl 1): 636-652.
180. Miranda, T. B. and P. A. Jones (2007). "DNA methylation: the nuts and bolts of repression." Journal of cellular physiology **213**(2): 384-390.
181. Mitani, F., K. Mukai, H. Miyamoto, M. Suematsu and Y. Ishimura (2003). "The undifferentiated cell zone is a stem cell zone in adult rat adrenal cortex." Biochimica et Biophysica Acta (BBA)-General Subjects **1619**(3): 317-324.
182. Moll, I., M. Roessler, J. M. Brandner, A.-C. Eispert, P. Houdek and R. Moll (2005). "Human Merkel cells–aspects of cell biology, distribution and functions." European journal of cell biology **84**(2-3): 259-271.
183. Morgenstern, D. A., R. A. Asher, M. Naidu, T. Carlstedt, J. M. Levine and J. W. Fawcett (2003). "Expression and glycanation of the NG2 proteoglycan in developing, adult, and damaged peripheral nerve." Molecular and Cellular Neuroscience **24**(3): 787-802.
184. Moriya, C., Y. Shida, Y. Yamane, Y. Miyamoto, M. Kimura, N. Huse, K. Ebisawa, Y. Kameda, A. Nishi and D. Du (2013). "Subcutaneous administration of sodium alginate oligosaccharides prevents salt-induced hypertension in Dahl salt-sensitive rats." Clinical and Experimental Hypertension **35**(8): 607-613.

185. Moskowitz, A. J. and S. M. Horwitz (2017). "Targeting histone deacetylases in T-cell lymphoma." Leukemia & lymphoma **58**(6): 1306-1319.
186. Moya, M. L., M. Morley, O. Khanna, E. C. Opara and E. M. Brey (2012). "Stability of alginate microbead properties in vitro." Journal of Materials Science: Materials in Medicine **23**: 903-912.
187. Mozzetta, C., G. Minetti and P. L. Puri (2009). "Regenerative pharmacology in the treatment of genetic diseases: the paradigm of muscular dystrophy." The international journal of biochemistry & cell biology **41**(4): 701-710.
188. Mund, C., B. Brueckner and F. Lyko (2006). "Reactivation of epigenetically silenced genes by DNA methyltransferase inhibitors: basic concepts and clinical applications." Epigenetics **1**(1): 8-14.
189. Nakano, Y., M. C. Kelly, A. U. Rehman, E. T. Boger, R. J. Morell, M. W. Kelley, T. B. Friedman and B. Bánfi (2018). "Defects in the alternative splicing-dependent regulation of REST cause deafness." Cell **174**(3): 536-548. e521.
190. Navarro, X., M. Vivó and A. Valero-Cabré (2007). "Neural plasticity after peripheral nerve injury and regeneration." Progress in neurobiology **82**(4): 163-201.
191. Niehrs, C. (2009). "Active DNA demethylation and DNA repair." Differentiation **77**(1): 1-11.
192. Nikulina, E., J. L. Tidwell, H. N. Dai, B. S. Bregman and M. T. Filbin (2004). "The phosphodiesterase inhibitor rolipram delivered after a spinal cord lesion promotes axonal regeneration and functional recovery." Proceedings of the National Academy of Sciences **101**(23): 8786-8790.
193. Noce, B. (2024). "Novel bona-fide NOXs inhibitors and dual EZH2/HDACs epigenetic modulators: innovative strategies to fight cancerous and non-cancerous diseases."
194. Nohno, T., E. Koyama, F. Myokai, S. Taniguchi, H. Ohuchi, T. Saito and S. Noji (1993). "A chicken homeobox gene related to Drosophila paired is predominantly expressed in the developing limb." Developmental biology **158**(1): 254-264.
195. Ohle, S. J., A. Anandaiah, A. J. Fabian, A. Fine and D. N. Kotton (2012). "Maintenance and repair of the lung endothelium does not involve contributions from marrow-derived endothelial precursor cells." American Journal of Respiratory Cell and Molecular Biology **47**(1): 11-19.
196. Orta, M. L., N. Pastor, E. Burgos-Morón, I. Domínguez, J. M. Calderón-Montaño, C. H. Castaño, M. López-Lázaro, T. Helleday and S. Mateos (2017). "Zebularine induces replication-dependent double-strand breaks which are preferentially repaired by homologous recombination." DNA repair **57**: 116-124.
197. Pagella, P., L. Jiménez-Rojo and T. A. Mitsiadis (2014). "Roles of innervation in developing and regenerating orofacial tissues." Cellular and molecular life sciences **71**: 2241-2251.
198. Park, H., H. J. Lee, H. An and K. Y. Lee (2017). "Alginate hydrogels modified with low molecular weight hyaluronate for cartilage regeneration." Carbohydrate polymers **162**: 100-107.
199. Park, J. Y., Y. W. Kang, B. Y. Choi, Y. C. Yang, B. P. Cho and W. G. Cho (2017). "CCL11 promotes angiogenic activity by activating the PI3K/Akt pathway in HUVECs." Journal of Receptors and Signal Transduction **37**(4): 416-421.
200. Pellettieri, J. (2019). Regenerative tissue remodeling in planarians–The mysteries of morphallaxis. Seminars in cell & developmental biology, Elsevier.
201. Peña-Quintana, L., M. Llarena, D. Reyes-Suarez and L. Aldamiz-Echevarria (2017). "Profile of sodium phenylbutyrate granules for the treatment of urea-cycle disorders: patient perspectives." Patient preference and adherence: 1489-1496.
202. Podolak-Popinigis, J., B. Górnikiewicz, A. Ronowicz and P. Sachadyn (2015). "Transcriptome profiling reveals distinctive traits of retinol metabolism and neonatal parallels in the MRL/MpJ mouse." BMC genomics **16**: 1-17.

203. Podolak-Popinigis, J., A. Ronowicz, M. Dmochowska, A. Jakubiak and P. Sachadyn (2016). "The methylome and transcriptome of fetal skin: implications for scarless healing." Epigenomics **8**(10): 1331-1345.
204. Ponting, C. P., P. L. Oliver and W. Reik (2009). "Evolution and functions of long noncoding RNAs." Cell **136**(4): 629-641.
205. Porrello, E. R., A. I. Mahmoud, E. Simpson, J. A. Hill, J. A. Richardson, E. N. Olson and H. A. Sadek (2011). "Transient regenerative potential of the neonatal mouse heart." Science **331**(6020): 1078-1080.
206. Portela, A. and M. Esteller (2010). "Epigenetic modifications and human disease." Nature biotechnology **28**(10): 1057-1068.
207. Qiang, L., S. Yang, Y.-H. Cui and Y.-Y. He (2021). "Keratinocyte autophagy enables the activation of keratinocytes and fibroblastsand facilitates wound healing." Autophagy **17**(9): 2128-2143.
208. Rajesh, A., L. Wise and M. Hibma (2019). "The role of Langerhans cells in pathologies of the skin." Immunology and cell biology **97**(8): 700-713.
209. Ramaiah, M. J., A. D. Tangutur and R. R. Manyam (2021). "Epigenetic modulation and understanding of HDAC inhibitors in cancer therapy." Life sciences **277**: 119504.
210. Reinke, J. and H. Sorg (2012). "Wound repair and regeneration." European surgical research **49**(1): 35-43.
211. Reynolds, S. D., A. Giangreco, J. H. Power and B. R. Stripp (2000). "Neuroepithelial bodies of pulmonary airways serve as a reservoir of progenitor cells capable of epithelial regeneration." The American journal of pathology **156**(1): 269-278.
212. Richardson, R., K. Slanchev, C. Kraus, P. Knyphausen, S. Eming and M. Hammerschmidt (2013). "Adult zebrafish as a model system for cutaneous wound-healing research." Journal of Investigative Dermatology **133**(6): 1655-1665.
213. Rink, S., H. Bendella, S. M. Akkin, M. Manthou, M. Grosheva and D. N. Angelov (2019). "Experimental studies on facial nerve regeneration." The Anatomical Record **302**(8): 1287-1303.
214. Rittié, L. (2016). "Cellular mechanisms of skin repair in humans and other mammals." Journal of cell communication and signaling **10**: 103-120.
215. Romeika, J., M. Wurzelmann and D. Sun (2017). "TrkB receptor agonist 7, 8-dihydroxyflavone and its therapeutic potential for traumatic brain injury." New Therapeutics for Traumatic Brain Injury: 225-234.
216. Rowlatt, U. (1979). "Intrauterine wound healing in a 20 week human fetus." Virchows Archiv A **381**: 353-361.
217. Ruvinov, E. and S. Cohen (2016). "Alginate biomaterial for the treatment of myocardial infarction: progress, translational strategies, and clinical outlook: from ocean algae to patient bedside." Advanced drug delivery reviews **96**: 54-76.
218. Sabino, C. P., A. M. Deana, T. M. Yoshimura, D. F. Da Silva, C. M. França, M. R. Hamblin and M. S. Ribeiro (2016). "The optical properties of mouse skin in the visible and near infrared spectral regions." Journal of Photochemistry and Photobiology B: Biology **160**: 72-78.
219. Sami, D. G., H. H. Heiba and A. Abdellatif (2019). "Wound healing models: A systematic review of animal and non-animal models." Wound Medicine **24**(1): 8-17.
220. Sanders, J. A., C. Schorl, A. Patel, J. M. Sedivy and P. A. Gruppuso (2012). "Postnatal liver growth and regeneration are independent of c-myc in a mouse model of conditional hepatic c-myc deletion." BMC physiology **12**: 1-15.
221. Santos, N. C., J. Figueira-Coelho, J. Martins-Silva and C. Saldanha (2003). "Multidisciplinary utilization of dimethyl sulfoxide: pharmacological, cellular, and molecular aspects." Biochemical pharmacology **65**(7): 1035-1041.
222. Sarabia-Sánchez, M. A. and M. Robles-Flores (2024). "WNT signaling in stem cells: a look into the non-canonical pathway." Stem Cell Reviews and Reports **20**(1): 52-66.

223. Saraswati, S., S. M. Marrow, L. A. Watch and P. P. Young (2019). "Identification of a pro-angiogenic functional role for FSP1-positive fibroblast subtype in wound healing." Nature communications **10**(1): 3027.
224. Sariola, H. and M. Saarma (2003). "Novel functions and signalling pathways for GDNF." Journal of cell science **116**(19): 3855-3862.
225. Sass, P., P. Sosnowski, J. Podolak-Popinigis, B. Górnikiewicz, J. Kamińska, M. Deptuła, E. Nowicka, A. Wardowska, J. Ruczyński and P. Rekowski (2019). "Epigenetic inhibitor zebularine activates ear pinna wound closure in the mouse." EBioMedicine **46**: 317-329.
226. Satish, L. and S. Kathju (2010). "Cellular and molecular characteristics of scarless versus fibrotic wound healing." Dermatology research and practice **2010**(1): 790234.
227. Satoh, A., A. Hirata and Y. Satou (2011). "Blastema induction in aneurogenic state and Prrx-1 regulation by MMPs and FGFs in Ambystoma mexicanum limb regeneration." Developmental biology **355**(2): 263-274.
228. Schmidt, B. A. and V. Horsley (2013). "Intradermal adipocytes mediate fibroblast recruitment during skin wound healing." Development **140**(7): 1517-1527.
229. Schneider, C. A., W. S. Rasband and K. W. Eliceiri (2012). "NIH Image to ImageJ: 25 years of image analysis." Nature methods **9**(7): 671-675.
230. Schuettengruber, B., H.-M. Bourbon, L. Di Croce and G. Cavalli (2017). "Genome regulation by polycomb and trithorax: 70 years and counting." Cell **171**(1): 34-57.
231. Seal, R. L., S. Tweedie and E. A. Bruford (2023). "A standardised nomenclature for long non-coding RNAs." IUBMB life **75**(5): 380-389.
232. Seifert, A. W., S. G. Kiama, M. G. Seifert, J. R. Goheen, T. M. Palmer and M. Maden (2012). "Skin shedding and tissue regeneration in African spiny mice (Acomys)." Nature **489**(7417): 561-565.
233. Seifert, A. W., J. R. Monaghan, M. D. Smith, B. Pasch, A. C. Stier, F. Michonneau and M. Maden (2012). "The influence of fundamental traits on mechanisms controlling appendage regeneration." Biological Reviews **87**(2): 330-345.
234. Seifert, A. W. and K. Muneoka (2018). "The blastema and epimorphic regeneration in mammals." Developmental biology **433**(2): 190-199.
235. Sephel, G. C. and S. C. Woodward (2001). Repair, regeneration, and fibrosis, Lippincott, Williams & Wilkins, Baltimore**:** 84-117.
236. Serezani, A. P., G. Bozdogan, S. Sehra, D. Walsh, P. Krishnamurthy, E. A. S. Potchanant, G. Nalepa, S. Goenka, M. J. Turner and D. F. Spandau (2017). "IL-4 impairs wound healing potential in the skin by repressing fibronectin expression." Journal of Allergy and Clinical Immunology **139**(1): 142-151. e145.
237. Shah, R., T. M. Spektor, D. J. Weisenberger, H. Ding, R. Patil, C. Amador, X.-Y. Song, S. T. Chun, J. Inzalaco and S. Turjman (2023). "Reversal of dual epigenetic repression of non-canonical Wnt-5a normalises diabetic corneal epithelial wound healing and stem cells." Diabetologia **66**(10): 1943-1958.
238. Shi, H., X. Wang, Z. Lu, B. S. Zhao, H. Ma, P. J. Hsu, C. Liu and C. He (2017). "YTHDF3 facilitates translation and decay of N6-methyladenosine-modified RNA." Cell research **27**(3): 315-328.
239. Shkand, T. V., M. O. Chizh, I. V. Sleta, B. P. Sandomirsky, A. L. Tatarets and L. D. Patsenker (2016). "Assessment of alginate hydrogel degradation in biological tissue using viscosity-sensitive fluorescent dyes." Methods and Applications in Fluorescence **4**(4): 044002.
240. Shyh-Chang, N., H. Zhu, T. Y. De Soysa, G. Shinoda, M. T. Seligson, K. M. Tsanov, L. Nguyen, J. M. Asara, L. C. Cantley and G. Q. Daley (2013). "Lin28 enhances tissue repair by reprogramming cellular metabolism." Cell **155**(4): 778-792.
241. Silva, J., J. Nichols, T. W. Theunissen, G. Guo, A. L. van Oosten, O. Barrandon, J. Wray, S. Yamanaka, I. Chambers and A. Smith (2009). "Nanog is the gateway to the pluripotent ground state." Cell **138**(4): 722-737.

242. Sim, C. B., M. Ziemann, A. Kaspi, K. Harikrishnan, J. Ooi, I. Khurana, L. Chang, J. E. Hudson, A. El-Osta and E. R. Porrello (2015). "Dynamic changes in the cardiac methylome during postnatal development." The FASEB Journal **29**(4): 1329-1343.
243. Simkin, J., T. R. Gawriluk, J. C. Gensel and A. W. Seifert (2017). "Macrophages are necessary for epimorphic regeneration in African spiny mice." elife **6**: e24623.
244. Simkin, J., M. C. Sammarco, L. A. Dawson, P. P. Schanes, L. Yu and K. Muneoka (2015). "The mammalian blastema: regeneration at our fingertips." Regeneration **2**(3): 93-105.
245. Singh, A. K., S. Halder-Sinha, J. P. Clement and T. K. Kundu (2018). "Epigenetic modulation by small molecule compounds for neurodegenerative disorders." Pharmacological Research **132**: 135-148.
246. Skowron, P., Rodziewicz-Motowidło, S., Dzierżyńska, M., Sawucka, J., Sachadyn, P., Słonimska, P., Sosnowski P., Sass, P., Kamińska, J., Baczyński-Keller, J., Płatek, R. (2024). Pharmaceutical composition based on hydrogel formulation for use as a two-component preparation promoting tissue regeneration. **Patent Pat.246411**.
247. Słonimska, P., J. Baczyński-Keller, R. Płatek, M. Deptuła, M. Dzierżyńska, J. Sawicka, O. Król, P. Sosnowski, M. Koczkowska and A. Kostecka (2024). "Development of a small-molecule epigenetic regenerative therapy. Subcutaneous administration of alginate formulations with high loads of zebularine and retinoic acid promotes tissue growth, vascularization and innervation and induces extensive epigenetic repatterning." bioRxiv: 2024.2009. 2018.613177.
248. Słonimska, P., P. Sachadyn, J. Zieliński, M. Skrzypski and M. Pikuła (2024). "Chemotherapy-mediated complications of wound healing: An understudied side effect." Advances in Wound Care **13**(4): 187-199.
249. Słonimska, P., Sachadyn P. (2022). Regenerative potential of bioflavonoids tested in an ear punch wound model. EMBO Conference – Molecular and cellular basis of tissue regeneration and repair 2022. Barcelona, Spain.
250. Solandt, O. (1941). "Some observations upon sodium alginate." Quarterly Journal of Experimental Physiology and Cognate Medical Sciences: Translation and Integration **31**(1): 25-30.
251. Song, Z., A. Jadali, B. Fritzsch and K. Y. Kwan (2017). "NEUROG1 regulates CDK2 to promote proliferation in otic progenitors." Stem Cell Reports **9**(5): 1516-1529.
252. Sosnik, A. (2014). "Alginate particles as platform for drug delivery by the oral route: state-of-the-art." International Scholarly Research Notices **2014**(1): 926157.
253. Sosnowski, P., P. Sass, P. Słonimska, R. Płatek, J. Kamińska, J. Baczyński Keller, P. Mucha, G. Peszyńska-Sularz, A. Czupryn and M. Pikuła (2022). "Regenerative drug discovery using ear pinna punch wound model in mice." Pharmaceuticals **15**(5): 610.
254. Stroncek, J. D. and W. M. Reichert (2008). "Overview of wound healing in different tissue types." Indwelling neural implants: strategies for contending with the in vivo environment.
255. Sun, Z., C. Song, C. Wang, Y. Hu and J. Wu (2019). "Hydrogel-based controlled drug delivery for cancer treatment: a review." Molecular pharmaceutics **17**(2): 373-391.
256. Suzuki, M., S. Ebara, T. Koike, S. Tonomura and K. Kumamoto (2012). "How many hair follicles are innervated by one afferent axon? A confocal microscopic analysis of palisade endings in the auricular skin of thy1-YFP transgenic mouse." Proceedings of the Japan Academy, Series B **88**(10): 583-595.
257. Suzuki, M., A. Satoh, H. Ide and K. Tamura (2005). "Nerve-dependent and-independent events in blastema formation during Xenopus froglet limb regeneration." Developmental Biology **286**(1): 361-375.
258. Suzuki, M., A. Satoh, H. Ide and K. Tamura (2007). "Transgenic Xenopus with prx1 limb enhancer reveals crucial contribution of MEK/ERK and PI3K/AKT pathways

in blastema formation during limb regeneration." Developmental biology **304**(2): 675-686.
259. Szekalska, M., A. Puciłowska, E. Szymańska, P. Ciosek and K. Winnicka (2016). "Alginate: current use and future perspectives in pharmaceutical and biomedical applications." International journal of polymer science **2016**(1): 7697031.
260. Szuts, E. Z. and F. I. Harosi (1991). "Solubility of retinoids in water." Archives of Biochemistry and Biophysics **287**(2): 297-304.
261. Szymański, Ł., R. Skopek, M. Palusińska, T. Schenk, S. Stengel, S. Lewicki, L. Kraj, P. Kamiński and A. Zelent (2020). "Retinoic acid and its derivatives in skin." Cells **9**(12): 2660.
262. Takahashi, K. and S. Yamanaka (2006). "Induction of pluripotent stem cells from mouse embryonic and adult fibroblast cultures by defined factors." cell **126**(4): 663-676.
263. Takeo, M., W. C. Chou, Q. Sun, W. Lee, P. Rabbani, C. Loomis, M. M. Taketo and M. Ito (2013). "Wnt activation in nail epithelium couples nail growth to digit regeneration." Nature **499**(7457): 228-232.
264. Takeo, M., W. Lee and M. Ito (2015). "Wound healing and skin regeneration." Cold Spring Harbor perspectives in medicine **5**(1): a023267.
265. Talbott, H. E., S. Mascharak, M. Griffin, D. C. Wan and M. T. Longaker (2022). "Wound healing, fibroblast heterogeneity, and fibrosis." Cell stem cell **29**(8): 1161-1180.
266. Tan, F. H. and M. E. Bronner (2024). "Regenerative loss in the animal kingdom as viewed from the mouse digit tip and heart." Developmental Biology **507**: 44-63.
267. Tecilazich, F. and A. Veves (2018). Role of peripheral neuropathy in the development of foot ulceration and impaired wound healing in diabetes mellitus. Nutritional and Therapeutic Interventions for Diabetes and Metabolic Syndrome, Elsevier**:** 95-104.
268. Tekcham, D. S., D. Chen, Y. Liu, T. Ling, Y. Zhang, H. Chen, W. Wang, W. Otkur, H. Qi and T. Xia (2020). "F-box proteins and cancer: an update from functional and regulatory mechanism to therapeutic clinical prospects." Theranostics **10**(9): 4150.
269. Thoniyot, P., M. J. Tan, A. A. Karim, D. J. Young and X. J. Loh (2015). "Nanoparticle–hydrogel composites: Concept, design, and applications of these promising, multi-functional materials." Advanced Science **2**(1-2): 1400010.
270. Thuret, S., M. Thallmair, L. L. Horky and F. H. Gage (2012). "Enhanced functional recovery in MRL/MpJ mice after spinal cord dorsal hemisection." PloS one **7**(2): e30904.
271. Togo, T., A. Utani, M. Naitoh, M. Ohta, Y. Tsuji, N. Morikawa, M. Nakamura and S. Suzuki (2006). "Identification of cartilage progenitor cells in the adult ear perichondrium: utilization for cartilage reconstruction." Laboratory Investigation **86**(5): 445-457.
272. Tokuzawa, Y., E. Kaiho, M. Maruyama, K. Takahashi, K. Mitsui, M. Maeda, H. Niwa and S. Yamanaka (2003). "Fbx15 is a novel target of Oct3/4 but is dispensable for embryonic stem cell self-renewal and mouse development." Molecular and cellular biology **23**(8): 2699-2708.
273. Tomasso, A., V. Disela, M. T. Longaker and K. Bartscherer (2024). "Marvels of spiny mouse regeneration: cellular players and their interactions in restoring tissue architecture in mammals." Current Opinion in Genetics & Development **87**: 102228.
274. Trevor, L. V., K. Riches-Suman, A. L. Mahajan and M. J. Thornton (2020). "Adipose tissue: a source of stem cells with potential for regenerative therapies for wound healing." Journal of clinical medicine **9**(7): 2161.
275. Uchiyama, A., S. Nayak, R. Graf, M. Cross, K. Hasneen, J. S. Gutkind, S. R. Brooks and M. I. Morasso (2019). "SOX2 epidermal overexpression promotes cutaneous wound healing via activation of EGFR/MEK/ERK signaling mediated by EGFR ligands." Journal of Investigative Dermatology **139**(8): 1809-1820. e1808.

276. Ud-Din, S., S. W. Volk and A. Bayat (2014). "Regenerative healing, scar-free healing and scar formation across the species: current concepts and future perspectives." Experimental dermatology **23**(9): 615-619.
277. Uniyal, S., A. K. Tyagi and J. P. Muyal (2020). "All trans retinoic acid (ATRA) progresses alveolar epithelium regeneration by involving diverse signalling pathways in emphysematous rat." Biomedicine & Pharmacotherapy **131**: 110725.
278. Van Dongen, J. A., M. C. Harmsen, B. Van der Lei and H. P. Stevens (2018). "Augmentation of dermal wound healing by adipose tissue-derived stromal cells (ASC)." Bioengineering **5**(4): 91.
279. VandenBosch, L. S. and T. A. Reh (2020). Epigenetics in neuronal regeneration. Seminars in cell & developmental biology, Elsevier.
280. VanderMolen, K. M., W. McCulloch, C. J. Pearce and N. H. Oberlies (2011). "Romidepsin (Istodax, NSC 630176, FR901228, FK228, depsipeptide): a natural product recently approved for cutaneous T-cell lymphoma." The Journal of antibiotics **64**(8): 525-531.
281. Vanhoutte, P. M. (2010). "Regeneration of the endothelium in vascular injury." Cardiovascular drugs and therapy **24**: 299-303.
282. Varani, J., R. S. Mitra, D. Gibbs, S. H. Phan, V. M. Dixit, R. Mitra Jr, T. Wang, K. J. Siebert, B. J. Nickoloff and J. J. Voorhees (1990). "All-trans retinoic acid stimulates growth and extracellular matrix production in growth-inhibited cultured human skin fibroblasts." Journal of investigative dermatology **94**(5): 717-723.
283. Verheijen, M., M. Lienhard, Y. Schrooders, O. Clayton, R. Nudischer, S. Boerno, B. Timmermann, N. Selevsek, R. Schlapbach and H. Gmuender (2019). "DMSO induces drastic changes in human cellular processes and epigenetic landscape in vitro." Scientific reports **9**(1): 4641.
284. Vériter, S., J. Mergen, R.-M. Goebbels, N. Aouassar, C. Grégoire, B. Jordan, P. Levêque, B. Gallez, P. Gianello and D. Dufrane (2010). "In vivo selection of biocompatible alginates for islet encapsulation and subcutaneous transplantation." Tissue Engineering Part A **16**(5): 1503-1513.
285. Vestita, M., P. Tedeschi and D. Bonamonte (2022). "Anatomy and Physiology of the Skin." Textbook of plastic and reconstructive surgery: basic principles and new perspectives: 3-13.
286. Votruba, I., A. Holý and R. Wightman (1973). "The mechanism of inhibition of DNA synthesis in Escherichia coli by pyrimidin-2-one β-d-ribofuranoside." Biochimica et Biophysica Acta (BBA)-Nucleic Acids and Protein Synthesis **324**(1): 14-23.
287. Waikel, R. L., Y. Kawachi, P. A. Waikel, X.-J. Wang and D. R. Roop (2001). "Deregulated expression of c-Myc depletes epidermal stem cells." Nature genetics **28**(2): 165-168.
288. Wakizono, T., H. Nakashima, T. Yasui, T. Noda, K. Aoyagi, K. Okada, Y. Yamada, T. Nakagawa and K. Nakashima (2021). "Growth factors with valproic acid restore injury-impaired hearing by promoting neuronal regeneration." JCI insight **6**(22): e139171.
289. Wang, B., Y. Zhan, L. Yan and D. Hao (2022). "How zoledronic acid improves osteoporosis by acting on osteoclasts." Frontiers in Pharmacology **13**: 961941.
290. Wang, J., Y. Wang, X. Sun, D. Liu, C. Huang, J. Wu, C. Yang and Q. Zhang (2019). "Biomimetic cartilage scaffold with orientated porous structure of two factors for cartilage repair of knee osteoarthritis." Artificial cells, nanomedicine, and biotechnology **47**(1): 1710-1721.
291. Wang, L., J. Li, P. Tang, D. Zhu, L. Tai, Y. Wang, T. Miyata, J. R. Woodgett and L.-j. Di (2025). "GSK3β deficiency expands obese adipose vasculature to mitigate metabolic disorders." Circulation Research **136**(1): 91-111.
292. Wang, X., Z. Lu, A. Gomez, G. C. Hon, Y. Yue, D. Han, Y. Fu, M. Parisien, Q. Dai and G. Jia (2014). "N 6-methyladenosine-dependent regulation of messenger RNA stability." Nature **505**(7481): 117-120.

293. Webster, D. B. (1966). "Ear structure and function in modern mammals." American Zoologist **6**(3): 451-466.
294. Wei, J. J., H. S. Kim, C. A. Spencer, D. Brennan-Crispi, Y. Zheng, N. M. Johnson, M. Rosenbach, C. Miller, D. H. Leung and G. Cotsarelis (2020). "Activation of TRPA1 nociceptor promotes systemic adult mammalian skin regeneration." Science immunology **5**(50): eaba5683.
295. Werner, A. and M. Rape (2017). "Powering stem cell decisions with ubiquitin." Cell Death and Differentiation **24**(11): 1823.
296. Widelitz, R. B. (2008). "Wnt signaling in skin organogenesis." Organogenesis **4**(2): 123-133.
297. Wietecha, M. S., M. Pensalfini, M. Cangkrama, B. Müller, J. Jin, J. Brinckmann, E. Mazza and S. Werner (2020). "Activin-mediated alterations of the fibroblast transcriptome and matrisome control the biomechanical properties of skin wounds." Nature communications **11**(1): 2604.
298. Wijermans, P., B. Rüter, M. Baer, J. Slack, H. Saba and M. Lübbert (2008). "Efficacy of decitabine in the treatment of patients with chronic myelomonocytic leukemia (CMML)." Leukemia research **32**(4): 587-591.
299. Wilken, M. S., J. A. Brzezinski, A. La Torre, K. Siebenthall, R. Thurman, P. Sabo, R. S. Sandstrom, J. Vierstra, T. K. Canfield and R. S. Hansen (2015). "DNase I hypersensitivity analysis of the mouse brain and retina identifies region-specific regulatory elements." Epigenetics & chromatin **8**: 1-17.
300. Williams-Boyce, P. K. (1982). "Mammalian ear tissue regeneration."
301. Williams-Boyce, P. K. and J. C. Daniel Jr (1980). "Regeneration of rabbit ear tissue." Journal of Experimental Zoology **212**(2): 243-253.
302. Wood, M. D., S. W. Kemp, C. Weber, G. H. Borschel and T. Gordon (2011). "Outcome measures of peripheral nerve regeneration." Annals of Anatomy-Anatomischer Anzeiger **193**(4): 321-333.
303. Wulff, B. C., A. E. Parent, M. A. Meleski, L. A. DiPietro, M. E. Schrementi and T. A. Wilgus (2012). "Mast cells contribute to scar formation during fetal wound healing." Journal of Investigative Dermatology **132**(2): 458-465.
304. Xia, H., M. P. Krebs, S. Kaushal and E. W. Scott (2011). "Enhanced retinal pigment epithelium regeneration after injury in MRL/MpJ mice." Experimental eye research **93**(6): 862-872.
305. Xu, P., K. Jin, J. Zhou, J. Gu, X. Gu, L. Dong and X. Sun (2022). "G9a inhibition promotes the formation of pacemaker-like cells by reducing the enrichment of H3K9me2 in the HCN4 promoter region." Molecular Medicine Reports **27**(2): 21.
306. Xu, Z., H. Li and P. Jin (2012). "Epigenetics-based therapeutics for neurodegenerative disorders." Current Geriatrics Reports **1**: 229-236.
307. Yadav, A., T.-C. Huang, S.-H. Chen, T. S. Ramasamy, Y.-Y. Hsueh, S.-P. Lin, F.-I. Lu, Y.-H. Liu and C.-C. Wu (2021). "Sodium phenylbutyrate inhibits Schwann cell inflammation via HDAC and NFκB to promote axonal regeneration and remyelination." Journal of Neuroinflammation **18**: 1-16.
308. Yamanaka, S. (2013). "The winding road to pluripotency (Nobel Lecture)." Angewandte Chemie International Edition **52**(52).
309. Yamazaki, T., W. Li, L. Yang, P. Li, H. Cao, S.-i. Motegi, M. C. Udey, E. Bernhard, T. Nakamura and Y.-s. Mukouyama (2018). "Whole-mount adult ear skin imaging reveals defective neuro-vascular branching morphogenesis in obese and type 2 diabetic mouse models." Scientific reports **8**(1): 430.
310. Yin, D., X. Zhang, Q. Jiang, S. Luo, Y. Luo, P. Cheng, G. Jin and C. Liu (2022). "Epidermal stem cells participate in the repair of scalds via Nanog and Myc regulation." Molecular Medicine Reports **26**(6): 364.
311. Yokoyama, H. (2008). "Initiation of limb regeneration: the critical steps for regenerative capacity." Development, growth & differentiation **50**(1): 13-22.

312. Yokoyama, H., T. Maruoka, H. Ochi, A. Aruga, S. Ohgo, H. Ogino and K. Tamura (2011). "Different requirement for Wnt/β-catenin signaling in limb regeneration of larval and adult Xenopus." PLoS One **6**(7): e21721.
313. Yousefi, S., Z. Zhi and R. K. Wang (2014). "Label-free optical imaging of lymphatic vessels within tissue beds in vivo." IEEE J Sel Top Quantum Electron **20**(2): 6800510.
314. Zen, A. A. H., D. A. Nawrot, A. Howarth, A. Caporali, D. Ebner, A. Vernet, J. E. Schneider and S. Bhattacharya (2016). "The retinoid agonist tazarotene promotes angiogenesis and wound healing." Molecular Therapy **24**(10): 1745-1759.
315. Zhang, Q.-S., D. S. Kurpad, M. G. Mahoney, M. J. Steinbeck and T. A. Freeman (2017). "Inhibition of apoptosis signal-regulating kinase 1 alters the wound epidermis and enhances auricular cartilage regeneration." PloS one **12**(10): e0185803.
316. Zhang, S., X. Wang, J. Man, J. Li, X. Cui, C. Zhang, W. Shi, D. Li, S. Zhang and J. Li (2020). "Histone deacetylase inhibitor-loaded calcium alginate microspheres for acute kidney injury treatment." ACS Applied Bio Materials **3**(9): 6457-6465.
317. Zhang, X., S. Zhang, X. Yan, Y. Shan, L. Liu, J. Zhou, Q. Kuang, M. Li, H. Long and W. Lai (2021). "m6A regulator-mediated RNA methylation modification patterns are involved in immune microenvironment regulation of periodontitis." Journal of Cellular and Molecular Medicine **25**(7): 3634-3645.
318. Zhang, Y., F. Madiai and K. V. Hackshaw (2001). "Cloning and characterization of a novel form of mouse fibroblast growth factor-1 (FGF-1) mRNA, FGF-1. G: differential expression of FGF-1 and FGF-1. G mRNAs during embryonic development and in postnatal tissues." Biochimica et Biophysica Acta (BBA)-Gene Structure and Expression **1521**(1-3): 45-58.
319. Zhou, P., Y. Lu and X.-H. Sun (2011). "Zebularine suppresses TGF-beta-induced lens epithelial cell–myofibroblast transdifferentiation by inhibiting MeCP2." Molecular vision **17**: 2717.
320. Zhou, T.-B., G. P. Drummen and Y.-H. Qin (2012). "The controversial role of retinoic acid in fibrotic diseases: analysis of involved signaling pathways." International journal of molecular sciences **14**(1): 226-243.
321. Zhou, W., K. He, C. Wang, P. Wang, D. Wang, B. Wang, H. Geng, H. Lian, T. Ma and Y. Nie (2024). "Pharmacologically inducing regenerative cardiac cells by small molecule drugs." eLife **13**: RP93405.

LIST OF FIGURES

LIST OF TABLES

ACADEMIC ACHIEVEMENTS

Publications:

- **Słonimska, P.**, Sachadyn, P., Zieliński, J., Skrzypski, M., Pikuła, M. (2024). Chemotherapy-mediated complications of wound healing. An understudied side effect. Advances in Wound Care., DOI: 10.1089/wound.2023.0097, IF (2024): 4.9
- Sosnowski, P., Sass, P., **Słonimska, P.**, Płatek, R., Kamińska, J., Baczyński-Keller, J., Mucha, P., Peszyńska-Sularz, G., Czupryn, A., Pikuła, M., Piotrowski, A., Janus, Łukasz, Rodziewicz-Motowidło, S., Skowron, P., & Sachadyn, P. (2022). Regenerative Drug Discovery Using Ear Pinna Punch Wound Model in Mice. Pharmaceuticals, 15, 610., DOI: 10.3390/ph15050610, IF (2022): 4.3
- Stańczak, M., Wyszomirski, A., **Słonimska, P.**, Kołodziej, B., Jabłoński, B., Stanisławska-Sachadyn, A., Karaszewski, B. (2024). Circulating miRNA profiles and the risk of hemorrhagic transformation after thrombolytic treatment of acute ischemic stroke: a pilot study. Frontiers in Neurology, 15, 1399345.; DOI: 10.3389/fneur.2024.1399345 IF (2024): 2.7
- Mania S., Banach-Kopeć A., Tylingo R., Maciejewska N., Czerwiec K., **Słonimska P.**, Deptuła M., Pikuła M., Baczyński-Keller J., Sachadyn P., „From Bioink to Tissue: Exploring Chitosan-Agarose Medium in the Context of Printability and Cellular Behaviour“, Molecules, 29(19), 4648., DOI: 10.3390/molecules29194648, IF (2023): 4,2
- Deptuła, M., Zawrzykraj, M., **Słonimska, P.**, Pikuła, M. (2024). Isolation of Human Progenitor Epidermal Cells on Collagen Type IV and Analysis of Their Markers with Flow Cytometry and PCR Methods. DOI: 10.1007/7651_2024_541

Patent and patent aplications:

- Patent Pat. 246411 “Pharmaceutical composition based on hydrogel formulations for use as a two-component preparation stimulating tissue regeneration” granted by the Patent Office of the Republic of Poland on September 18 2024, INVENTORS: **Paulina Słonimska**, Paweł Sachadyn, Piotr Skowron, Paweł Sosnowski, Piotr Sass, Sylwia Rodziwicz-Motowidło, Justyna Sawicka, Maria Dzierżyńska, Jolanta Kamińska, Jakub Baczyński-Keller, Rafał Płatek, APPLICANTS: University of Gdańsk, Gdańsk University of Technology, Medical University of Gdańsk, Innovabion Sp. z o.o.
- PCT/PL2019/000008 Composition for use in the treatment of skin wound. Filing date 2019-01-23. Publication date 2020-07-30 WO/2020/153855 INVENTORS: Paweł Sachadyn, Paweł Sosnowski, Piotr Sass, Jolanta Kamińska, Jakub Baczyński-Keller, **Paulina Słonimska,** APPLICANT: Gdańsk University of Technology
- EP22214353.9A Hydrogel formulation comprising zebularine and retinoic acid. Filing date 2022-12-16 EP4197526A1 Publication date: 2023-06-21 INVENTORS: **Paulina Słonimska**, Paweł Sachadyn, Piotr Skowron, Paweł Sosnowski, Piotr Sass, Sylwia Rodziewicz-Motowidło, Justyna Sawicka, Maria Dzierżyńska, Jolanta Kamińska, Jakub Baczyński-Keller, Rafał Płatek, Michał Pikuła, Milena Deptuła. APPLICANTS: University of Gdańsk, Gdańsk Univerity of Technology, Medical University of Gdańsk, Innovabion Sp. z o.o.

Conference reports:

- Poster presentation entitled "Regenerative potential of bioflavonoids tested in an ear punch wound model" **Słonimska Paulina**, Sachadyn Paweł, EMBO Conference – Molecular and cellular basis of tissue regeneration and repair 2022, 23-26.09.2022, Barcelona, Spain
- Oral presentation entitled "Application of hydrogel bioflavonoid preparations in tissue regeneration" **Słonimska Paulina**, Sachadyn Paweł, 2nd Scientific Conference "Interdisciplinary perspective on health sciences" named after Professor Piotr Lass, 23-25.11.2022, Gdańsk, Poland

- Poster presentation entitled "Searching for compounds stimulating regeneration", **Słonimska Paulina**, Baczyński-Keller Jakub, Sachadyn Paweł, XIV Interdisciplinary Scientific Conference TYGIEL 2022, March 24-27, 2022, Lublin, Poland
- Co-authorship of the conference report entitled "Biological properties of chitosan-agarose composite as a potential bioink component for 3D printing", **Słonimska Paulina**, Czerwiec Katarzyna, Baczyński-Keller Jakub, Deptuła Milena, Pikuła Michał, Tylingo Robert, Banach-Kopeć Adrianna, Mania Szymon, Sachadyn Paweł, 4th International Conferences on Advances Functional Materials & Biomaterials & Biodevices, 16.11.2023, Rome, Italy
- Co-authorship of the conference report entitled "The expression of bitter taste receptors in human arterial endothelium," Kochany Paweł, Opiełka Mikołaj, **Słonimska Paulina**, Mickiewicz Agnieszka, Woźniak Michał, Sachadyn Paweł, Gruchała Marcin, Górska-Ponikowska Magdalena, 28th International Student Conference in Gdansk, 13-15.04.23, Gdansk, Poland
- Co-authorship of the conference report entitled "Epigenetic therapy activates endogenous regenerative potential", Sass Piotr, **Słonimska Paulina**, Płatek Rafał, Baczyński-Keller Jakub, Sosnowski Paweł, Kamińska Jolanta, Sachadyn Paweł, Eurobiotech, 22.06.2022, Krakow, Poland
- Co-authorship of the conference report entitled "Epigenetic basis of regeneration", Górnikiewicz Bartosz, Sass Piotr, Baczyński-Keller Jakub, **Słonimska Paulina**, Podolak-Popinigis Justyna, Sosnowski Paweł, Kamińska Jolanta, Sachadyn Paweł, 53rd Symposium of the Polish Society for Histochemistry and Cytochemistry, 15-18.09.2019, Gdańsk, Poland

Grants:

- **2019 - 2023** BIONANOVA a research project funded by the National Centre for Research and Development of Poland „New generation bioactive molecules delivery systems, based on chemically synthesised and obtained through genetic engineering nanobiomaterials”, TECHMATSTRATEG2/410747/11/2019 – as an investigator
- **2021 - 2024** A research project funded by the National Centre for Research and Development of Poland NCN OPUS, „The effect of adipose tissue stem cells on

in vitro cultured skin cells from patients undergoing chemotherapy", UMO-2019/31/Z/NZ8/04028 – as an investigator

- **2024** Faculty Grant for the Interdepartmental Research Team in cooperation with the Department of Chemistry, Technology and Biotechnology of Food and the Laboratory for Regenerative Biotechnology **(**Department of Biotechnology and Microbiology), entitled "Assessment of the effect of chitosan-agarose composition on wound healing in an animal model" – as an investigator
- **2018 – 2019** „Drug candidate for wound healing" a grant under the project Incubator of Innovation+ - Support for management of scientific research and commercialisation of R&D results in scientific units and enterprises", implemented under the Intelligent Development Operational Program 2014-2020 (Action 4.4) – as an investigator
- **since 2025** A research project funded by the National Centre for Research and Development of Poland NCN OPUS, „Molecular factors and pathomechanism of cancer cachexia ", UMO-2024/53/B/NZ5/04166 – as an investigator